PHOTOGRAPHIC EMULSION STUDIES OF NUCLEAR REACTIONS AT HIGH AND INTERMEDIATE ENERGIES.

by

G. C. Morrison

Department of Natural Philosophy

University of Glasgow

Presented as a thesis for the degree of

Ph.D., in the University of Glasgow.

ProQuest LLC.
789 East Eisenhower Parkway
P.O. Box 1346
Ann Arbor, MI 48106 – 1346

PREFACE

The research described in this thesis has been carried out by the author while a postgraduate student in the Department of Natural Philosophy, Glasgow University, under the supervision of Professor P. I. Dee. During this time (1951 - 1954) the author was a member of the nuclear emulsion group under the direction of Dr. H. Muirhead. The programme of research has been concerned with the nuclear interactions of particles of energy below that at which meson production becomes possible.

At the present time there is no unified description of the interaction of nucleons with atomic nuclei which can satisfactorily account for the experimental results obtained for all energies of the bombarding particles. The results are interpreted by consideration of phenomenological models of the nucleus which are appropriate for different regions of energy of the incident nucleons. These models appear adequate in their regions of applicability. Their relationship to each other and their underlying physical significance is only partly understood.

In order to give the perspective to the thesis of this dissertation, the early chapters are devoted to a critical review of the subject.

This entails discussion in Chapter 1 of the various models of the nucleus which have been proposed to describe the interaction of nucleons at different incident energies. The application of photographic emulsion technique in the study of nuclear reactions is considered in Chapter 2. An appendix to this chapter describes the determination of the range-energy relationships for protons and alpha particles in diluted Ilford G5 emulsions carried out by the author in collaboration with Dr. Rosser.

The results have been published in the Proceedings of the Physical Society.

The review is followed by an account of the author's research. For reasons of conciseness here, certain details of procedure are included in the form of appendices.

In Chapter 3 an investigation of the interaction of protons at an energy of 140 MeV with the nuclei of the photographic emulsion is described. Cross sections are obtained for the disintegrations produced in the light and heavy atomic constituents of the emulsion by comparison of events in normal and diluted emulsions. A satisfactory description of the nature of the disintegrations is obtained by assuming, on the Goldberger model, that the incident proton interacts directly with individual nucleons inside the struck nucleus. A nucleon cascade is set up inside the nucleus which continues until the nucleons escape from the nucleus or are absorbed to leave the residual nucleus in an excited state. An estimate is made for the mean free path of nucleons inside nuclear matter at different energies when possible nucleon-nucleon collisions are restricted by the application of the Pauli Exclusion Principle.

The study was carried out by the author in collaboration with Dr. Muirhead and Dr. Rosser. The experimental procedure adopted to separate the cross sections for the disintegrations in the light and heavy nuclei of the photographic emulsion is due to Dr. Muirhead. The results of this investigation have been published in the Philosophical Magazine.

In Chapter 4 an experimental attempt to assess the importance of the emission of nucleons at intermediate energies by direct collision process

inside the nucleus is described. This has been carried out by studying the distributions in energy and angle of the protons emitted from the interaction of 13.2 MeV neutrons with iron. The protons are produced in iron foils and are detected in photographic emulsions. Exposures to aluminium and rhodium foils were also made to allow a comprehensive study of the (n,p) reactions in different elements to be made. The results which have been subsequently obtained from these exposures are also given in chapter 4.

The investigation was initiated by the author and carried out with the assistance and subsequent collaboration of Mr. Brown. The experimental procedure adopted and the method of analysis of the observations were developed by the author. The correction which was applied to the observed energy spectra to allow for the reduction in energy of the protons in passing through the iron foils was calculated by Mr. Brown. The results of this investigation have been published in the Philosophical Magazine.

In chapter 5, the scattering of nucleons at low and intermediate energies by nuclei is treated theoretically by an extension of the semi-classical method of Goldberger. The nucleus is described by a simplified free particle model in which account is taken of the Pauli Principle in excluding dynamically possible collisions inside nuclear matter. The model is applied in a calculation of the dependence of the imaginary part of the Weisskopf nuclear potential on the energy of the incident nucleon. Good agreement is obtained with the values of the scattering potentials which have been derived from the analysis of nucleon nucleus scattering

experiments by the optical model. The application of the model in predicting the direct emission of nucleons from nuclear reactions at these energies is considered.

The calculation of the scattering potentials was carried out by Dr. Muirhead with the collaboration of the author. The results of the investigation have been published in the Philosophical Magazine.

The dissertation concludes in chapter 6, emphasis being placed on the connection of the research presented in the thesis with current ideas.

ACKNOWLEDGEMENTS

The author wishes to record his thanks to his supervisor, Professor P. I. Dee, F.R.S., for his continued interest in this work. It is his pleasure to acknowledge the direction and encouragement received by the author from Dr. H. Muirhead.

PUBLICATIONS

(1) The Range-Energy Relation for Protons and Alpha-Particles in Diluted Ilford G5 Emulsions.

Lees, Morrison and Rosser, 1953, Proc. Phys. Soc. A, 66, 13.

(2) The Cross Section for Star Production in Nuclear Emulsions by 130 MeV Protons.

Lees, Morrison, Muirhead and Rosser, 1953, Phil. Mag. 44, 304.

(3) The Nuclear Disintegrations Produced by High Energy Protons.

Morrison, Muirhead and Rosser, 1953, Phil. Mag. 44, 1326.

(4) A Study of Protons Emitted from Aluminium, Iron and Rhodium on Bombardment with Neutrons of 13.2 MeV.

Brown, Morrison, Muirhead and Morton, 1957, Phil. Mag. 2, 785.

(5) On the Selection of Potentials in Nucleon Nuclear Scattering Problems.

Morrison, Muirhead and Murdoch, 1955, Phil. Mag. 46, 795.

C O N T E N T S

Chapter 1

A Review of the Interaction of Nucleons with Nuclei.

Section 1.1: Introduction

An exact theory of the interaction of nucleons with nuclei must be based upon a knowledge of the forces existing between nucleons inside the nucleus. Most attempts to discover the nature of the inter-nucleon forces have proceeded along one of two paths, namely, the study of the interaction of only two nucleons in order to arrive at an understanding of the elementary forces between isolated nuclear particles and the interpretation of the properties of complex nuclei in terms of the interaction between the nuclear constituents. Up to the present time these two approaches have not led to a consistent theory of nuclear forces. Indeed it is far from certain that the forces active within the nucleus are the same as found between isolated nucleons.

Because of this lack of knowledge of the nature of the forces within the nucleus, any present theory which describes a nuclear reaction must necessarily be phenomenological. Various models of the mechanism of the nuclear interaction which do not depend on a detailed account of the interactions between the elementary particles have been applied at different energies of the incident particle. With the aid of these models it has been possible to describe the nucleus in terms of a limited number of parameters. In this way a consistent picture of the structure of the nucleus is being developed.

It is convenient for the purpose of discussion to specify three energy regions, namely: $E < 1$ MeV, $1 < E < 50$ MeV and $E > 50$ MeV (the

low, intermediate and high energy regions respectively). In general the character of a nuclear reaction is determined by the energy region of the incident particle. However, as would be expected there is considerable overlap in the classification of nuclear reactions, with a gradual change of character from one energy region to another.

At low energies nuclear reactions are characterised by sharp resonances in the cross sections. At intermediate energies the nucleus appears effectively black to an incident particle and the cross sections for scattering and absorption are about equal to the geometrical area of the nucleus. At high energies the nucleus appears partially transparent to an incident nucleon and the cross sections for absorption are considerably less than the geometrical area for the light nuclei.

The observed interaction of nucleons with the nucleus has been described on the basis of two very different models: the compound nucleus model and the optical model. At the time this work was started, the compound nucleus model, based on strong interaction, appeared adequate to account for the results of experiments at low and intermediate energies. Its antithesis, the optical model, gave a satisfactory interpretation of the experimental results obtained at high energies. During the period of this research the optical model was extended in application to describe the scattering and absorption of nucleons at low energies.

The work presented in this thesis is concerned with the study of nuclear reactions at high and intermediate energies. In this chapter a critical review of the interaction of nucleons with nuclei is given within the above models.

Section 1.2: The Definition of Cross Sections

The total cross section, σ_t, which includes all effects that remove a particle from the incident beam can be subdivided into two parts. Thus,

$$\sigma_t = \sigma_{el} + \sigma_r$$

where σ_{el} denotes the elastic scattering cross section and σ_r denotes the combined cross section for all events other than elastic scattering, referred to as the reaction cross section. The reaction cross section plays the part of an absorption cross section since it describes the removal of particles from the 'entrance channel' of the reaction.

The detailed cross sections of the different nuclear reactions are all contained in σ_r, which can be split into the sum of the cross sections for specific reactions. Thus,

$$\sigma_r = \sigma_{in} + \sum\sigma(a,b)$$

where σ_{in} is the cross section for inelastic scattering of the incident particle and the sum of the $\sigma(a,b)$ takes into account all other reactions in which the incident particle is not re-emitted.

Ideally the task of a comprehensive theory of nuclear reactions is to predict the individual cross sections for all the energetically allowed reactions that can be initiated by the incident particle. However, it is convenient to distinguish between the prediction of the elastic and reaction cross sections and the detailed cross sections. The former are concerned exclusively with the scattering or absorption of the incident beam. The latter cross sections, however, reflect the mechanism of energy transfer inside the nucleus and depend, therefore, on a specific description of the

course of the nuclear reaction.

The elastic and reaction cross sections can be further divided into partial cross sections $\sigma_{el,\ell}$ and $\sigma_{r,\ell}$ which represent the cross sections for events initiated by incident particles with angular momentum ℓ. General expressions have been obtained for these cross sections by considering the effect of the target nucleus on the wave function of the incident particles in the entrance channel. The interaction with the nucleus changes the outgoing wave only. The partial elastic and reaction cross sections are then given by the following expressions:

$$\sigma_{el,\ell} = \frac{\pi}{k^2}(2\ell+1)\left|1 - S_\ell\right|^2 \quad \text{and} \quad \sigma_{r,\ell} = \frac{\pi}{k^2}(2\ell+1)\left\{1 - \left|S_\ell\right|^2\right\} ,$$

where k is the wave number of the incoming particles and S_ℓ is the amplitude of the ℓ_{th} partial outgoing wave.

In general the amplitudes, S_ℓ, can be calculated only if the internal structure of the nucleus is known. However, it is a feature of the different models used to describe the nuclear interaction that these amplitudes can be determined on making certain general assumptions about the structure of the nucleus. In particular if the existence of a well defined nuclear surface is assumed, then S_ℓ can be determined from the conditions at the nuclear surface.

The radial wave function outside the nucleus $u_\ell(r)$, can be obtained from the solution of the radial Schrodinger equation. The amplitude, S_ℓ, will be contained in the wave function, $u_\ell(r)$. Since the radial wave function and its derivative must be continuous at the surface, then, if f_ℓ is the logarithmic derivative of the interior wave function,

$$f_\ell = R\left(\frac{du_\ell/dr}{u_\ell}\right)_{r=R}$$

From this equation, the amplitudes, S_ℓ, and hence the cross sections can be expressed quite generally in terms of the f_ℓ's.

The determination of cross sections can therefore be reduced to finding plausible values of the f_ℓ's. In the compound nucleus model, the f_ℓ's are determined by postulating suitable values of u_ℓ in the interior of the nucleus. In the optical model, the f_ℓ's are derived directly in terms of the parameters of the complex potential well.

As the energy of the incident particle increases, the number of ℓ values which must be considered in the partial wave analysis also increases. At high energies, the analysis becomes exceedingly complicated. However, at high energies the wavelength of the incident particle is very small, so that the nuclear surface is not well defined. On the transparent nucleus model of high energy scattering, the reflection at the nuclear surface is neglected so that the phase change of the outgoing wave can be simply evaluated. In this approximation, therefore, the cross sections can be calculated without using an exact partial wave analysis.

Section 1.3: The Compound Nucleus Description of a Nuclear Reaction at Low and Intermediate Energies.

3(a) The Compound Nucleus

Until recently the generally accepted description of the interaction of nucleons with nuclei was based on the strong interaction or compound nucleus theory of Bohr (1936). On this theory the nuclear reaction was described as proceeding in two successive stages; firstly, the formation of a compound nucleus between the bombarding particle and target nucleus

and secondly, the decay of the compound system into the products of the reactions. It was assumed that the two stages of the reaction could be considered as independent processes so that the decay of the compound system did not depend specifically on the way it was formed. This has been referred to as the Bohr assumption. According to this assumption, the cross section for a nuclear reaction X(a,b)Y, expressed as $\sigma(a,b)$, can be written as,

$$\sigma(a,b) = \sigma_c(a) \cdot G_c(b)$$

where $\sigma_c(a)$ is the cross section for formation of the compound nucleus and $G_c(b)$ is the probability that the compound nucleus will decay with emission of b.

The Bohr assumption is based on a picture of the nucleus in which the interaction between the nucleons is so strong that the energy of the incident particle, once it strikes the nucleus, is rapidly absorbed and completely distributed among the nuclear constituents. A necessary condition for the quick sharing of energy is that the incident nucleon has a short mean free path in nuclear matter. A necessary condition for the complete 'mixing' of the energy of the incident particle is that the compound nucleus has a long lifetime. In addition, the stability of the compound nucleus requires that the average energy of a particle, after the excitation energy of the compound nucleus has been shared out, should be much less than the separation energy of the particle from the nucleus. When the energy of the incident particle is less than 50 Me V, it was estimated that these conditions should be valid (c.f. Blatt and Weisskopf 19

1952). The compound nucleus description has been applied in this energy range.

3(b) The Formation of the Compound Nucleus: Continuum and Resonance Theory

The formal determination of cross sections using the concept of a compound nucleus has been based on two extreme theories, namely, continuum theory and resonance theory. Common to both theories are two general assumptions regarding the structure of the nucleus.

1. The nucleus has a well defined surface which is a sphere of radius R. The nuclear forces only act on a particle if the distance between the particle and the centre of the nucleus is less than R.

2. The particle is subject to very strong interactions inside the nucleus so that it rapidly exchanges its energy with the other nucleons. Neither theory is concerned, however, with any details of compound nucleus formation.

The further assumption peculiar to the continuum theory of nuclear reactions is that the compound nucleus has many modes of decay (Feshbach and Weisskopf 1949). This condition is fulfilled when the incident energy is sufficient to excite the compound nucleus above the region of discrete energy levels, i.e., to the continuum region of excitation levels. The continuum theory is therefore only strictly applicable to incident particles with energy of several Me V. However, Feshbach and Weisskopf showed that the continuum theory could also be applied at lower energies if the cross sections are averaged over resonances.

In view of the continuum assumption the incident particle is very unlikely to be re-emitted into the entrance channel once it has penetrated the nuclear surface. The radial wave function in the entrance channel is therefore expected to have the form of an ingoing wave only, so that it can be represented by $u_\ell \sim e^{-iKr}$, for $r < R$, where K is the wave number of the particle on entering the nucleus. This wave function is approximate, being used only to give an estimate for the logarithmic derivative f_ℓ at the nuclear surface. The continuum theory leads to values of the cross sections which are smooth functions of the energy and independent of any special properties of the target nucleus. The continuum theory does not predict nuclear resonances. Furthermore, the reaction cross section is identical with the cross section for the formation of the compound nucleus, because of the assumption that the incident particle is not re-emitted into the entrance channel.

A different description of the behaviour of $u_\ell(r)$, for $r < R$, is necessary to extend the above considerations to lower incident energies, where the return of the incident particle into the entrance channel cannot be neglected. If the continuum assumption is dropped, it can be shown that the main consequence is the appearance of resonances in the cross section (Feshbach et al. 1947). The cross section for forming a compound nucleus now shows a series of maxima and minima corresponding to the excitation of discrete energy levels in the compound nucleus.

In the resonance region the experimental results can be well represented by the theory in almost all cases. At higher energy the experimental

results as they appeared in 1949 were very limited. Feshbach and Weisskopf (1949) showed that their calculations gave only a fair measure of agreement with the experimental results. However, the main application of compound nucleus theory at that time was in the prediction of the detailed cross sections. In so far as the continuum theory appeared capable of providing an overall description of the cross section for forming a compound nucleus, the theoretical situation was considered to be satisfactory. It was not until much later that serious doubt was cast upon the correctness of the continuum assumption of the immediate formation of a compound nucleus.

3(c) The Decay of the Compound Nucleus.

The nuclear processes occurring after the formation of a compound nucleus were first considered by Weisskopf (1937). On the basis of the Bohr assumption, a connection between the rate of the two opposite processes of formation and decay of the compound system was derived by the application of reciprocity arguments. When the levels of both the compound and residual nuclei are assumed to form a continuum, the probability of decay of the compound nucleus by emission of particle b with energy ϵ, $I_b(\epsilon)d\epsilon$, is given by the following expression:

$$I_b(\epsilon)\, d\epsilon = \text{const.}\, \epsilon\, \sigma_{cb}(\epsilon)\, w(E)\, d\epsilon$$

where $\sigma_{cb}(\epsilon)$ is the cross section for formation of the compound nucleus by b in the inverse reaction and $w(E)$ is the level density of the residual nucleus with excitation energy E. From general thermodynamic considerations, the level density at an excitation energy E can be expressed in terms of the corresponding nuclear temperature T, as $\frac{1}{T} = \frac{d(\log w)}{dE}$. The resulting

expression for the energy distribution of the emitted particles, b, then describes the disintegration of the compound nucleus as analogous to an evaporation process.

The above considerations were extended to the calculation of the yields of nuclear reactions (Weisskopf and Ewing 1940). The decay of the compound nucleus is assumed to be governed by the free competition between all the different possible processes of de-excitation, the only difference between neutrons and protons, for example, being the effect on the latter of the Coulomb barrier. This is the statistical assumption. The theory of nuclear reactions founded on this basis is called the statistical theory.

The probability of the decay of the compound nucleus with emission of particle b, G_c (b), can be written as

$$G_c \ (b) \quad = \quad \frac{F_b}{\Sigma F_c}$$

where the quantity, F_b, is the emission probability of particle b, and the sum is over all possible types of decay including the emission of b. When the excited states of the residual nucleus are continuous, the quantity F_b is given by the integral of the intensity distribution I_b (ϵ) dϵ over all possible energies of the emitted particle

$$F_b \quad = \quad \int_o^{\epsilon_b} I_b \ (\epsilon) \, d\epsilon$$

$$= \text{const} \int_o^{\epsilon_b} \epsilon \, \sigma_{cb}(\epsilon) \, w(E) \, d\epsilon$$

where ϵ_b is the maximum possible energy of the emitted particle b. The functions F_b can be computed for each particle type if the form of the level density in the residual nucleus w(E) is known. An estimate of the

dependence of the level density w(E) on the excitation energy E can be deduced from the assumed energy dependence of the temperature T.

The cross section of a particular (a,b) reaction proceeding via the compound nucleus can therefore be calculated from the expression,

$$\sigma(a,b) = \sigma_c(a) \sum \frac{F_b}{F_c}$$

where $\sigma_c(a)$ is the cross section for forming the compound nucleus by particle a. When neutron emission is energetically possible, it is generally more likely to occur than charged particle emission, since the latter must penetrate the Coulomb barrier. The cross section for the reaction, $\sigma(a,n)$ is approximately equal to the cross section for forming a compound nucleus $\sigma_c(a)$ for energies below the Coulomb barrier.

Certain general conclusions can also be stated concerning the angular distribution of the reaction products from the decay of the compound nucleus It can be shown by statistical arguments that the angular distribution of particles emitted from a compound nucleus excited in the continuum region is symmetrical about 90° (Wolfenstein 1951). Moreover, the angular distribution of particles which leave the residual nucleus also excited in the continuum region is isotropic.

Experimental confirmation of the statistical theory of the decay of the compound nucleus has been obtained in a wide range of experiments. These include a comparison of the ratio of the yield of particular reactions proceeding through the same compound nucleus at the same excitation energy (Ghoshal 1950); a comparison of the variation of the yield of the (α,n)

and (α, 2n) reactions (Bradt and Tendam 1947, Bleuler et al. 1953) and the (p,n) reaction (Blaser et al. 1951) as a function of energy; a comparison of the energy spectrum of neutrons emitted in (n,n′) and (p,n) reactions (Graves and Rosen 1953, Gugelot 1951). However, significant deviations are observed in the study of reactions which, for statistical reasons, are not favoured in the decay of the compound nucleus, the emission of protons, for example, being more likely than theoretically predicted. Such differences will be discussed in section 1.5(a)

3(d) The Validity of the Compound Nucleus Description.

To appreciate the limitations of the compound nucleus picture, it is worthwhile making a closer study of the compound nucleus formed in the reaction. This will have a large probability of being formed if the incident energy is such that an energy level, E_s, in the compound nucleus is excited. Since the compound states decay, they have a finite lifetime τ_s and the level E_s has a width Γ_s related to τ_s by $\Gamma_s = \frac{\hbar}{\tau_s}$

The average distance between levels, D, can be related to the period, T, of the internal nucleon motion by the expression, $T = \frac{2\pi\hbar}{D}$ (Weisskopf 1950). For a level from which only a particle b can be emitted, the period T is the interval of time between successive appearances of the particle b at the nuclear surface; that is, between successive attempts at escape. The lifetime τ_b of the state is then given by $\tau_b = \frac{T}{P_b}$ where P_b is the penetrability of the surface for the particle b. Hence the particle width can be related to the level distance by the expression:

$$\Gamma_b = \frac{\hbar}{\tau_b} \approx P_b \frac{D}{2\pi}$$

In the resonance region, the level width, Γ_b is much less than the level distance, D. The occurrence of resonances implies, therefore, that the penetration of the nuclear surface is small and in consequence that the same motion is repeated many times before the decay of the compound state occurs. As a result, the Bohr assumption that the decay of the compound nucleus is independent of its mode of formation should be valid in the resonance region.

As the energy of the incident particle increases, the width of the compound state increases. Not only does every single particle width increase since each P_b becomes larger, but more modes of decay are possible since more levels become available in the residual nucleus. There is a region of excitation energy, therefore, at which the width Γ_s becomes greater than the level distance D. The spectrum of the compound nucleus becomes truly continuous and the formation of the compound nucleus is independent of the position of individual levels. This is the continuum region. The lifetime of the compound state, τ_s has become smaller than the period, T, so that the incident nucleon may not even complete one single cycle of its motion. A complete mixing of the excitation energy may not occur, and in consequence, the decay of the compound nucleus may not now be independent of the manner of formation.

Thus the assumption of an independent decay is strictly valid only in the resonance region. However, even at higher energies the lifetime of the compound nucleus, although shorter than the nuclear period, may be sufficiently long to allow a complete sharing of energy. This premise is

supported by the general success of the statistical theory of nuclear reactions. However, at still higher energies, the assumption of the sharing of energy among all the nuclear constituents can no longer be justified and the theory of nuclear reactions has to be treated on a different basis.

Section 1.4: The Optical Description of a Nuclear Reaction at High Energy

4(a) Nuclear Transparency

When the energy of the incident particle becomes so high that its wavelength is much smaller than the nuclear radius, the particle can interact with individual nucleons inside the nucleus (Serber 1947). Since the cross sections for interaction between nucleons are small at high energies, the mean free path for inelastic scattering by individual nucleons in nuclear matter becomes of the order of nuclear dimensions. It follows that the assumption of immediate absorption can no longer be considered valid so that the nuclear interaction can no longer be described on the compound nucleus model.

There is also a finite probability that a nucleon of high energy, because of its long mean free path will pass right through the nucleus without any collision - the phenomenon of nuclear transparency. The value of the reaction cross section at high energies is therefore expected to be less than the geometrical area presented by the nucleus to the incident particles. It is obvious, from size considerations that the light nuclei will show the greatest transparency.

4(b) The Transparent Nucleus Model

A theoretical description of the nuclear interaction of particles of high energy has been made by analogy with the scattering of light by optical systems. The nuclear matter is characterised by a complex index of refraction, which takes into account the change in wavelength of the nucleon on entering the nucleus (real part) and the absorption in the nucleus (imaginary part). Thus the wave train of incident nucleons is considered to preserve its identity as it moves through the nucleus apart from attenuation and refraction. This is the optical description. In particular, when the optical picture is applied to the prediction of cross sections, it is known as the 'transparent nucleus' model (Fernbach, Serber and Taylor 1949).

The transparent model is a high energy approximation which requires that the energy is high enough for the incident wavelength λ to be much less than R. In the model all nuclei are treated as spheres of uniform density having the same refractive index and absorption coefficient and differing from each other in size only. The complex propagation vector of the incident nucleons inside the nucleus can be written as $k + k_1 + \frac{1}{2}iK$ where k is the wave number of the incident nucleon outside the nucleus, k_1 is the increase in wave number inside the nucleus and K is the absorption coefficient in nuclear matter.

The increase in wave number k_1 can be related to the depth of the real potential well V inside the nucleus. The wave number inside the nucleus is given by:

$$k + k_1 = \left\{ \frac{2m}{\hbar^2} (E + V) \right\}^{\frac{1}{2}}$$

where E is the kinetic energy outside the nucleus. It follows then that:

$$k_1 = k \left\{ \left(1 + \frac{V}{E}\right)^{\frac{1}{2}} - 1 \right\}$$

If the absorption of the incident nucleon is assumed to take place by the mechanism proposed by Serber (loc. cit.), then the absorption coefficient K is given by the product of the particle density inside the nucleus and the average cross section $\bar{\sigma}$ for scattering of the incident nucleon N by a particle in the nucleus. Hence K can be related to the cross sections for free nucleon-nucleon scattering since $\bar{\sigma}$ can be expressed in terms of these cross sections by

$$\bar{\sigma} = \frac{\left[Z \sigma_{Np} + (A - Z) \sigma_{Nn} \right] \alpha}{A}$$

where α is a factor which reduces the cross sections in nuclear matter to allow for the restriction of the Pauli Exclusion Principle on the scattering of the incident nucleon by a proton or a neutron bound in the nucleus.

In the transparent nucleus model the cross sections are calculated in terms of these parameters by considering classical trajectories of the nucleon traversing the nucleus. Since the wavelength is assumed to be very much less than the nuclear radius, the general expressions for the cross sections (c.f. section 1.2) can be simplified by replacing the sum over the discrete partial waves by the integral over a continuous impact parameter. Moreover, if reflection at the surface is neglected, the outgoing wave has a relative phase and amplitude given by

$$S_\ell = e^{(ik_1 - \frac{1}{2}K) T}$$

where T is the distance travelled in the nucleus and can be directly

related to the impact parameter. Thus the cross sections can be obtained directly by integration of the expressions given in section 1.2 when S_ℓ has the form above.

The reaction cross section is given by

$$\sigma_r = \pi R^2 \left[1 - \left\{ 1 - (1 + 2KR)e^{-2KR} \right\} \frac{1}{2K^2R^2} \right]$$

The expression for the elastic cross section is more complicated and will not be given here. For a finite value of K, the reaction cross section has a value less than the geometrical cross section πR^2 which exhibits the transparency of the nucleus. When K tends to infinity which represents the case of a completely opaque nucleus, the reaction cross section tends to the geometrical value πR^2.

The transparent nucleus model has been employed as a basis for analysis of the observed variation of the total cross section for neutrons with energy above 80 MeV incident on different nuclei (Fernbach, Serber and Taylor loc. cit., Taylor 1953). It is found that the radius of different nuclei can be represented by $1.37\ A^{\frac{1}{3}} \times 10^{-13}$ cm, in agreement with the assumption of a constant nuclear density. The values of the real potential V and the absorption coefficient K which have been derived from the experimental results vary smoothly with the energy of the incident neutron. According to the model, K slowly decreases as the energy of the incident nucleon increases, whereas V rapidly decreases above an energy of 80 MeV to a constant value of a few MeV at an energy of 200 MeV.

The variation of K can be shown to agree well with that expected

from the measured nucleon-nucleon cross sections provided that account is taken of the restrictions imposed by the Pauli Exclusion Principle. Moreover, the observed decrease of V can be qualitatively explained by considering the nature of the nucleon-nucleon interaction. At high energies the wavelength of the incident particle is small and in consequence more details of the nucleon-nucleon interaction are explored: thus, the decrease in the effective nuclear potential could be expected if the interaction between two nucleons becomes highly repulsive at short distances. Hence the application of the model leads to a consistent description of the interaction of high energy neutrons in terms of the collisions with individual particles inside the nucleus.

The experimental determination of the cross sections for the interaction of protons is complicated by the charge of the proton which results in the attenuation of the proton beam by ionisation and Coulomb scattering. For this reason, the number of such experiments carried out with high energy protons has been limited. However, where the results of proton experiments have been obtained (e.g. Richardson et al. 1952), their analysis by the transparent nucleus model (Gatha and Riddell 1952) has been equally successful and indicates values of the parameters in good agreement with those derived from the neutron experiments.

The work described in the first part of chapter 3 on the inelastic scattering of protons of 130 MeV was carried out to examine the validity of the transparent nucleus model at an energy where previously no measurements had been performed.

4(c) The Reaction Produced at High Energy

On the transparent nucleus model, the cross section for the occurrence of a nuclear reaction is determined from the probability that the incident nucleon collides with a nucleon inside the nucleus. The result of the reaction can also be predicted by considering the interaction of the incoming nucleon with the individual nucleons of the target nucleus rather than with the nucleus as a whole. Because of the elastic nature of the collision, the struck nucleon may receive a large fraction of the incident energy, and thus leave the nucleus without further collision. On the other hand, the energy division may continue until the energy of the nucleons is so low that the nucleons are absorbed. Thereafter, the nucleons share their energy with the nucleus as a whole.

A detailed model which predicts the nature of the nuclear disintegrations at high energy was developed on this basis by Goldberger (1948). On the model the incident nucleon initiates a nucleonic cascade following the first collision inside the nucleus. Since the effects of wave interference can be neglected at high energy, the passage of the nucleons in nuclear matter can be defined by the application of classical mechanics. The scattering collisions are described by the free nucleon-nucleon cross sections. The influence of the other nucleons is felt only through the nuclear potential well, the internal momentum distribution of the nucleons inside the nucleus and the Pauli Exclusion Principle which forbids collisions corresponding to final states already filled by the other nucleons.

The cascade is considered to continue until either the nucleons reach

the surface of the nucleus and escape, or lose sufficient energy in a collision to be absorbed in the nucleus leaving it in an excited state. The emission of particles from the excited nucleus can then be described by the evaporation theory of Weisskopf (1937).

The existence of direct collision processes inside the nucleus has been confirmed by the observation of the high energy particles emitted in the reaction. Indeed, it was soon realised that the quasi-elastic nature of the first collision should allow a determination of the momentum distribution of the nucleons inside the nucleus (Cladis et al. 1952, Chamberlain and Segrè 1952). The only difference between such a collision and that of the free nucleon nucleon collision results from the motion of the struck particle inside the nucleus. The slowly varying yield of particular reactions observed at high energy, e.g. $C^{12}(p,pn)C^{11}$ (Hintz 1952) can again be interpreted in consequence of the direct emission of particles; the actual excitation energy remaining in the nucleus varies more slowly than the energy of the incident particle. Finally it has been shown that the detailed characteristics of the nuclear disintegrations produced by 400 MeV protons can be predicted by a statistical calculation of the development of a nucleon cascade (Bernardini et al. 1952). However, it appeared desirable to examine the extent to which direct collisions are important at lower energies.

The work described in the second part of chapter 3 is concerned with an investigation of the nuclear disintegrations produced by 130 MeV protons. It was anticipated that the comparatively low energy of the

incident proton might allow an estimate of the energy at which the reaction should no longer be described as the interaction of the incident nucleon with individual nucleons inside the nucleus but rather as an interaction with the nucleus as a whole.

Section 1.5: The Optical Description of a Nuclear Reaction at Low and Intermediate Energies.

5(a) Difficulties of Interpretation on the Compound Nucleus Model

In view of the success of two such different descriptions of the nuclear interaction as the optical model at high energy and the compound nucleus model at low and intermediate energies, it was natural that theoretical attention should be given to their region of applicability. The two models are generically related since absorption of a nucleon on the optical model is a necessary first step in the establishment of an excited compound nucleus. However, this is obviously not sufficient, since the nucleus may lose energy be inelastic emission in an early stage of the sharing and exchange processes. By taking a mean free path for the incident nucleon on the basis of the free particle cross sections, Peaslee (1952) estimated that compound nucleus theory should be applicable up to energies of the order of 30 MeV (c.f. section 1.3(a)) and that the optical model should be valid for energies greater than 80 MeV. In this lower region some recent experimental data are very difficult to reconcile with the predictions of compound nucleus theory.

Some of the difficulties arose in the interpretation of the measured scattering cross sections by continuum theory. The data consisted of

measurements of the total cross sections of a range of elements for neutrons of 42 MeV (Hildebrand and Leith 1950) and 14 MeV (Barschall et al. 1952) and measurements of the angular distributions of protons elastically scattered from different nuclei at 18 MeV (Levier and Saxon 1952) and 31 MeV (Britten 1952). However, the observed deviations from the predictions of continuum theory gave no indication of the manner in which the theory should be modified.

Other difficulties arose from the interpration of the yields and products of particular nuclear reactions on the statistical theory. Thus, Paul and Clarke (1953) have observed considerable differences between their experimental cross sections for the (n,p) reaction induced by 14.5 MeV neutrons and the predictions of theory. Similar difficulties have been encountered by Cohen et al. (1954) in attempting to interpret the measured cross sections for the (p,pn) reaction induced by 22 MeV protons. Discrepancies have also been noted by Gugelot (1954) and by Igo and Eisberg (1954) in the form of the energy spectra and angular distributions of inelastically scattered protons. The energy spectra contains more high energy protons than the statistical theory predicts; furthermore, the angular distribution of these protons is predominantly forward. Although some of these deviations might arise from the difficulties of interpretation in the continuum region discussed in section 1.3 (d), the character of the observed deviations is similar to that observed in nuclear reactions at high energies. However, it was not clear at what point the compound nucleus theory could be extended to include such direct interaction

effects.

An advance towards clarification of the situation was finally achieved when a detailed study of the scattering of neutrons of energies less than 3 MeV revealed striking disagreement with the smooth variation in cross sections predicted by continuum theory. It was observed that the total cross sections, averaged over resonances, exhibited a series of large scale maxima and minima as a function of the incident energy at positions which varied gradually from nucleus to nucleus (Barschall 1952). These features are inexplicable on a theory which assumes immediate absorption of the incident neutron. On the other hand, if the incident particle is assumed to move inside the nucleus with a weak interaction the observed maxima in the cross sections can be qualitatively understood. For certain values of the nuclear radius and neutron wavelength, standing waves can be set up inside the nucleus; in this event the penetration inside the nucleus and hence the interaction can be very great. Thus the nature of the results leads to the application of the optical model at low energies.

5(b) The Optical Model.

At low energies the effect of the nucleus on the incident nucleon can be described on the optical model by a complex potential,

$$V = V(r) + i\,W(r)$$

For the description to be physically realistic it is evidently necessary to restrict the potential to approximately the size of the target nucleus. The real part is a representation of the average potential energy to which the nucleon is subjected when passing through the nucleus; the imaginary

part indicates the strength of these processes which lead to energy exchange of the nucleon with the target nucleus.

Such a representation gives rise to a complex index of refraction of the nucleus as in the transparent nucleus model. Indeed, the parameters k_1 and K of the latter model are related to the real and imaginary potentials V and W by the equation

$$k + k_1 + \tfrac{1}{2} iK = k \left\{ 1 - \frac{V + iW}{E} \right\}^{\frac{1}{2}}$$

where k is the wave number corresponding to the energy E of the nucleon outside the nucleus. If W is small compared to V + E, it follows that:

$$\frac{k_1}{k} = \left(1 + \frac{V}{E} \right)^{\frac{1}{2}} - 1 \quad ,$$

$$\frac{K}{k} = \frac{W}{E\left(1 + \frac{V}{E}\right)^{\frac{1}{2}}}$$

In addition, since the absorption coefficient K is the reciprocal of the mean free path λ, the latter relation establishes a connection between W and λ; thus, a small imaginary potential implies a long mean free path of the incident nucleon in nuclear matter.

Although the parameters of the optical model at high and low energies are equivalent, the cross sections calculated on the transparent nucleus model areinvalid at low energies. It is only permissible to consider the scattering problem in terms of the passage of the incident nucleon through the nucleus at high energies. At low energies it is necessary to perform an exact phase shift analysis with proper concern for the boundary conditions at the surface of the nucleus (c.f. section 1.2). The analysis leads directly to expressions for the scattering cross sections in terms of

the real and imaginary potentials.

When the optical model was applied at low energies, it was found that the observed maxima and minima in the total cross sections could be reproduced accurately by employing a small value of the imaginary potential (Feshbach, Porter and Weisskopf 1953, 1954). Thus, the application of the model indicates that the incident nucleon experiences the weak interaction inside nuclear matter required to establish the validity of the optical description at low energies. In contrast to the assumption of immediate absorption which is the basis of the compound nucleus theory, the incident particle has a long mean free path in nuclear matter.

As the energy of the incident particle increases, analysis of the experimental results indicates that the value of the imaginary potential also increases (Woods and Saxon 1954). Since the imaginary potential corresponds to an increased absorption the position is similar to that considered on the compound nucleus theory. The optical model gives similar predictions to the continuum theory at intermediate energies. It can now be appreciated that the analysis of cross sections at intermediate energies did not lead to a clear distinction in favour of either model. However, even at intermediate energies the optical model predicts that the incident nucleon has a finite mean free path in nuclear matter; in consequence, further examination of the compound nucleus description would appear to be necessary.

5(c) Implications of the Optical Model

The optical model only provides an empirical description of the cross sections for elastic scattering and absorption (reaction) of the incident

nucleon. A description of the detailed cross sections requires the additional assumption that absorption on the optical model leads to the formation of a compound nucleus; then the formalism developed in section 1.3(c) could be carried over within the framework of the optical description of the interaction. The assumption appears valid at low energies, since the existence of resonances implies that absorption of the incident nucleon, although occurring with reduced probability, does lead to the formation of a compound nucleus. Furthermore, in view of the success of statistical theory it would appear that the majority of absorption processes again lead to compound nucleus formation at intermediate energies.

Nevertheless, it is consistent with the model that absorption does not always proceed in this way. Thus it may be possible to consider the course of a nuclear reaction on an extended basis and in particular to interpret the conflicting experimental results regarding the yield and products of nuclear reactions discussed in section 1.5(a). As has been suggested there, the products of a nuclear reaction may be separated into those emitted by direct collision processes and those emitted from the decay of a compound nucleus. Thus it would appear that direct interaction could be included as an absorption process on the optical model. However, if more than an empirical description is to be obtained it is necessary to specify the absorption process. In this respect, the optical description itself appears to provide the framework within which the compound nucleus and direct interaction aspects of a nuclear reaction at intermediate energies may be reconciled.

The optical model has indicated a reduced interaction of the incident

nucleon inside the nucleus. Thus the possibility exists that a particle may be emitted as a result of the direct collision of the incident particle with an individual nucleon inside the nucleus. On this basis the compound nucleus is only formed if the individual nucleons are absorbed before reaching the surface of the nucleus. Such a distinction between the two stages of a nuclear reaction is obviously analogous to that considered at high energies. Thus it would appear desirable to further study the nuclear reaction at intermediate energy to determine whether the occurrence of direct interaction should be recognised as a distinctive feature of nuclear reactions at these energies. In chapter 4, a study of the protons emitted in the reaction $Fe^{56}(n,p)\,Mn^{56}$ is reported.

Furthermore, a better understanding of the mechanism of energy transfer inside the nucleus is required in order to provide more than a qualitative description of the interaction. In chapter 5, an account is given of an attempt to establish the scattering of nucleons of low and intermediate energies by nuclei as a result of the collisions with individual nucleons inside the nucleus.

CHAPTER 2

Photographic Emulsion Technique.

Nuclear emulsions are photographic emulsions of very high silver concentration thickly coated on glass backings. Ionising particles which pass through the photographic emulsions alter a number of the silver bromide crystals in their path such that upon development they appear as microscopic rows of black grains of colloidal silver.

At the present time there is available commercially a range of nuclear emulsions of various sensitivities which will record tracks of charged particles of any energy. To appreciate this variation in sensitivity, it is necessary to consider the variation of ionisation with the velocity of a charged particle. The ionisation produced by a particle moving through matter decreases with increasing velocity, reaching a minimum value at a velocity corresponding to a kinetic energy of approximately twice the rest mass of the particle. This minimum occurs for electrons of energy about 1 MeV and for protons about 2,000 MeV. At higher energies the increase in ionisation is very gradual, amounting for electrons to a factor of only two in the range of 10^6 to 10^{10} eV of particle energy. The most sensitive emulsion (Ilford G.5) is, therefore, one in which a sufficient number of grains are rendered developable when the rate of loss of energy corresponds to this minimum value. Such sensitivity has been achieved by increasing the grain size and improving the sensitization process.

The use of nuclear emulsions in research involves three general stages:

(a) the exposure of the plates;

(b) the processing of the plates;

(c) the microscope examination of the plates.

Exposure

In general a photographic plate can be used either as a detector of charged particles produced in some reaction which takes place external to the emulsion, or of those produced in a reaction which takes place in a constituent of the emulsion itself. The nature and energy of the particles can then be determined from measurements performed on their tracks.

The application of photographic emulsion in each of these ways will be illustrated in the following chapters.

Processing

In contrast to the processing of ordinary photographic plates, the length of time required for the penetration of the various solutions through thick emulsions ($\sim$ 100 microns) entails the use of much more elaborate techniques. If development occurs while the developing solution penetrates the emulsion, the time taken for penetration would result in unequal development along the length of a track traversing from the surface of the emulsion to the glass. To overcome this difficulty Dilworth, Occhialini, and Payne (1948) devised the method of 'temperature development'. To facilitate penetration the plates are presoaked in cold distilled water. The emulsion is then placed in developer at a temperature sufficiently low (a few degrees Centigrade) to inhibit its action

until it has permeated the entire emulsion. Development is allowed to take place at a higher temperature, the emulsion being protected from the action of fresh developer at this stage. In the normal procedure, the plate is removed from the developer, and raised to a temperature between 25° and 30°C. Development is stopped by immersion in an acid stop bath. The degree of development can be varied as required by the concentration of the developing solution used, and the duration and temperature of the hot stage.

The fixing process is usually carried out at a temperature of 5° to 10° C, the time of fixing depending on the thickness of the emulsion involved. The washing of the emulsion after fixation consists of slow dilution of the hypo until all traces of hypo have been removed. When dry, the emulsion is ready for examination under the microscope.

Owing to the high concentration of silver bromide in nuclear emulsions when the ususued silver is removed after fixation, a considerable reduction in their thickness occurs. A determination of the ratio of the thickness of emulsion before and after processing, the shrinkage factor, allows a correction to be made to the length of track measured under the microscope to obtain that in the unprocessed emulsion. For plates at normal room humidity, the shrinkage factor is approximately 2.4 - 2.6 for Ilford C.2 and G.5 emulsions.

Microscope Examination

Observations can be made on the following characteristics of the track:-

(a) the residual range

(b) the multiple coulomb scattering

(c) the ionisation (grain density or delta rays).

For an emulsion of a given composition the residual range and the magnitude of the coulomb scattering of particles with the same mass, velocity and charge are always the same within the limits imposed by statistical deviations. These two properties may, therefore, be regarded as 'constants' of a nuclear emulsion of a given type and be related to its atomic composition. In appendix 1 is described a determination of the range-energy relationships for protons and alpha particles in diluted G5 emulsions.

The grain density produced by a charged particle depends on the rate of energy loss of the particle in the emulsion in a way that varies not only with the type of emulsion but also with the conditions of processing. There is proportionality, however, between the rate of energy loss and the grain density, provided that the rate of energy loss is less than the value at which saturation of the grain density occurs (Fowler and Perkins 1951). In the region of proportionality a direct calibration can be carried out which allows an interpretation of grain density measurements to be made.

The range, scattering and ionisation of a particle track are all related to the charge, rest mass and velocity of the particle; since the charge of the particle is usually apparent, a determination of two of these three parameters will define the nature and energy of the particle.

CHAPTER 3

The Interaction of Protons of 130 Me V with the Nuclei of the Photographic Emulsion.

Section 3.1: Introduction.

When high energy particles pass through matter nuclear reactions and elastic scattering occur. In principle, the total cross section can be obtained by measuring the attenuation of the beam of particles by the target under investigation with the detector placed in 'good' geometry; the inelastic or reaction cross section with the detector in 'bad' geometry. When the incident particle is a neutron, however, the measured reaction cross section will only be a lower limit since the threshold energy of available detectors may be insufficiently high to exclude all inelastically scattered neutrons. Most of the neutron experiments, therefore, have been designed to measure the total cross section (c.f. references given in Nedzel 1954). When the incident particle is a proton, it is in theory possible to determine the reaction cross section accurately by using absorbers to select only those protons transmitted or elastically scattered by the target. The experiments with protons, however, suffer the disadvantages of multiple scattering and energy loss in the target resulting from the Coulomb field. Moreover, at small angles the Rutherford scattering interferes with the diffraction scattering making a determination of the total cross section very difficult. For these reasons comparatively few cross section determinations have been carried out with high energy protons and of these, most have been designed to

measure the reaction cross section (c.f. references given in Chen et al. 1955).

The study of the nuclear interactions produced in photographic emulsion by high energy protons has several advantages over the attenuation experiments. In the nuclear emulsion a nuclear reaction can be easily recognised. For such events either a nuclear disintegration or star is produced or the incident proton loses energy in an inelastic process. For elastic scattering there is no appreciable change in energy and therefore the grain density of the proton track is almost the same before and after each scattering event. This enables the elastic scattering to be separated from the nuclear reactions produced in the emulsion. The determination of the reaction cross section can, therefore, be carried out by actual observation of the inelastic events. Furthermore, the characteristics of the charged particles emitted in the reaction can be observed at the same time and information thereby obtained on the nature of the processes leading to the disintegration of nuclei at high energies.

The photographic plate, however, has the disadvantage that it has more than one constituent element. This disadvantage can be partially removed by a classification of the observed disintegrations into two main groups: those produced in the light nuclei (carbon, nitrogen and oxygen) and those produced in the heavy nuclei (silver and bromide) of the emulsion.

In this chapter the interaction of 130 Me V protons with the nuclei of the photographic emulsion is investigated. In section 3.2 methods are

described whereby the stars are separated into those produced in the light and heavy nuclei of the emulsion and the separate interaction cross sections are determined. The values obtained permit an investigation of the applicability of the transparent nucleus theory to the prediction of the interaction cross sections for protons. In section 3.3, the characteristics of the observed nuclear disintegrations are examined and compared with those expected on the assumption that the incident proton interacts directly with individual nucleons inside the struck nucleus.

Section 3.2: Determination of Cross Sections.

2(a) Experimental Procedure.

Ilford normal and x4 diluted G5 plates were exposed to the external proton beam of the Harwell cyclotron. The G5 x4 emulsion is an electron sensitive emulsion which contains a much smaller ratio of silver halide to gelatin than the normal G5 emulsion (c.f. Appendix 1). The energy of the protons entering the plate assembly was 146 ± 3 Me V. After allowing for energy loss by ionisation in the plates, the protons producing the stars were shown by grain counting to have energies between 110 and 146 Me V.

The search for stars was carried out both by 'along the track' and 'area' scanning methods (Bernardini et al. 1952). A proton-induced star with n secondary charged prongs will be referred to as an np star. During the examination of the plates all scatterings of the type 1p were rejected in which the ionisation of the secondary particle was not statistically greater than the ionisation of the primary proton, since elastic

scatterings appear as events of this type. With this criterion, 251 and 122 stars were found by the 'along the track' method in the normal and diluted emulsion, corresponding to a total length of proton path of 8460 and 7290 cm. respectively. Before the true mean free paths can be calculated, however, the observed number of stars must be corrected for two factors:

(a) A fast proton can undergo collisions with free hydrogen in the emulsion which gives rise to events of the type 2p. The contribution of free proton proton collisions to be subtracted from the observed number of 2p events was estimated from the known values of the cross section for p-p collisions (Christain 1952).

(b) By rejecting all 1p events in which no change of ionisation is observed some genuine inelastic collisions were excluded. The lower limit of the energy loss that could be detected by grain counting on the incident and scattered track was about 25 Me V. This figure corresponds to around the maximum energy which can be transferred to the nucleus in an inelastic collision without giving rise to a slow charged secondary (Tiomno and Wheeler 1949, Fry 1952). Thus a 1p type of event can occur which is rejected owing to the criterion for selection of stars. If the fast secondary particle is a neutron, then a 0p star which has no secondary charged prongs is produced. The event can be unambiguously recognised since the track of the incident proton suddenly ends at the point of interaction. The number of genuine 1p stars rejected can therefore be estimated from

the observed number of 0p stars. From the known free p-p and n-p scattering cross sections the ratio of the number of stars with a single secondary proton of high energy to the number of stars with a secondary neutron of high energy was calculated to be 2.5. Therefore 2.5 times the number of 0p stars observed was added to the 1p star accepted in the original measurements.

After making these corrections, the mean free paths for star production in normal and x4 diluted emulsions were found to be $32.6^{+2.5}_{-2.0}$ and 54^{+6}_{-5} cm. respectively (the errors quoted throughout are the standard deviations).

2(b) Separation of Stars.

Prong Distribution in Normal and Diluted Emulsions

The measurement of the mean free paths in normal and diluted emulsion allows a statistical separation of the stars into those produced in light and heavy components. The mean free path, λ_n, for the production of a star with n prongs is related to the cross section for production by the equation:

$$N_H \sigma_{H_n} + N_L \sigma_{L_n} = \frac{1}{\lambda_n} \quad \ldots\ldots\ldots (1.1)$$

where N_H = number of silver and bromine atoms per cm^3 in the emulsion ($N_H = 2.06 \times 10^{22}$ and 0.92×10^{22} atoms per cm^3 for normal and x 4 diluted emulsions respectively), N_L = number of carbon, nitrogen and oxygen atoms per cm^3 ($N_L = 2.69 \times 10^{22}$ and 4.33×10^{22} atoms per cm^3 for normal and x 4 diluted emulsions respectively), σ_{H_n} = mean cross section for the

production of a star with n prongs in silver and bromine nuclei, and σ_{I_n} = the corresponding cross section for carbon, nitrogen and oxygen nuclei.

This if λ_n is known, the cross section σ_{H_n} and σ_{I_n} may be derived by applying the above equation to normal and x 4 emulsions. The total cross section for star production in light and heavy nuclei may be obtained in a similar fashion.

In order to improve the statistics for the prong distribution, data on stars found by area scanning was added to that obtained by along the track scanning. It was found that although the mean free path obtained from area scanning was longer by a factor of 1.5 than that obtained from along the track scanning, the relative prong distributions were identical for stars other than of the Op type. This result can be attributed to the difficulty of properly overlapping scans, when using high power objectives with very small fields of view, and has been observed by other workers (Bernardini et al., loc. cit.) The data obtained from area scanning was normalised to the overall mean free path obtained by along the track scanning for all stars other than of the type Op. The frequency distribution of prong size for stars produced by 130 Me V protons in normal and x 4 emulsion is given in figure 3.1. The number of stars with n prongs is given in terms of the parameter $1/\lambda_n$. Using these values for $1/\lambda_n$, σ_{H_n}, and σ_{I_n} were calculated. The results are shown in table 3.1; it can be seen that σ_{I_n} only becomes larger than σ_{H_n} for 5 and 6 prong stars and that for all practical purposes the 1, 2 and 3p

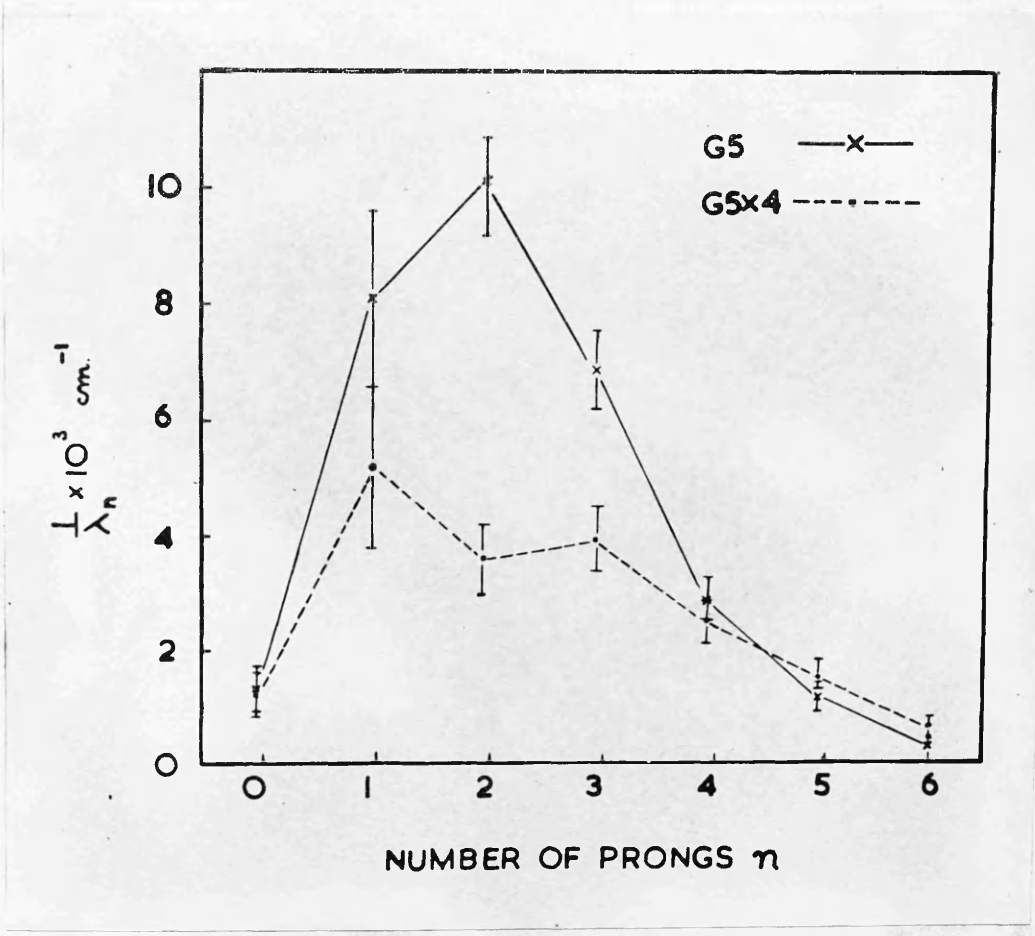

Figure 3.1: The frequency distribution of prong size for stars produced by 130 MeV protons in normal and x 4 emulsions.

Table 3.1: Cross Sections determined for heavy and light nuclei

Type of Star	σ_{H_n} ($\times 10^{26}$ cm^2)	σ_{L_n} ($\times 10^{26}$ cm^2)
0	4 ± 3	2 ± 1.5
1	32 ± 12	5 ± 5
2	53 ± 7	$-(3 \pm 4)$
3	30 ± 5	3 ± 2
4	9 ± 3	4 ± 1.5
5	1 ± 2	3.5 ± 1
6	$-(1 \pm 1)$	1.5 ± 0.5

stars are all produced in heavy nuclei.

The overall cross sections obtained for star production were found to be (128 ± 16) x 10^{-26} cm^2 in heavy nuclei, and (16 ± 7) x 10^{-26} cm^2 in light nuclei.

Alpha-particle method.

A separation of stars into those produced in the light and heavy constituents of the emulsion can also be carried out from an examination of the α- particles appearing from the stars. Considerable work has been performed on the numbers of α- particles which emerge from stars formed by the cosmic radiation. It has been found that the ratio of α-particles to all tracks of energy less that 30 Me V is 0.27 for silver and bromine nuclei and 0.5 for gelatin nuclei (Rochester and Rosser 1951). The numbers and energies of the α-particle tracks appearing from stars initiated by 130 Me V protons in normal emulsions was examined. The energy of the α-particles was determined by range measurements.

In this analysis an α-particle was given the overall definition of a particle whose track has a range greater than 5 microns, and whose charge was 2e. The differentiation between α-particles and singly charged particles was carried out from the characteristics of protons and alpha particles at the end of their ranges. To facilitate their identification, plates exposed to protons and α-particles were permanently set up while the analysis was being carried out.

The ratio of the number of α-particle tracks to total number of prongs as a function of the latter figure is given in figure 3.2. The

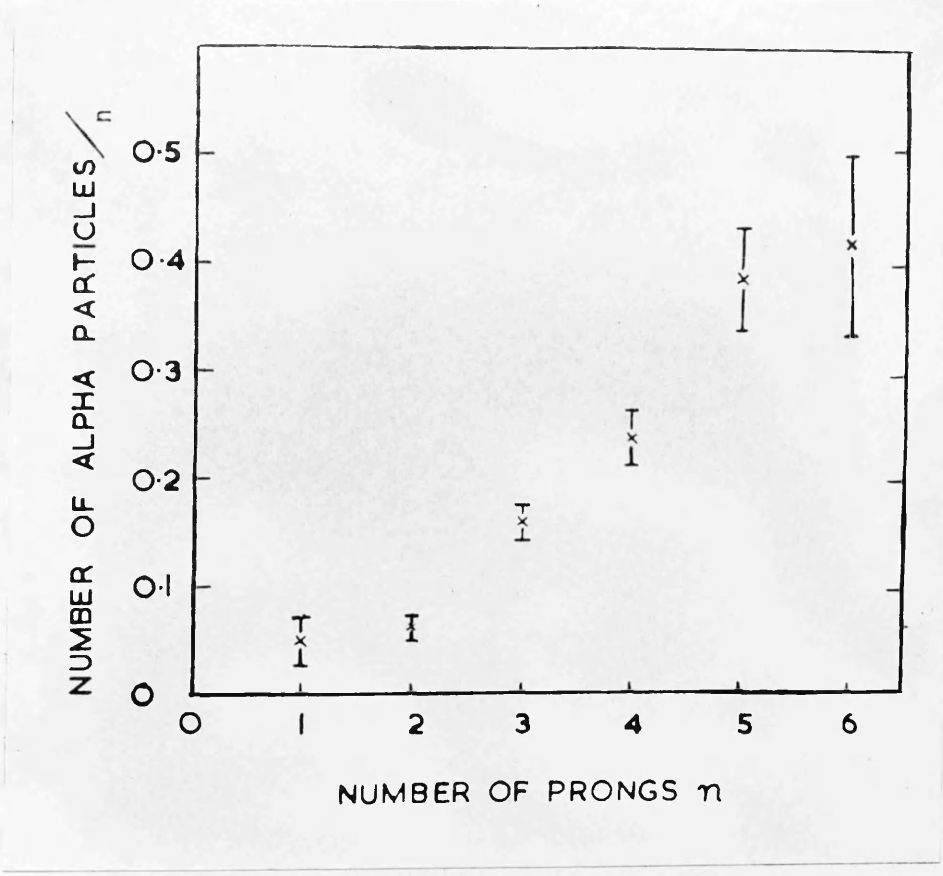

Figure 3.2: The ratio of the number of α-particle tracks to total number of prongs as a function of the total number of prongs for stars produced by 130 MeV protons.

The ratio steadily increases with the number of prongs associated with a star and appears to flatten at the value of about 0.4 for 5 and 6p stars. The energy distributions of α-particles also shows a difference for 1, 2 and 3p stars compared with 5 and 6p stars. This is illustrated in figure 3.3.

The data presented in figures 3.2 and 3.3 support the conclusion regarding 5 and 6p stars, namely, that they are mainly formed by the disintegration of the light gelatin nuclei. The peak in the energy distribution in the region of 4 Me V for 5 and 6p stars is consistent with the low potential barrier confronting the α-particles in light nuclei, while the value of 0.4 for the ratio of α-particles to total prong number for 5 and 6p stars is in good agreement with that found for stars formed by the cosmic radiation in pure gelatin.

In the 1, 2 and 3p stars the ratio of α-particles to total prong number is considerably lower than that found in stars formed in silver and bromine nuclei by the cosmic radiation. This result will be interpreted in the next section in terms of protons directly knocked on in collisions produced by the primary particle. The cosmic ray stars involve much greater excitation of the nucleus than that produced by 130 Me V protons so that most of the particles ejected with energy < 30 Me V are evaporation particles. The peak in the region of 12 Me V for the energy distribution of α-particles emitted in 1, 2 and 3p stars is consistent with the high potential barrier presented to α-particles by silver and bromine nuclei. Thus the data obtained on the 1, 2 and 3p stars again supports the

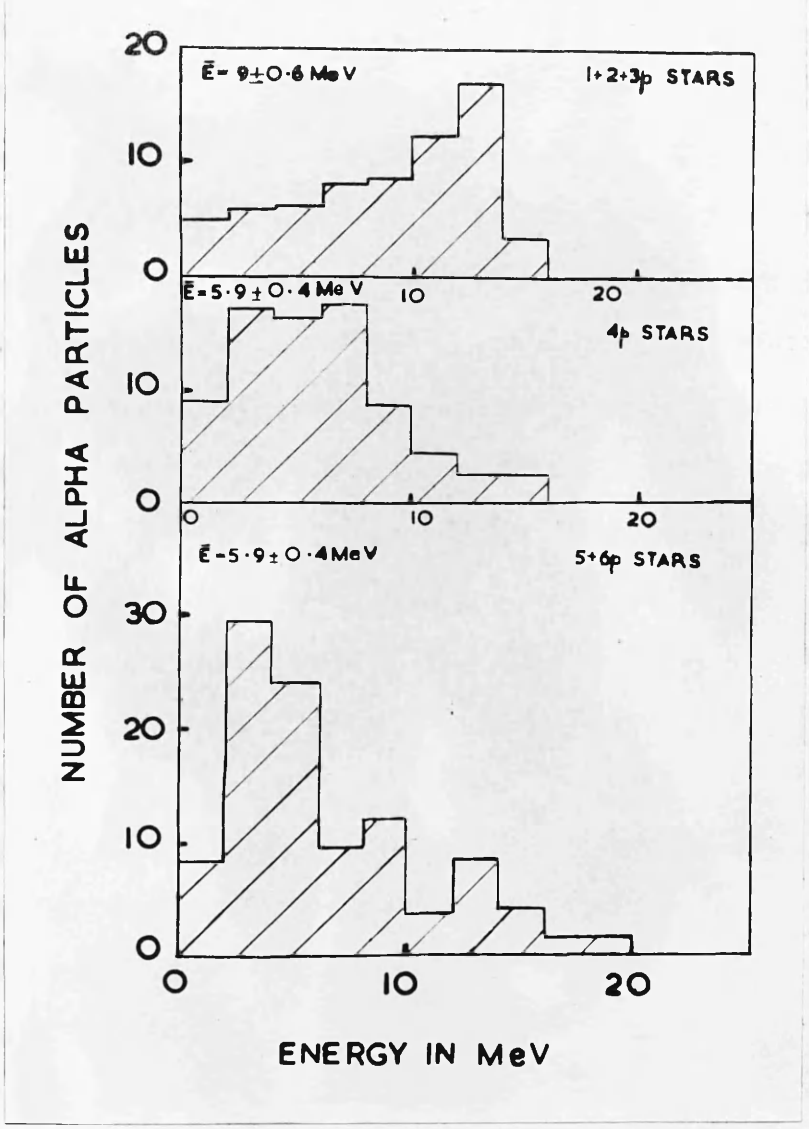

Figure 3.3: The energy distributions of α-particles emitted in stars produced by 130 MeV protons.

conclusion reached previously.

A rough cross section for star production in light nuclei was estimated by assuming that all the 5 and 6p stars, and all the other stars with at least one α-particle of kinetic energy less than 9 Me V were produced in carbon, nitrogen or oxygen (Menon et al. 1950). This yielded a value of about 15×10^{-26} cm^2 for the total cross section for star production in light nuclei. This method possesses certain limitations. Occasionally a light nucleus will disintegrate and emit no α-particle; on the other hand some α-particles of low energy may occasionally penetrate the Coulomb barrier in the disintegration of a heavy nucleus. Although these two effects might be expected to cancel in the above estimate, nevertheless the value obtained can only be considered approximate.

2(c) Discussion.

The cross sections for star production in the light and heavy nuclei.

Since the completion of the work reported here, Cassels and Lawson (1954) have extended the measurement of the reaction cross sections to a number of elements by a study of the attenuation of 134 Me V protons. The mean cross sections for nuclear interaction in the light and heavy nuclei of the photographic emulsion (within the limits of their large experimental error) are in agreement with those obtained from an interpolation of the results of Cassels and Lawson over the elements of the periodic table.

Although the comparison of stars in normal and x 4. diluted emulsions allows a statistical separation of the stars produced in the light and heavy

nuclei to be made, it does not show the characteristics of the individual stars. Nevertheless, it can be concluded that 130 Me V protons produce larger stars in light nuclei than in heavy nuclei. Furthermore, the individual stars formed in the light nuclei may be recognised in many cases by the high ratio of the number of α-particles to the total number of prongs and by the low energy of the α-particles emitted.

Interpretation of the cross sections on the Transparent Nucleus Model.

The measured cross section for star production in the light and heavy nuclei can be compared with the predictions of the transparent nucleus theory (Fernbach et al. 1949). In this theory the cross section for a nuclear reaction at high energy has the following form (c.f. section 1.4)

$$\sigma_r = \pi R^2 \left[1 - \left\{ 1 - (1 + 2KR) e^{-2KR} \right\} \frac{1}{2K^2R^2} \right] \quad \ldots\ldots (3.2)$$

where R = nuclear radius, K = absorption coefficient. The absorption coefficient K can also be related to the nuclear radius R by the expression

$$K = \frac{3A}{4R^3} \times \bar{\sigma} \quad , \quad \ldots\ldots\ldots (3.3)$$

where $\bar{\sigma}$ is the average proton nucleon cross section inside the nucleus $\bar{\sigma}$ can be written in terms of σ_{pp} and σ_{pn}, the free proton-proton and proton-neutron cross sections respectively:

$$\bar{\sigma} = \frac{[Z\sigma_{pp} + (A - Z)\sigma_{pn}]\alpha}{A} \quad , \quad \ldots\ldots (3.4)$$

where α is a reduction factor to allow for the effect of the Pauli Exclusion Principle.

The quantities σ_{pn} and σ_{pp} have been measured (Christian 1952, Pickavance and Cassels 1952) and α may be calculated by assuming a Fermi gas model of the nucleus (Goldberger 1948). Hence a value of $\bar{\sigma}$ can be obtained and equation 3.3 may be used to express the absorption coefficient K in terms of the nuclear radius R. Since the cross section is uniquely determined by these two parameters, the measured values of σ_r in a particular experiment can be used to derive values of R and hence K.

The following values of the radii in the light and heavy nuclei, R_L and R_H respectively, have been derived in this way:

$$R_L = (2.6 \pm 0.7) \times 10^{-13} \quad \text{and} \quad R_H = (6.9 \pm 0.6) \times 10^{-13} \text{cm} .$$

The error in R does not include the uncertainty in $\bar{\sigma}$ arising from the experimental uncertainties in σ_{pp} and σ_{pn}. An interpretation of these radii in terms of the relationship, $R = r_o A^{\frac{1}{3}}$, which assumes a constant nuclear density, leads to values for r_o of $(1.1 \pm 0.3) \times 10^{-13}$ and $(1.5 \pm 0.1_5) \times 10^{-13}$cm. for the light (A = 14) and heavy nuclei (A = 94) respectively. This difference cannot be considered significant. The values are consistent with a value of $\sim 1.4 \times 10^{-13}$cm deduced from the analysis of neutron and proton scattering at high energies (Taylor 1953, Chen et al. 1955). However, the large uncertainties in the measured values of σ_r do not permit an accurate determination of the parameters of the transparent nucleus model to be made in this experiment.

It is also of interest to derive the cross sections for star production from the mean free path observed in normal G5 emulsion. In this way any uncertainty associated with the scanning of diluted emulsion

should be avoided. The method is due to Perry (1952) who has shown that K and hence σ_r can be obtained from a single measurement of λ (the total mean free path for star production in any emulsion) if the correctness of equation 3.2 is assumed. His method is equivalent to inserting the expression for σ_r in equation 3.2 into equation 3.1, giving:

$$\sum_i N_i \pi R_i^2 \left[1 - \left\{1 - (1 + 2KR_i)\, e^{-2KR_i}\right\} \frac{1}{2K^2 R_i^2}\right] = \frac{1}{\lambda}, \quad \ldots\ldots (3.5)$$

where the subscripts i refer to the atomic constitution of the emulsion. Since both N_i and λ are known in this equation, K may be obtained if a suitable figure for the nuclear radius is assumed.

In table 3.2 the value of K obtained from equation 3.5 applied for the case of normal G5 emulsion is compared with that expected from the free particle cross sections (equations 3.3 and 3.4). Values of R equal to $1.37\, A^{\frac{1}{3}} \times 10^{-13}$cm and $1.47\, A^{\frac{1}{3}} \times 10^{-13}$cm were assumed. In addition to the comparison at 130 Me V, the values of K expected from equations 3.3 and 3.4 are also compared with those obtained from the published values of λ at 220 Me V (Perry 1952) and 375 Me V (Bernardini et al. 1952). All these results are again consistent with the transparent nucleus model without permitting the nuclear radius to be chosen uniquely.

In table 3.3 the values of the cross sections determined for star production in the light and heavy nuclei are compared with those obtained by substitution of K from table 3.2, column 3, into equation 3.2. The cross section σ_H and σ_L obtained by the two methods are in satisfactory agreement indicating that equation 3.2 is reasonably accurate for both

Table 3.2: Comparison of the absorption coefficient K

Nuclear Radius $\times 10^{-13}$ cm	Energy of Protons in MeV	K $\times 10^{-12}$ cm^{-1}	
		Transparent Nucleus	Expected from Eqns. 3.3 & 3.4
$1.37A^{1/3}$	130	$2.9 \pm \begin{matrix}0.8\\0.4\end{matrix}$	2.6
	220	$2.9 \pm \begin{matrix}0.8\\0.4\end{matrix}$	2.5
	375	$1.7 \pm \begin{matrix}1.2\\0.5\end{matrix}$	2.4
$1.47A^{1/3}$	130	$2.0 \pm \begin{matrix}0.4\\0.3\end{matrix}$	2.1
	220	$1.9 \pm \begin{matrix}0.3\\0.3\end{matrix}$	2.0
	375	$1.1 \pm \begin{matrix}0.7\\0.3\end{matrix}$	1.9

Table 3.3: Comparison of inelastic cross sections in light and heavy nuclei.

Cross sections $\times 10^{26}$ cm^2	σ_H	σ_L
Measured	128 ± 16	16 ± 7
Transparent $R = 1.37A^{1/3} \times 10^{-13}$ cm	$110 \pm \begin{matrix}5\\4\end{matrix}$	$25 \pm \begin{matrix}3\\2\end{matrix}$
nucleus theory $R = 1.47A^{1/3} \times 10^{-13}$ cm	$111 \pm \begin{matrix}6\\5\end{matrix}$	$23 \pm \begin{matrix}2\\2\end{matrix}$

heavy and light constituents of the emulsion.

Section 3.3: The Nature of the Disintegrations.

3(a) Experimental Analysis.

The analysis of the charged products of the nuclear disintegration was carried out for events produced in normal G5 emulsions. The experimental results were based on stars obtained by area scanning. The analysis determined the nature, energy and angle with respect to the incident proton of all charged particles emitted in the star.

The differentiation between protons and α-particles which come to the end of their range in the emulsion was carried out as described in the previous section. In addition further examination and measurements were carried out in underdeveloped plates which facilitated the separation of protons and α-particles. It was impossible to separate particles of single charge into protons, deuterons and tritons; in the analysis all singly charged particles were classified as protons. The probability of 'pick-up' processes leading to deuteron and triton emission is expected to be small. The range and projected angle of emission of the proton tracks ending in the emulsion were measured. The energies of the protons were determined from the range in G5 emulsion.

For protons of high energy, the true angle of emission relative to the direction of the incident proton was determined from measurements of the horizontal projected angle and the angles of dip of the two particles. In general, however, such protons left the emulsion before coming to the end of their range. Nevertheless, the energy of the proton could be

determined from the grain density of the track. The energy of the incident proton could also be determined from a similar measurement and only those fast particles emitted from stars produced by protons of energy greater than 130 Me V were considered for analysis.

The relation between the grain density of a track and the energy of the particle depends on the type of emulsion and the conditions of processing (c.f. chapter 2). The ionisation of a particle increases as the energy decreases. For a normally developed G5 emulsion the energy of the protons greater than 55 Me V can be determined by grain counting. The grain density of a proton of 55 Me V energy is about six times the grain density at minimum ionisation. For protons of energy less than 55 Me V the error in estimating the grain density becomes considerable, especially for tracks at an angle to the horizontal plane. In addition to this, the curve of grain density versus specific energy loss shows saturation as the energy loss increases, so that the relation between the energy and the grain density becomes unreliable when applied to protons of energy less than approximately 50 Me V.

The normally developed G5 emulsions had been previously calibrated for protons in the energy region 150 to 50 Me V (Bosley and Muirhead 1952). A plot of the logarithm of the ratio of their grain density to that at minimum ionisation against the logarithm of the corresponding proton energy had been found to be linear. As no variation of grain density with depth in emulsion was found in the plates examined, the energies of the protons greater than 50 Me V could be determined from this curve.

Some of the G5 emulsions were underdeveloped so that the determination of energy by grain counting could be extended to lower energies. For these emulsions it was found that there was a variation of the grain density of a track with depth in the emulsion. It was therefore necessary to determine the grain density v energy relationship for proton tracks at different depths in the emulsion. Curves of grain density v depth for protons of particular energies up to 65 MeV were obtained from measurements on tracks of residual range up to 1.5 cm. The grain densities of the tracks of primary protons coming from the surface were also determined at different depths in the emulsion. From these results were derived the calibration curves of grain density v energy at different depths in the emulsion. The energies of protons as low as 30 MeV could be obtained as a result of the examination of the underdeveloped emulsion.

3(b) Calculation of the Nuclear Interaction of 140 MeV Protons.

The Goldberger Model of the Nuclear Interaction

It has been suggested that the emission of particles in anuclear reaction at high energies can be considered to take place in two stages (Serber 1947, Goldberger 1949). There is a certain probability that a nucleon will escape directly following the first and subsequent collisions of the incident nucleon inside the nucleus. The end of the first stage or 'cascade stage' of the reaction comes when all individual nucleons have lost sufficient energy in their collisions to be absorbed in the nucleus leaving it in an excited state. The emission of particles from the excited nucleus constitutes the second stage of the reaction. Such a

description will be referred to as the Goldberger model.

It is of interest to obtain evidence for the relative importance of these processes from the observed characteristics of the nuclear disintegrations in the emulsion. As a result of the preceding analysis the charged particles emitted in the nuclear disintegrations could be grouped into regions of energy and angle. In the first instance, however, the character of the individual events was examined.

In general it was found that a nuclear disintegration was characterised by the emission of a charged particle of high energy and several charged particles of much lower energy. In addition, it was observed that particular events could perhaps be considered as examples of a single collision of the incident proton with a nucleon inside the nucleus. The energies of the incident and outgoing proton, E_{in} and E_{out} respectively, and the angle, θ, between the two protons approximately satisfied the relation, $E_{out} = E_{in} \cos^2\theta$ which would hold for a non-relativistic collision between the incident proton and a free nucleon at rest. The momentum distribution of the struck nucleon inside the nucleus and the possibility of subsequent scattering of the outgoing proton inside the nucleus, however, remove the restriction imposed by energy and momentum conservation in collisions between free nucleons. These two effects limited an assessment of the importance of two body collisions from the analysis of single events.

In order to obtain statistical evidence of the occurrence of such collisions between individual particles inside the nucleus it was necessary to have some detailed predictions based on this description to compare with

the experimental results. A complete analytical description of the development of a nucleon cascade had not so far proved feasible. Calculation of the result of the first and second collision has been carried out analytically but the method becomes tedious for higher order collisions (Mandl and Skyrme 1952). This means, in particular that the method is unable to predict the energy left in the excited nucleus at the end of the cascade process. Goldberger, however, suggested that numerical results could be obtained by considering the passage of sufficient number of nucleons through the nucleus and allowing the position and nature of the collisions to be determined by the law of chance - the Monte Carto method (Ulam and Neumann 1947).

The approach to the problem is essentially classical, since the particles are considered to possess a definite trajectory inside the nucleus. One follows in detail, collision by collision, their passage through the nucleus. Whenever it is necessary to make a choice of a number of equally probable events the choice is made by a random process. For a sufficiently large number of calculations it would be possible to obtain an exact solution to the problem. However, it can be shown that the distribution curves obtained as a result of N calculations should possess the same inherent statistical fluctuations as one obtains for results based on N experimentally observed events.

While this work was in progress, the Goldberger model was shown to be satisfactory for describing the stars produced by 400 Me V protons in photographic emulsions (Bernardini et al. 1952). However, it was of

increased interest to compare the predictions of the model with the experimental results of the analysis of the disintegrations produced by protons of lower energy since the validity of the assumptions made in the calculation may then be in doubt.

The Method of the Monte Carlo Calculation.

The calculations were carried out for a heavy nucleus (Z = 41, A = 94), and a light nucleus (Z = 7, A = 14). The nuclear radius was taken as $1.42 \times 10^{-13} A^{\frac{1}{3}}$ cm., a value intermediate between those assumed in section 3.2. One hundred primary protons were followed in each case.

A Fermi gas model was used for the nucleons inside the nucleus; their maximum energy was taken as 22 Me V. The binding energy of the nucleons was taken as 8 Me V, making the depth of the potential well equal to 30 Me V. It was assumed that a 140 Me V incident proton gained a kinetic energy of 30 Me V on entering the nucleus.

In making the calculation a two dimensional geometry was used in which the spherical nucleus was replaced by a circle of nuclear radius. Ten 'locations' of the incident protons on the nucleus were chosen by dividing half the circle by a series of chords parallel to the incident direction and an equal distance apart. For convenience, only half a circle was used since the final distributions must be symmetrical about the incident direction. The three dimensional nature of the first collision was preserved by choosing the number of particles incident on each location to be proportional to the area of the ring presented normal to the beam by the actual nucleus.

The position of the first collision was determined from the following distribution law

$$p = e^{-x/\lambda}$$

where p is the probability of penetrating a distance x from the surface without suffering a collision and λ is the mean free path for free nucleon nucleon collision (that is, neglecting the Pauli Principle). Collisions with protons and neutrons were considered separately. The path lengths were found from the relation $x_n = \lambda \log \frac{1}{p_n}$, where p_n is a number between 0 and 1 selected at random and designates which of the N equally likely intervals is the site of a collision. It was obtained from the relation $p_n = \frac{n}{N}$ by selecting random numbers (0 - N) for n.

The value of the momentum of the struck nucleon was selected at random. Allowance was made for the spherical symmetry of the momentum distribution of the nucleons inside the nucleus in choosing the direction of the struck nucleon in the representative two dimensional geometry. The kinetic relations in the centre of mass system were next calculated from the momenta of the colliding nucleons. The directions and energies of the scattered nucleons were then obtained from a random choice of the scattering angles of the two nucleons in the centre of mass system. The variation of the angular distribution of the nucleon nucleon scattering was taken into account in the division of the scattering angles into intervals of equal probability.

The above procedure which determined the result of the first collision was repeated for all the individual nucleons set in motion during the

cascade. It was assumed that at all energies only single nucleon nucleon collisions took place and therefore at all energies the free particle cross sections were used. In determining the position of the subsequent collisions, allowance was made for the variation of the free nucleon nucleon scattering cross sections with energy. In determining the result of each encounter, the variation of the angular distribution of the nucleon nucleon scattering in the centre of mass with energy was taken into account. If either particle had an energy less that 22 Me V after a collision, the collision was assumed forbidden by the Pauli Exclusion Principle and the particle passed on undisturbed to the next location.

The development of the cascade was plotted on a diagram representing the nucleus in two dimensions. The cascade was followed until the nucleons reached the nuclear surface or were absorbed. Reflection at the surface was neglected. A value of 6 Me V, which is smaller than the accepted value of 8-9 Me V, was used for the Coulomb potential barrier for protons in the heavy nucleus. This value was chosen to allow for some Gamow penetration of the barrier. If after a collision the energy of the proton inside the heavy nucleus was less than 36 Me V, or 30 Me V in the case of a neutron, it was assumed that the particle was absorbed, leaving the nucleus in an excited state. The excitation energy U of the nucleus following the cascade is given by

$$U = \left[140 - \sum_{i=1}^{N} E_i - 8\,(n-1) \right] \text{ Me V}, \quad \ldots\ldots \quad (3.6)$$

where E_i is the energy of the knock-on nucleon outside the nucleus

(obtained by subtracting 30 Me V from the energy of the particle as it left the nucleus) and N is the total number of knock-on nucleons emerging from the nucleus. The calculations were not extended to nucleons with energies below 60 Me V inside the light nucleus (section 3.3c)

As a result of the calculations the cross sections for nuclear disintegrations produced by 140 Me V protons in the light and heavy nuclei were determined. The number, energy and angle of the products of the disintegration and the excitation energy of the residual nucleus were also tabulated.

3(c) Comparison of the Numerical Prediction of the Model with the Experimental Results.

The Cross Sections

In table 3.4 the cross sections for nuclear interactions of 140 Me V protons in the light and heavy nuclei derived from the Monte Carlo method are compared with those obtained experimentally as described in section 3.2. Up to the first collision the Monte Carlo method is equivalent to the optical model. The close similarity between the values given in rows 3 and 5 of table 3.4 is then to be expected since it was seen in section 3.2 that there was a close correspondence between the experimentally derived absorption coefficient in nuclear matter and that expected from the free nucleon nucleon scattering cross sections.

In addition, from the result of the Monte Carlo calculations the fraction of the collisions allowed for 140 Me V protons can be derived. The value obtained was (0.75 ± 0.11) which was consistent with the value

Table 3.4: Cross Sections for nuclear interactions

	Heavy Nucleus	Light Nucleus	
No. of primary protons	100	100	Monte Carlo Calculations
No. of nuclear interactions	81	59	
Cross section for nuclear interactions	$(104 \pm 15).10^{-26} cm^2$	$(21 \pm 3).10^{-26} cm^2$	
Cross section for nuclear interaction - Experimental	$(128 \pm 16).10^{-26} cm^2$	$(16 \pm 7).10^{-26} cm^2$	Section 3.2
Cross section for nuclear interaction - Perry's method	$(110 \pm 5).10^{-26} cm^2$	$(23 \pm 2).10^{-26} cm^2$	

of 0.8 used in section 3.2. It is of interest to note the effect of the Pauli Exclusion Principle at lower energies. In figure 3.4 the mean free path resulting from the Monte Carlo calculations for nucleons in nuclear matter is shown as a function of energy. For comparison the uncorrected mean free path of nucleons in matter and the same path length corrected using the relation given by Goldberger (loc. cit. equation (14)) are shown (unbroken and broken lines respectively).

The Disintegration Products.

The model of successive single nucleon nucleon collisions inside the nucleus is most likely to hold for high energy particles whose mean free path for such collisions is considerably longer than the average inter nucleon distance. This was considered to be the case for nucleons of energy greater than 60 Me V inside the nucleus (Peaslee, 1952). Furthermore the number of evaporation particles emitted from the excited nucleus with energies above 30 Me V is negligible. For these reasons the calculated and experimentally observed products of the disintegrations were divided into three groups:-

(i) protons of energy greater than 30 Me V.

(ii) protons of energy less than 30 Me V.

(iii) alpha-particles of energy less than 30 Me V.

(i) Protons of energy greater than 30 Me V.

The results obtained by the Goldberger method for heavy and light nuclei were combined in the proportion of the geometrical area presented

by each to protons in Ilford G5 emulsions, that is approximately 3 to 1. It has been also pointed out in section 3.2 that 0p stars are difficult to detect in 'area' scanning and that 1p events in which the primary proton lost less than 25 Me V cannot be distinguished from elastic scattering of the primary proton. The effective number of stars in the calculated data was therefore made to correspond to the experimental conditions by rejecting from the calculated results all the 0p stars, and the 1p stars in the above category.

The experimental energy and angular distributions of the protons emitted with energies greater than 30 Me V are compared with those calculated on the Monte Carlo procedure in tables 3.5 and 3.6. The agreement is satisfactory.

(ii) Protons of energy less than 30 Me V

On the compound nucleus picture of nuclear reactions (Peaslee 1952) one would expect very few knock-on protons of energy < 30 Me V to emerge from the nucleus. The model of single nucleon-nucleon collisions is also more likely to break down at low energies where simultaneous collisions of more than two nucleons may take place. In making the Monte Carlo calculations, however, the nucleons were followed through the nucleus assuming single nucleon-nucleon collisions, until the particles either left the nucleus or were absorbed. A large proportion of the protons whose energy after a collision was less than 30 Me V then escaped from the nucleus as the chance of their subsequent collision was reduced by the action of the Pauli Exclusion Principle. It is therefore important to compare the Monte

Table 3.5: Energy distribution of protons of energy greater than 30 MeV.

Energy in MeV.	30-49	50-69	70-89	90-109	> 110
No. of protons per star - Experimental	.23±.04	.13±.02	.07±.02	.11±03	.05±.02
No. of protons per star - Calculated	.22±.04	.16±.04	.21±.04	.12±.03	.08±.03

Table 3.6: Angular distribution of protons of energy greater than 30 MeV

Angle in degrees	0-19	20-39	40-59	60-79	80-99	100-119	>120
Experimental	22	46	27	11	3	5	3
Calculated	22	41	26	20	4	2	2

Carlo calculations with the experimental results for protons of energy below 30 Me V.

The results of the calculations on the heavy nucleus were compared with the experimental data on stars produced in the heavy component of the emulsion, since a fairly reliable evaporation theory is available for silver and bromine (Le Couteur 1950, 1952); such a theory would not be reliable for light nuclei because of the small number of nucleons. In section 3.2, it was shown that 95% of the 1, 2 and 3p stars and 70% of the 4p stars were produced in silver and bromine. The results of the calculation for the heavy nucleus were therefore compared with the sum of the experimental results for 1, 2, 3 and 4p stars. Stars in this category, however, which had one or more α-particle of energy less than 9 Me V were not included since these stars also were probably produced in the light nuclei. In the following discussion all protons of energy less than 30 Me V will be called black.

Size Frequency Distribution.

A calculated size frequency distribution for stars in silver and bromine was obtained from the results of the Monte Carlo calculation. For each interaction, the excitation of the residual nucleus, and the number of knock-on protons is known. The calculated excitation energies varied from 2 to 148 Me V, the mean value being 44 Me V. From a knowledge of the excitation energy the number of charged evaporation particles emitted can be calculated for each star separately (Le Couteur, 1950 and 1952). The total number of charged prongs per interaction can thus be calculated.

Table 3.7: Size frequency distribution

of stars in Silver and Bromine

Type of Star	Calculated number of stars	Calculated Cross Section x 10^{26} cm^2	Experimental Cross Section x 10^{26} cm^2
0p	11	14	4±3
1p	23	29.5	32±12
2p	31	39	53±7
3p	13	17	30±5
4p	3	4.5	9±3
5p	-	—	1±2
6p	-	-	-(1±1)
Totals	81	104	128

The resulting size frequency distribution is compared with the experimental results for silver and bromine in table 3.7. There is satisfactory agreement.

Energy Distribution

The experimental energy distribution of the black protons is shown in figure 3.5 (histogram). It is based on measurements on 388 stars; the total number of black protons emitted in these stars after applying a geometrical correction for those leaving the emulsion was 420. For comparison the calculated data for the heavy nucleus was normalised to 388 stars where allowance was made for the 0p and 1p stars which would not be found by area scanning as previously discussed.

On the basis of the Monte Carlo calculations, 180 protons should be emitted from 388 stars in evaporation processes. In obtaining this result, allowance was again made for the variation of excitation energy in each star. Their number is not sufficient to account for the total number of tracks observed experimentally. However, the Goldberger model also predicts that an additional 190 protons of energy below 30 Me V would be emitted from the heavy nuclei in direct collision processes: thus the calculated number of protons emitted is in satisfactory agreement with experimental number.

In figure 3.5, the shaded area represents the calculated number of knock-on protons emitted in the energy range 6 to 30 Me V. Below 20 Me V, however, the effects of the knock-on protons is completely masked by the evaporation protons. The energy distribution of the evaporation protons

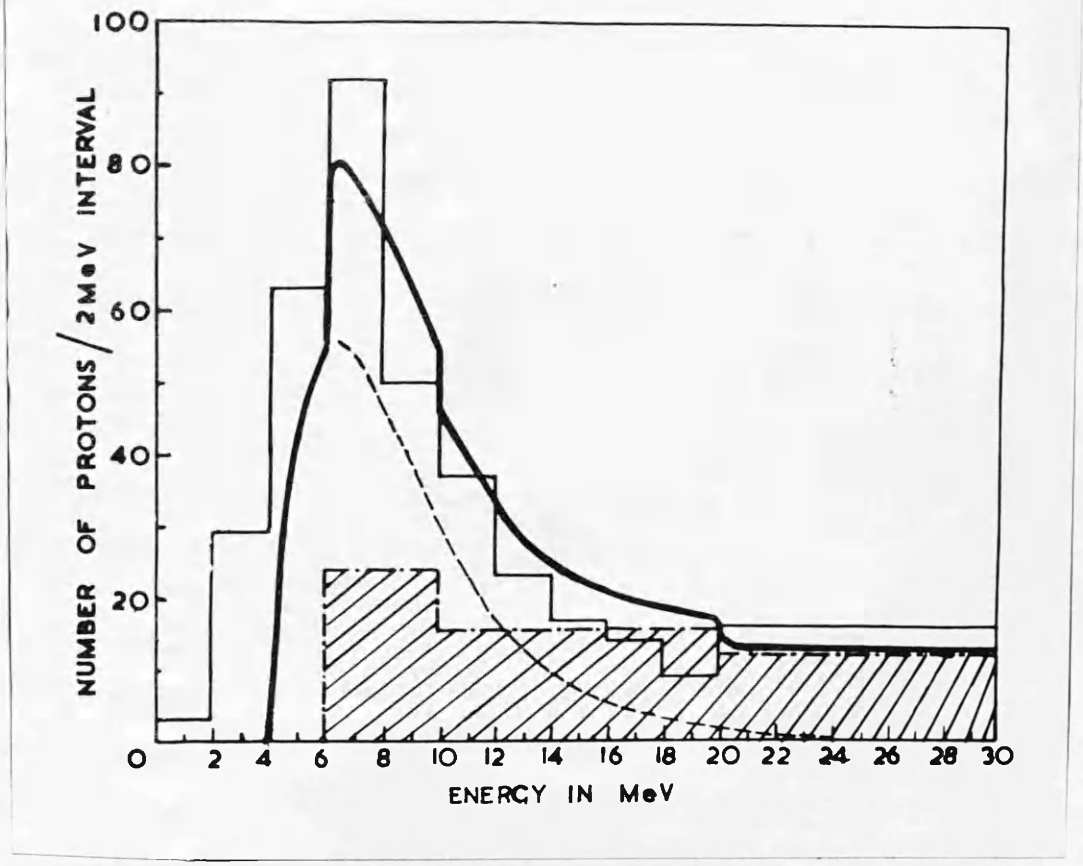

Figure 3.5: Energy distribution of protons below 30 MeV;

⊓ experimental results;

—·—·— calculated spectrum of knock-on protons;

– – – calculated evaporation spectrum on basis of Monte Carlo calculations;

——— calculated knock-on plus evaporation spectrum.

was calculated for the average nuclear excitation energy of 44 Me V (Weisskopf 1937). The resulting curve for 180 evaporation protons is shown in figure 3.5; it is also shown added to the calculated knock-on spectrum (broken line and heavy line, respectively). The agreement of the combined spectrum with the experimental spectrum is satisfactory.

The results obtained by assuming the cascade continues at all energies are, therefore, adequate to account for both the numbers and energy distribution of protons below 30 Me V emitted from stars produced by 140 Me V protons. It should be pointed out, however, that processes different from those assumed in the calculation could account for the experimental data below 20 Me V. If at energies below 50 Me V inside the nucleus, it was assumed that nucleons lose energy rapidly by some process other than that proposed previously and were absorbed, then the excitation energy of the nucleus would be raised from 44 to 66 Me V. The total number of protons expected to be evaporated with energies between 0 and 20 Me V would be 310 compared with 340 protons observed experimentally. The energy spectrum of the evaporation protons was recalculated on this basis and is shown in figure 3.6. However, even if it were assumed that all nucleons of energy less than 60 Me V inside the nucleus were absorbed, the form of the evaporation spectra would not be substantially different from that shown in figure 3.6 and would not be able to account for the number of protons in the energy range 20 - 30 Me V observed experimentally. It, therefore, seems probable that some knock-on protons of energy between 20 and 30 Me V escape from the nucleus.

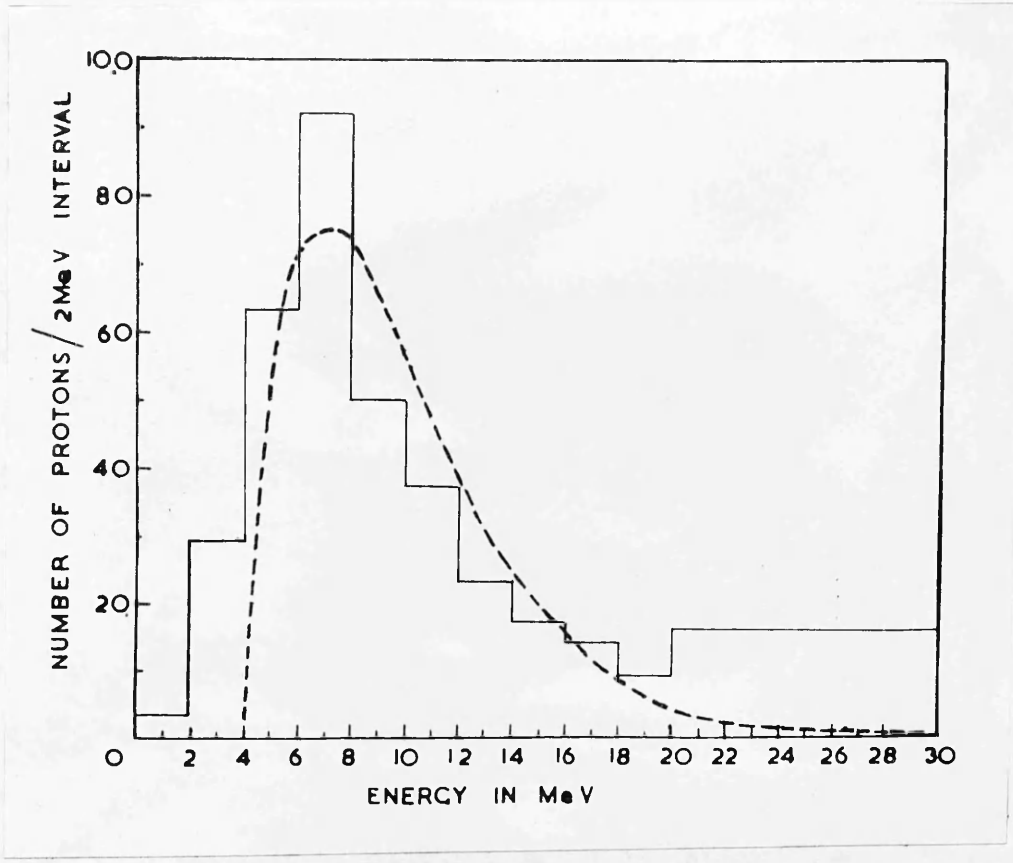

Figure 3.6: Energy distribution of protons below 30 MeV.

⊓ experimental results,

– – – – calculated evaporation spectrum assuming that nucleons of energy less than 50 MeV inside the nucleus contribute to the nuclear excitation energy.

Angular Distribution

The distribution of protons emitted during the evaporation process should be approximately isotropic in the laboratory system since the velocity of the recoiling nucleus is small. It has been shown that an evaporation process could not easily account for the number of protons observed with energies in the region from 20 to 30 Me V. In this energy region, 20 protons were observed travelling in the forward direction and 3 in the backward direction giving additional evidence for this view.

The experimental angular distribution of all protons of energies less than 30 Me V emitted from stars in silver and bromine was also determined. For such stars the ratio of the number of black protons in the forward direction to the number in the backward direction was 1.9 ± 0.2. The calculated forward to backward ratio obtained by combining the calculated angular distribution for black knock-on protons (peak in the forward direction) with the angular distribution for the evaporation protons (assumed isotropic) was 1.9 ± 0.5. These figures are in good agreement which again confirmed that some knock-on protons of energy less than 30 Me V escape from the nucleus.

These observations can be extended to protons of energies less than 20 Me V. The Monte Carlo calculations gave a forward to backward ratio of 1.7 ± 0.5 for such protons. The experimental forward to backward ratios for protons ending in the emulsion were 1.5 ± 0.2 and 1.4 ± 0.2 for protons in the energy ranges 0 - 20 Me V and 0 - 10 Me V respectively. It is therefore not possible to conclude with certainty that knock-on protons c

of energies < 20 Me V were emitted in the stars produced in silver and bromine.

(iii) Alpha particles

According to Le Couteur (1950), the ratio of the number of α-particles to the total number of charged evaporation particles emitted from silver and bromine should be 0.25. The ratios of the number of α-particles to the total number of particles emitted in these stars could then be obtained as a function of star size from the results of the Monte Carlo calculation. This ratio will be referred to as the $\frac{\alpha}{\text{total}}$ ratio. The calculated ratios are compared in table 3.8 with the experimental results given in section 3.2.

The agreement for 1p and 2p stars is very good so that the low $\frac{\alpha}{\text{total}}$ ratio found experimentally again shows that an appreciable number of knock-on protons are emitted in the stars with energy less than 30 Me V. If it were again assumed that all nucleons of energy less than 50 Me V inside the nucleus were absorbed, the increase in excitation energy would approximately double the calculated number of charged evaporation prongs, thereby doubling the ratio. The calculated ratio for 3p stars is lower than the experimental value. This is thought to be due to the fact that some of the 3p stars found experimentally were produced in light nuclei for which the measured ratio is about 0.5.

3(d) Discussion

The Existence of the Nucleonic Cascade.

For protons emitted with energy greater than 30 Me V it can be

Table 3.8: α/total ratios for stars in Silver and Bromine.

Type of Star	α/Total	
	Calculated for Ag and Br	Experimental
1p	0.04 ± 0.02	0.05 ± 0.02
2p	0.08 ± 0.02	0.07 ± 0.01
3p	0.10 ± 0.03	0.16 ± 0.02

concluded that the model used in the Monte Carlo calculation of successive nucleon nucleon collisions inside the nucleus is adequate to account for the experimental results in both the light and heavy nuclei. Furthermore, the very nature of the experimental results strongly implies the necessity of this mechanism for their explanation. The angular distribution of the high energy protons is strongly peaked in the forward direction and about one proton in every four stars has an energy greater than half the energy of the incident proton. It would be expected that any multiple nucleon type of collisions would smear out the assymetry of the nucleonic cascade and result in entirely different characteristics of the high energy protons.

For nucleons of energy less than 60 MeV inside the nucleus the simplifications and poor statistics inherent in the Monte Carlo calculations do not allow the exclusion of the possibility of the sharing of the energy of a nucleon between three or more particles. Nevertheless, from the number of protons occurring with energies greater than 20 MeV and less than 30 MeV and the experimental forward to backward ratio for protons in this energy range, it can be concluded that some nucleons with these energies escape during the nucleonic cascade in the heavy nuclei. Below 20 MeV, there is no definite evidence for the existence of such knock-on protons but the forward to backward ratio for protons of energy less than 20 MeV and the α/total ratios found experimentally for 1p and 2p stars suggest that some nucleons of energies less than 20 MeV may also escape from the heavy nucleus during the nucleonic cascade. Indeed the

assumption that some nucleon-nucleon collisions occur at low energies appears necessary to account for the properties of the stars produced in silver and bromine which have been observed in this experiment.

As the energy of the incoming particle increases, the extent of the cascade throughout the nucleus also increases. The calculation of the interaction of protons of 400 MeV in the heavy nuclei showed that the emission of knock-on protons of low energy would be approximately isotropic as a result of the large number of collisions occurring in the cascade (Bernardini et al 1952). The characteristics of the low energy protons emitted in the cascade would then be similar to the evaporation protons. For this reason, the agreement which was obtained at 400 MeV between the predictions of the model and the experimental results provided inconclusive evidence for the existence of the nucleonic cascade for nucleons of energy less than 60 MeV inside the nucleus.

The procedure which has been adopted in the present calculation could be applied to predict the results of the nuclear interaction of protons and neutrons at still higher energy if the possibility of meson production is included. The effect of meson production has been considered by Lock et al. (1955) in an analysis of the nuclear interaction of protons of 950 MeV energy.

The Mean Free Path of Nucleons inside Nuclear Matter.

As a result of the Monte Carlo calculation the mean free path for nucleons in nuclear matter has been determined as a function of energy. This was shown in figure 3.4. As the energy decreases the Pauli

Exclusion Principle becomes increasingly more important in reducing the number of allowed collisions so that the mean free path goes through a minimum value and increases again at low energies. At very low energies the mean free path has a value of about 10^{-12} cm which is of the order of the nuclear diameter of a medium weight nucleus. In contrast, the mean free path uncorrected for the Pauli Principle has a value of 10^{-13} cm which reflects the increase in the free nucleon-nucleon cross sections at low energies.

Other evidence for a finite mean free path at low energies was presented at the time this work was completed by Feshbach, Porter and Weisskopf (1953, 1954). In an analysis of the total cross sections of nuclei for the scattering of neutrons with energies between 0.1 and 3 MeV these authors concluded that the incident neutrons penetrate a distance of about 2×10^{-12} cm into nuclear matter. However, the empirical nature of their analysis gave no explanation of such a surprisingly long mean free path. Furthermore, it was assumed that the absorption of the incident neutron led to the formation of a compound nucleus.

The work presented in this chapter was therefore of considerable importance. It suggested that the restrictions of the Pauli Principle might lead to the required increase of the mean free path at low energies. Moreover, by suggesting that the absorption process was by single nucleon-nucleon collisions, it implied that the direct emission of particles was possible even at low energies. Thus, the course of a nuclear reaction at low and intermediate energies might be capable of a description analogous to that invoked at high energies. The work described in the

remainder of the thesis was carried out to further study the importance of such high energy effects in reactions at lower energies.

CHAPTER 4

A Study of the Protons Emitted by the Interaction of 13.2 Me V Neutrons with Iron

Section 4.1 Introduction.

In chapter 3, evidence is presented which strongly suggests that direct interaction is possible inside the nucleus between two nucleons of intermediate energy. However, it was believed at that time that the course of a nuclear reaction induced at these energies could be described by the compound nucleus model. In this model it is assumed that the energy of the incident particle is rapidly shared out among the constituents of the nucleus; thus, the subsequent emission of particles is determined by the excitation energy of the compound nucleus. That the additional process of direct interaction might be possible necessarily implies an extension of this model. Since it was important to verify this conclusion a further investigation was undertaken.

In the preceding experiment, the observation of the direct emission of protons of low energy was confused by the considerable number of evaporation protons emitted in the decay of the highly excited nuclei remaining after the nucleon cascade. It was decided that a study of the interaction of nucleons of lower energy could provide more definite information concerning the probability of direct collisions inside the nucleus. The presence of direct interaction should again be revealed by the form of the energy spectrum and angular distributions of the emitted particles.

At the time of these considerations, a survey of the cross sections for reactions of the type (n,p γ) for neutrons with an energy of 14.5 Me V was published (Paul and Clarke, 1953). The survey showed that the experimental cross sections were, in many cases, larger than would be expected on the basis of the statistical theory of Weisskopf and Ewing (1940). It was suggested (McManus and Sharp 1952) that these results were evidence for some direct interaction of the incident neutron with the nucleons of the nucleus. It was therefore decided to study the protons emitted by the interaction of neutrons of this energy in elements of different atomic number.

When this work was started, no previous study of the protons emitted in nuclear reactions at intermediate energies had been reported. Observations on the inelastic scattering of protons with energies of 18 Me V (Gugelot 1954) and of 31 Me V (Igo and Wisberg 1954) have been published subsequently.

In this chapter an investigation of the protons emitted from the interaction of 13.2 Me V neutrons with natural iron using photographic emulsion is described. The experimental procedure developed here has been subsequently applied by others to the investigation of the protons emitted from aluminium and rhodium. The results of the latter work will therefore be introduced in section 4.5 to allow a complete discussion of the evidence for direct interaction obtained in the study of (n,p) reactions.

Section 4.2 Experimental Procedure:

2(a) The Neutron Source

The neutrons were produced in the reaction T (d,n) He^4 by the bombardment of tritium absorbed in a target of zirconium with deuterons accelerated in the Glasgow H.T. set.

The total flux of neutrons produced per sec, N, by a beam of deuterons of energy E_1 incident on a zirconium target is given by

$$N = n_T \, n_D \int_{E_F}^{E_1} \sigma(E) \Big/ \frac{dE}{dx}(E) \cdot dE$$

where n_T is the number of tritium atoms per cc of target,

n_D is the number of deuterons incident per sec on the target,

$\sigma(E)$ is the cross section of the reaction at an energy, E,

$\frac{dE}{dx}(E)$ is the rate of loss of energy of a deuteron in the target,

E_F is the energy of the deuteron after passing through the zirconium.

This formula takes into account the variation in cross section of the T (d,n) reaction due to the reduction in energy of the deuteron in passing through the target. The variation of the cross section as a function of energy is shown in figure 4.1 (Conner et al. 1952).

Since the cross sections for the neutron induced reactions to be studied are small it was necessary that the neutron flux was as large as possible. A zirconium target, $1 mg/cm^2$ thick, containing 0.054 cc of tritium per cm^2 was obtained from A.E.R.E., Harwell. This was the thickest target available containing a uniform distribution of tritium. Its thickness is equivalent to the full range of a deuteron of 250 keV energy. When account is taken of the variation of cross section shown in figure 4.1, the

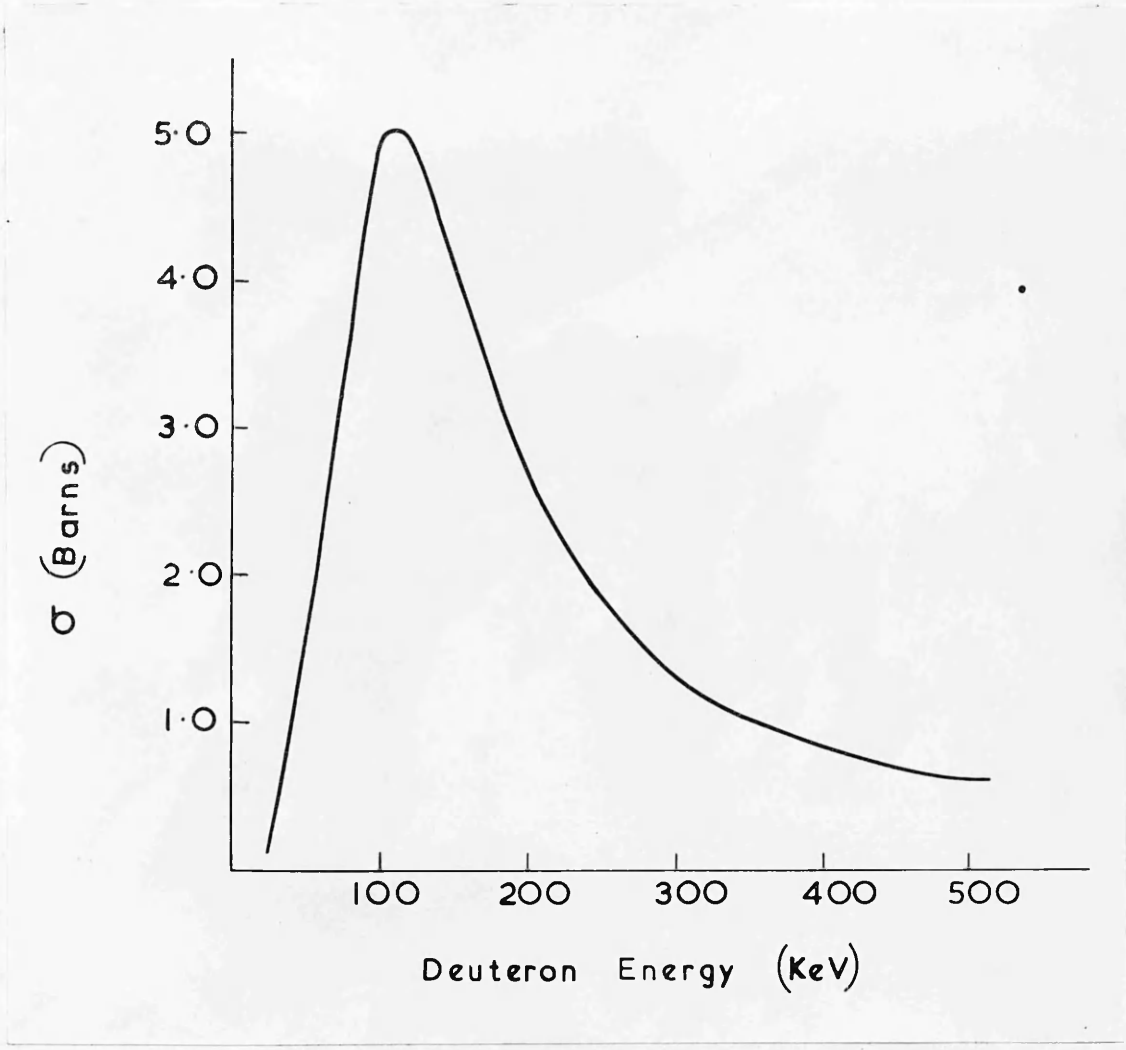

Figure 4.1: The variation in cross section of the reaction T(d,n) He^4.

maximum neutron intensity for a given current of deuterons should be obtained for deuterons of energy within the range 250 - 350 keV. Unfortunately, at these energies the current of deuterons available on the Glasgow H.T. set was very small. Above 500 keV, the current of deuterons is much increased but the effective cross section in the target is reduced and furthermore the greater dissipation of energy in the target may result in evaporation of some of the tritium.

The maximum flux of neutrons was obtained when the machine was run at 350 keV. At this energy the maximum current available was 10 μamp of deuterons which resulted in a flux of neutrons of 4×10^8 per sec.

2(b) Experimental Arrangements

Critical consideration was given to the experimental arrangements which would allow a simultaneous investigation of the energy and angle distributions of the protons emitted in an (n,p) reaction. In an experiment in which the nuclear reaction is induced by neutrons, the photographic plate suffers the disadvantage as a detector of particles that collision of neutrons from the source with free hydrogen present in the emulsion gives rise to a background of recoil proton tracks. Thus it may be necessary to choose a particular experimental arrangement in which the photographic plate is shielded from neutrons. Alternatively, since measurements are made by actual observation of the particles in the emulsion, it may be possible to distinguish tracks as background events in an unshielded emulsion. In any exposure, however, the background arising from proton recoils in the

emulsion must be kept below a certain level to preserve the optical clarity of the photographic plate.

In principle the experiment could be carried out in the schematic arrangement shown in figure 4.2 (Frye 1953). Protons are produced in a foil of the element by neutrons from the source, A, and are detected in photographic plates placed around the foil. From measurements made on the protons starting at the surface of the emulsion the energy spectrum of protons emitted in the (n,p) reaction could be obtained at an angle defined by the direction of the photographic plate. The plates are shielded from the direct beam so that almost all the protons recorded in the emulsion are those produced in the foil. Such an arrangement therefore possesses a high intrinsic efficiency for the detection of real events.

It possesses a low overall efficiency when the number of protons recorded for a given flux of neutrons from the source is considered. With the maximum flux of neutrons available on the H.T. set (c.f. section 4.2(a)) and for an (n,p) cross section of 100 mb, it was calculated that the required time of exposure to obtain a density of 10^4 protons per cm^2 of emulsion was approximately $\frac{d^2 r^2}{t}$ hours, where d is the distance in cm between the foil and the neutron source, r is the distance in cm between the foil and emulsion and t is the foil thickness in microns. These parameters cannot, however, be varied freely. The thickness of the foil is limited since the loss in energy of protons produced in a foil must be minimised. Furthermore, there is a minimum distance between the source and foil if adequate shielding of the source is required and between the foil and

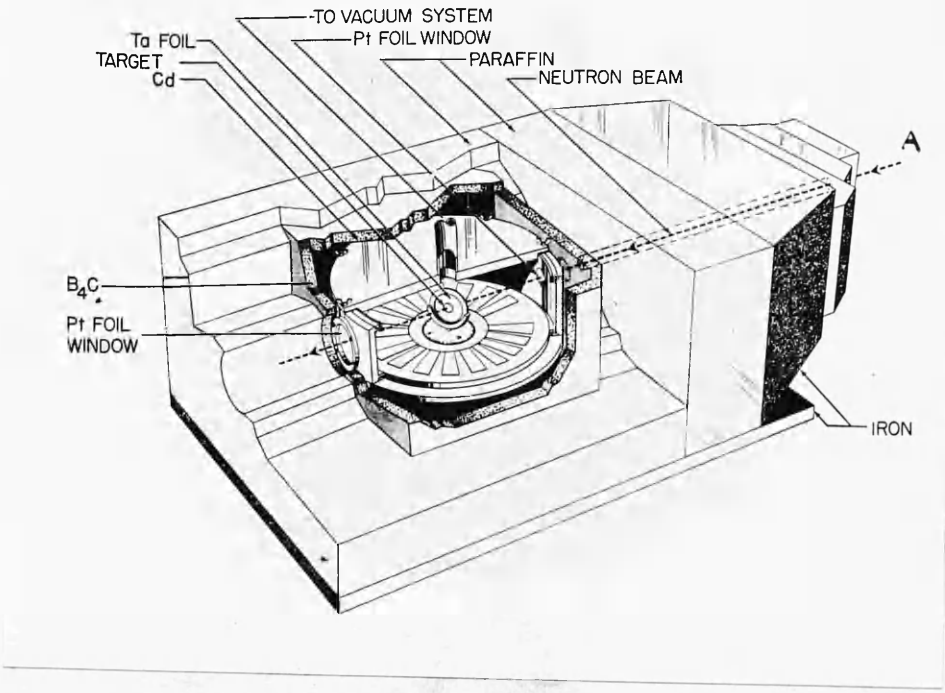

Figure 4.2: The experimental arrangement used by Frye (1953).

emulsion if the angular resolution of the detecting arrangement is to be preserved.

It was calculated that to carry out the experiment in this arrangement with the available flux of neutrons was only possible if exposures were made for 100 hours.

An alternative arrangement was considered in which the protons emitted following the (n,p) reaction in a foil were detected in a photographic emulsion placed in contact with the foil. From direct measurement of the proton entering the surface of the emulsion, the energy and angle with respect to the direction of the incident neutrons of the protons can be found. The proton angle is now no longer uniquely defined by the direction of the emulsion to the direction of the neutron beam but can be separately determined for each proton recorded. This arrangement possesses the obvious advantage that a large fraction of the protons produced in the foil are recorded in the emulsion.

It was decided that the assembly of the foil and emulsion should be irradiated close to the neutron source. An exposure carried out in this position has the following advantages:

(a) The (n,p) reaction in the foil is mainly due to the neutrons of full energy since the intensity at the foil of neutrons directly from the source is much greater than that arising from secondary scattered neutrons.

(b) The background of recoil protons although largest in this position is mainly due to the primary flux of neutrons and can be

distinguished by the dynamical conditions satisfied by the free n-p collision.

(c) The time of irradiation for a given flux of neutrons is a minimum in this position.

An upper limit to the time of exposure in this arrangement is reached when the number of recoil protons produced inside the emulsion is so large that the measurement of individual tracks is impossible. This limit corresponds to a flux of 10^9 neutrons incident per cm^2 of emulsion. This limit to the time of exposure therefore restricts the minimum thickness of a foil. The thickness must be sufficient that enough protons are produced in the foil to ensure that the subsequent examination of the emulsion is not too laborious. It was calculated that a foil thickness of about 12 mg/cm^2 of iron would satisfy this condition.

2(c) The Exposure of the Plates.

In view of the above considerations, the scattering chamber shown in figure 4.3 was constructed. This apparatus could be connected to the end of the accelerating column of the H.T. set. The essential features are the following. Only a small portion of the tritium target, 1/16 inch in diameter, was exposed to the beam of deuterons; thus the neutrons could be considered to arise from a point source. Collimation of the deuteron beam above the plate holder ensured that the deuterons were incident upon the uncovered portion of the tritium target. The scattering chamber was insulated from the H.T. set so that the integrated current of deuterons incident on the target could be measured. The plate holder itself con-

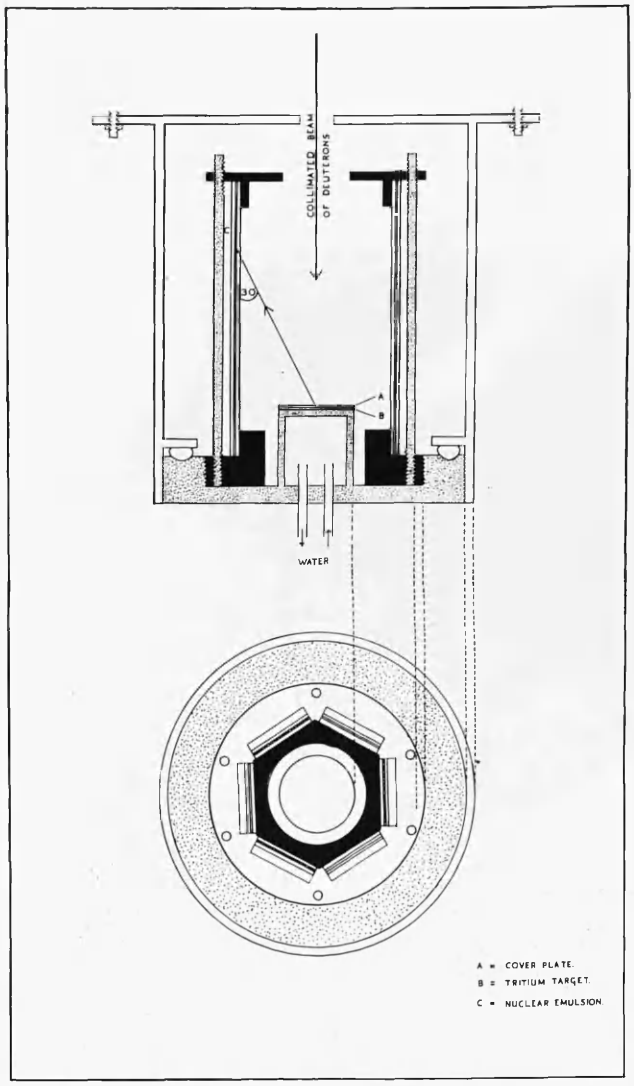

Figure 4.3: The scattering chamber employed in the present study of the (n,p) reaction.

sisted of a hexagonal base and matching hexagonal top plate. A photographic plate could be clipped to each of the six sides of the baseplate and held rigidly in position by six supporting struts through the top plate. The design of the plate holder therefore ensured that the minimum amount of material was near the nuclear emulsion.

The exposures were carried out under vacuum conditions with six nuclear emulsions (Ilford C2, 4" x 1" x 400μ) mounted hexagonally around the target. Foils, 4" x 1" of the element to be investigated were placed in contact with the alternate emulsions. These foils and the surfaces of the other three emulsions were covered by gold strips of size, 4" x 1" x 400μ. The gold, which has a very small (n,p) cross section, was used to shield the surface of the emulsion from external sources of protons. The three surfaces covered with gold strip alone were included so that allowance could be made for the small number of protons arising from the gold. The arrangement is shown schematically in figure 4.4.

Irradiation of the iron foils was carried out in this arrangement. The foils were kept in a dry box before being placed in contact with the emulsion surface. Nevertheless it was found necessary to keep the time of contact before exposure on the H.T. set as short as possible since the surface of the emulsion was rapidly attacked under normal conditions of humidity.

The time of the exposure was controlled by the current integrator. Collimation of the deuteron beam resulted in a maximum current of deuterons incident on the target of 1μamp. An integrated current of 2μamp hours was found to give a satisfactory intensity of protons incident on the

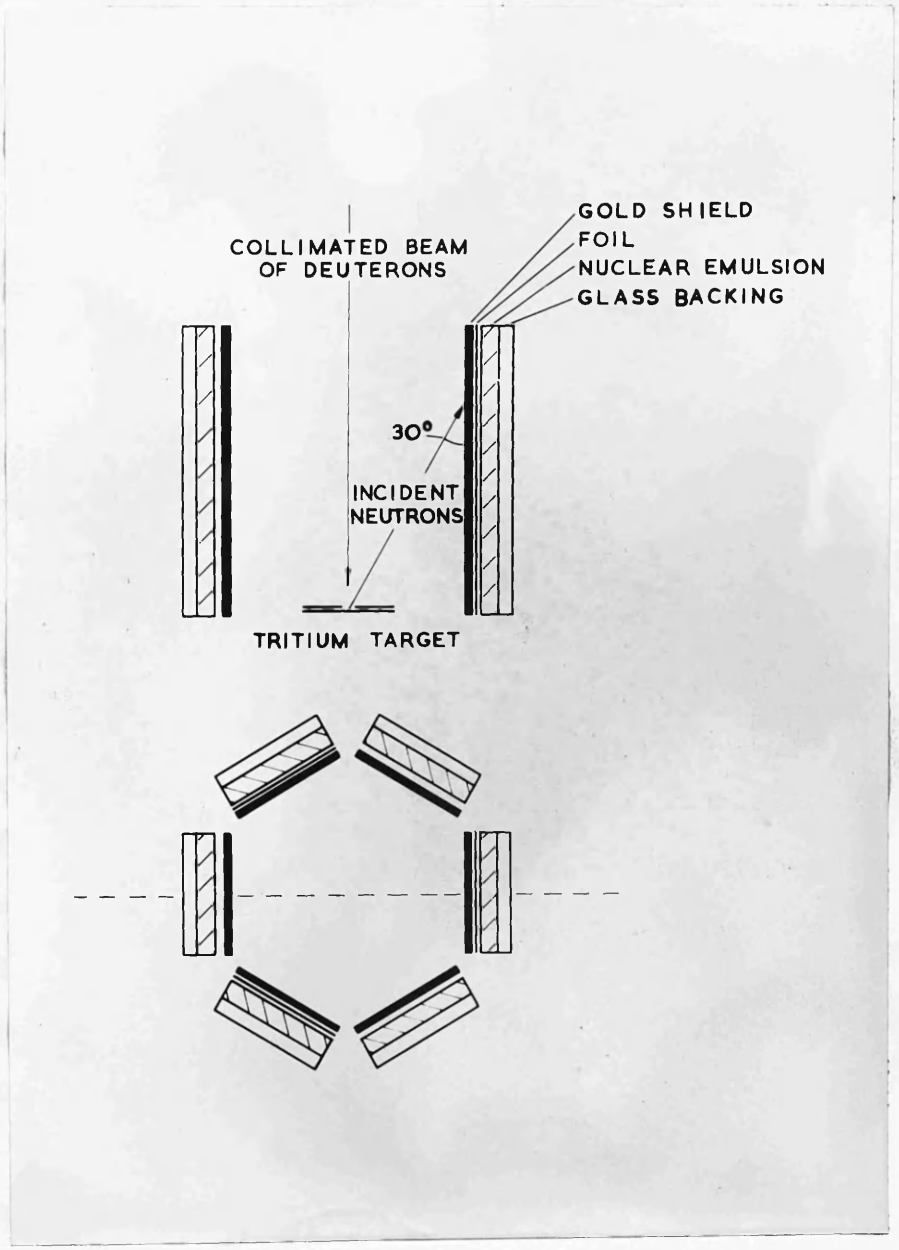

Figure 4.4: The photographic plate assembly.

emulsion compatible with the requirement of good track discrimination. Immediately after an exposure, before the emulsion had time to reabsorb water, the combined thickness of each photographic plate (emulsion and glass backing) was measured.

2(d) Development of the Plates

The plates were developed by the usual two stage 'temperature development' of Dilworth et al. (1948). However, precautions were necessary to ensure that a minimum amount of silver was deposited on the surface of the emulsion. Cleaning of the emulsion surface could not be considered in this experiment in case a layer of emulsion to a depth of a few microns might be removed. In this way tracks which were produced inside the emulsion might subsequently appear to have entered the emulsion from outside

The following precautions were successful in obtaining a surface free from silver:

(a) The developer was filtered to remove grains of undissolved amidol

(b) Upon removal of the plates from the cold developer the excess solution was carefully dried off with filter paper before transference to the hot plate.

(c) Throughout the fixing stage and in particular during the initial period, the fix was changed frequently so that silver grains were not deposited on the surface.

Upon development, the total thickness of the glass backing and processed emulsion was measured. The thickness of the processed emulsion was also measured directly under the microscope. From these and the

previous results the thickness of the emulsion at the time of exposure was determined.

2(e) Examination of the Plates

The photographic plates were examined in a region corresponding to neutrons incident at an angle of $30^{\circ} \pm 2^{\circ}$. The area of emulsion examined on each plate was 6 mm x 0.3 mm. The energy of the neutrons incident over this area was calculated from the dynamics of the T (d,n) He^4 reaction to be 13.2 $\pm$ 0.2 MeV.

The plates were scanned with x 45 objectives and x 10 eyepieces for tracks of protons* entering the surface of the emulsion; x 90 eyepieces were used to distinguish between tracks which entered the surface and those which started in the emulsion. Those tracks whose angle of dip was less than 30° were selected for measurement. The limitation on dip angle ensured that all tracks that started at the surface ended inside the emulsion The position of the scan was such that measurements on protons making angles greater than 150° to the direction of the incident neutrons could not be made. Scanning was also carried out inside a known volume of emulsion for all protons that satisfied the same geometrical conditions as imposed at the surface.

The range, the angle in the plane of the emulsion with respect to the direction of the incident neutron and the angle of dip were determined for

---

* It was assumed that all tracks of unit charge were protons since it was impossible to separate protons and deuterons of low energy by grain counting in C2 emulsion. The validity of this assumption will be discussed in the presentation of the results.

every track selected. The daily variation of the thickness of the processed emulsion was taken into account in the computation of the angle of dip and the range. The energies of the protons were determined from their ranges in dry C2 emulsion (Rotblat 1951). The angles in space of the protons with respect to the direction of the incident neutron were calculated from their dips and projected angles.

Section 4.3 Analysis.

3(a) Separation of Events.

Not all protons that were observed to start at the surface of the emulsion originated from the elements in contact with the emulsion. Protons starting in the emulsion within a distance of 1 or 2 microns from the surface are optically unresolvable from those entering the emulsion. Protons in this category were divided into two groups:

1) Recoil protons produced as a result of the collision of the incident neutrons of 13.2 MeV energy with hydrogen present in the emulsion.

2) Protons produced as a result of the interaction of the incident neutrons with the nuclei of the emulsion, or as a result of the collision of neutrons of lower energy with hydrogen atoms. These will be called background protons.

The recoil protons (1) were distinguished in the first instance by applying the relationship

$$Ep = (13.2 \pm 0.2) \cos^2\theta$$

where Ep = energy of the recoil proton,

θ = spatial angle between the direction of the recoil proton and the direction of the incident neutron.

Allowance was also made for errors in the measurements of Ep and θ in the classification of recoil protons.

As a further check on the identification of the recoil protons, the angular distribution of the protons which satisfied the above relation was plotted. This is shown in figure 4.5 for protons recorded at the surface of the emulsion in contact with the iron foils. The full curve represents the angular distribution expected from considerations of the angular distribution of the protons in the laboratory system and the solid angle available for their observation. The two distributions have been normalised at 30° It can be seen that at angles greater than 30° the number of recoil protons observed to start at the surfaces in contact with the iron foils was greater than the calculated distribution. This has been attributed to a contribution of protons which are emitted from the iron foil with an energy and angle satisfying the above relation. The Q-value of the (n,p) reaction in iron excludes the possibility of emission of protons of an energy which would satisfy the relation for angles less than 30°. The correctness of this interpretation was borne out by the agreement between the theoretical curve and the distribution of proton recoils observed to start at the surface of the emulsion in contact with the gold. The recoil protons (1) were therefore subtracted from the protons observed to start at the surface of the emulsions according to the full curve of figure 4.5.

The manner in which protons were produced in the top surface of the

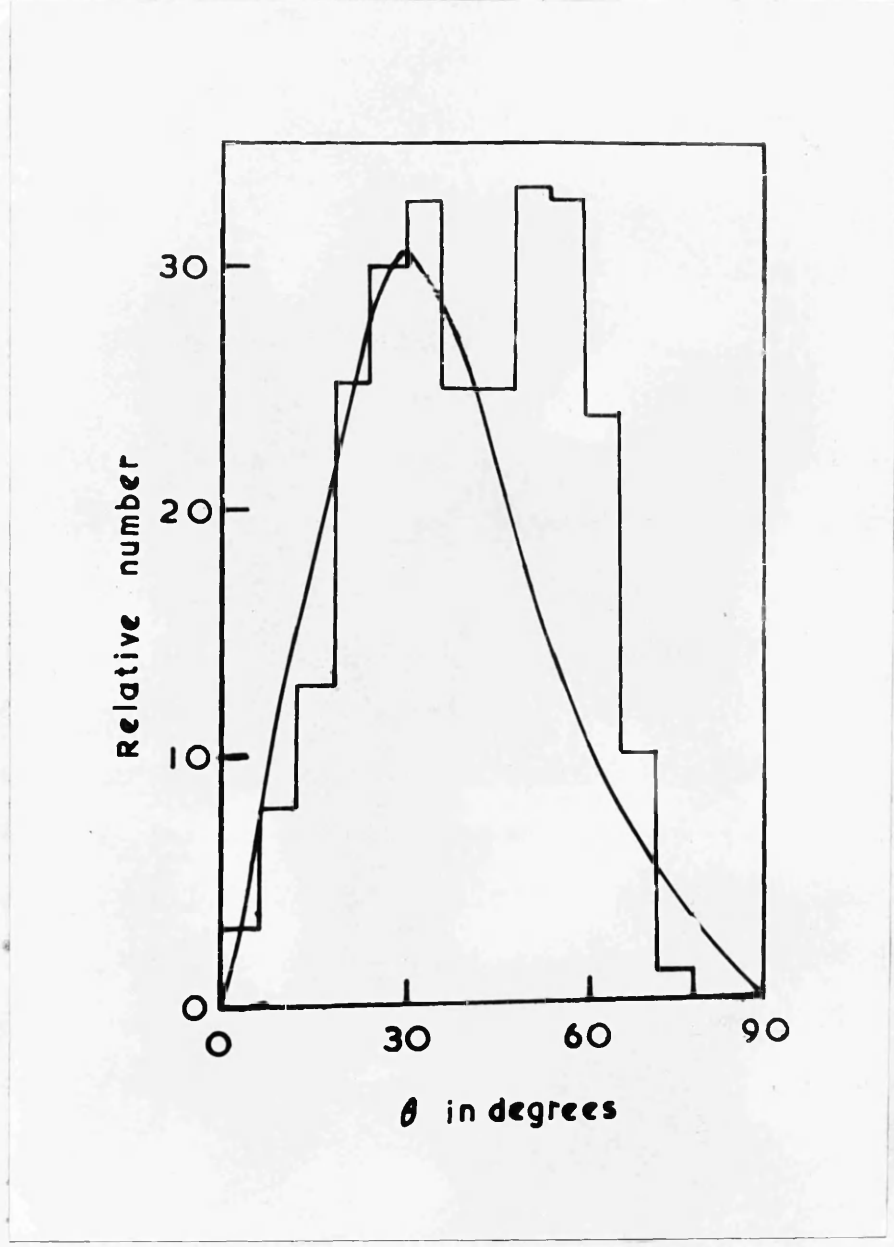

Figure 4.5: The angular distribution of the recoil protons recorded at the surface of the emulsions in contact with the iron foils.

emulsion by other processes has been outlined in (2). It was impossible to distinguish these protons by the application of any relation between their energy and angle. However, a correction for these background protons was obtained from the measurements made on the protons occurring inside the emulsion.

A volume of 8×10^{-3} cc was scanned inside the emulsion. With the same limitation of dip angle as were applied at the surface, 950 protons were identified as recoil protons and 350 protons were classified as background protons; of the latter, approximately 80% had energies below 3 MeV*. The angular distribution of the proton recoils was in good agreement with the full curve of figure 4.5; thus the above interpretation of the excess number of recoil protons at an angle greater than 30° at the surface of the emulsion in contact with the iron foils is again borne out. Under the same criteria of selection of tracks, the ratio of background to to recoil protons starting at the surface and at points inside the emulsion should be the same. The number of surface tracks subtracted as background

---

* It is believed that the most probable source of low energy neutrons which would result in recoil protons of these energies is the interaction of the bombarding deuterons with deuterium which has accumulated in the target and in the collimating slit above the target. The inelastic scattering of neutrons from the source should in general lead to neutrons of energy less than 2 MeV (Graves and Rosen 1953) and hence would result in recoil protons of energy lower than observed.

events was therefore made proportional to that for protons identified as recoil tracks in the ratio found to hold inside the emulsion. The grouping of the subtracted tracks in intervals of energy and spatial angle was made in the same relative numbers as those observed inside the emulsion.

The remaining surface protons could have arisen only in the materials placed in contact with the photographic emulsion. The effect of protons originating in the gold strip was eliminated by considering the energy and angle of the protons left (after subtraction of (1) and (2)) at the emulsion surfaces in contact with the gold strips alone. Before subtraction from the data obtained on the emulsions exposed to the foils in intervals of energy and spatial angle, allowance was made for the form that this spectrum would take after the traversal of the foil.

The complete procedure described above may be conveniently summarised by the schematic equation:

protons from foil = protons observed at the surface

$$- \left[(1) + (2) + \text{modified protons from gold.} \right]$$

The number of tracks entering the various categories for the exposure to the iron foil is shown in table 4.1. For proton energies of less than 4 MeV, about 25% of the observed data was removed in the subtraction. The results which have been subsequently obtained from the analysis of the exposures to aluminium and rhodium are also shown in table 4.1: for rhodium the area scanned on each plate was twice that for iron or aluminium. The consistency between the ratios of the various back-

Table 4.1: Separation of Events

Element (angle of dip)	Protons observed	Recoils	Background	Modified Gold	Protons from Foil
Fe (10° - 30°)	1190	200	55	50	885
Al (10° - 45°)	1600	220	30	70	1280
Rh (10° - 45°)	1140	490	60	90	500

ground categories for the different exposures serves to establish the correctness of the adopted procedure.

3(b) The Correction for the Energy Loss of Protons produced in the Foil.

The thickness of the foil used in the investigation was 13 mg/cm^2 of iron. However, the protons that were accepted for analysis had traversed the foil obliquely so that the effective thickness of a foil was greater than the figure quoted. A proton of 5 MeV energy that passes through a foil at an angle of dip of 30° loses an energy of 1.2 MeV in iron. The energy of a proton produced within a foil may therefore be considerably modified, particularly at low energy, by its passage through the foil to the surface of the emulsion. For this reason protons observed with angles of dip less than 10° were discarded because of the large thickness of foil they might have traversed.

A relaxation method was adopted to correct for the energy loss of protons produced in a semi-thick target. The observed angular distribution was then related to the true energy spectrum to obtain the true angular distribution in each energy interval. The procedure is given in appendix 2.

3(c) The Determination of the Cross Section for the Emission of Protons.

The differential cross section, $\left(\frac{d\sigma}{d\omega}\right)_\theta$, for the emission of protons at an angle θ, may be related to the number of protons $N_p(\theta)$, observed at an angle θ by the expression

$$N_p(\theta) = F\left(\frac{d\sigma}{d\omega}\right)_\theta d\Omega_\theta \, nV$$

where F = total flux of neutrons per cm^2 at the foil,

$d\Omega_\theta$ = solid angle available for acceptance of a proton emitted at an angle θ.

n = number of atoms per cc of the foil,

V = volume of the portion of the foil under examination.

The total flux of neutrons incident on the foil was determined by counting the number of recoil protons observed within a known volume of emulsion. The results obtained from the scanning carried out inside the emulsion were utilised in this procedure. The number of proton recoils, $N(\theta_1)$, which start in a volume, V, of emulsion at an angle, θ_1, to the direction of the incident neutron is related to the total flux of neutrons F, by the following expression (Rosen 1953)

$$F = \frac{N(\theta_1)\ d\theta_1}{\cos\theta_1\ d\Omega_{\theta_1}} \times \frac{\pi}{\sigma_{np}\, n_H\, V}$$

where $d\Omega_{\theta_1}$ = solid angle available for acceptance of a recoil proton at an angle θ_1.

σ_{np} = total corss section for free neutron-proton scattering

n_H = number of hydrogen atoms per cc of the emulsion.

A plot of $\frac{N(\theta_1)\ d\theta_1}{\cos\theta_1\ d\Omega_{\theta_1}}$ against θ_1, was found to be constant; this was anticipated from the agreement found previously between the angular distribution of the recoils inside the emulsion and the full curve of figure 4.5

Before the total flux was estimated, however, a correction was necessary for the efficiency of detection of recoil protons inside the emulsion. At the surface of the emulsion the efficiency for detection of

protons was practically 100% since relatively few protons were present in any one ~~microscope~~ field of view of the microscope. Inside the emulsion, however, there were a large number of tracks crossing a field of view so that the efficiency for detection of tracks which start in a field of view was reduced. By examination of the same volume of emulsion by different observers the efficiency for detection of recoil tracks inside the emulsion was estimated to be 80 $\pm$ 10%. The consequent error in the determination of the neutron flus, however, was only taken into account in the calculation of the total cross section for emission of protons, since the error was systematic and would not affect the relative differential cross sections*.

The solid angle, $d\Omega_\theta$, was restricted by the geometry of the exposure and the limitations imposed upon the angle of dip of the tracks selected for measurements. The variation of the solid angle was taken into account in the determination of the differential cross sections. The method of calculation of this solid angle as a function of θ is given in the appendix 3. Because of the position of the scan and the rejection of protons with angles of dip less than 10°, the differential cross sections could only be determined over the angular range from 0 - 140°.

---

* In practice it was unnecessary to calculate a value of the total neutron flux. Instead the differential cross sections could be simply determined from the known value of the free neutron-proton scattering cross section, σ_{np}, on resubstitution of the expression for F into the equation relating $N_p(\theta)$ and $\left(\frac{d\sigma}{dw}\right)_\theta$.

Section 4.4 Results

The energy spectra of the protons emitted from iron over different ranges of angle and over the entire range from 0° - 140° are shown in figures 4.6 and 4.7 respectively. The angular distributions for different ranges of energy are shown in figure 4.8.

A total cross section of 150 $\pm$ 30 millibarns for the emission of protons from iron was obtained by integration of the angular distributions extrapolated to 180°. However, a target of natural iron was used in this experiment. To obtain an estimate of the total cross section for Fe^{56} (92% of natural iron) a small background ($\sim$ 30 mb) due to the presence of Fe^{54} (Allan, private communication) was subtracted from the observed cross section. The total cross section of 120 $\pm$ 30 millibarns for the emission of protons from Fe^{56} can be compared with a total cross section of 190 millibarns deduced by Allan (private communication) from a study of the emission of protons from Fe^{56} at an angle of observation of $34^\circ \pm 20^\circ$. When account is taken of the forward peak in the angular distribution found in the present experiment the cross sections obtained by Allan would be reduced by about 20% giving a favourable comparison with the present results.

The nuclear reactions in Fe^{56} leading to the production of protons that can be induced by neutrons with an energy of 13.2 MeV are as follows:

$$_{26}Fe^{56} + n \rightarrow {}_{26}Mn^{56} + p + \gamma \qquad -2.9 \text{ MeV} \qquad \text{(a)}$$

$$_{25}Mn^{55} + p + n \qquad -10.2 \text{ MeV} \qquad \text{(b)}$$

$$_{25}Mn^{55} + n + p \qquad -10.2 \text{ MeV} \qquad \text{(c)}$$

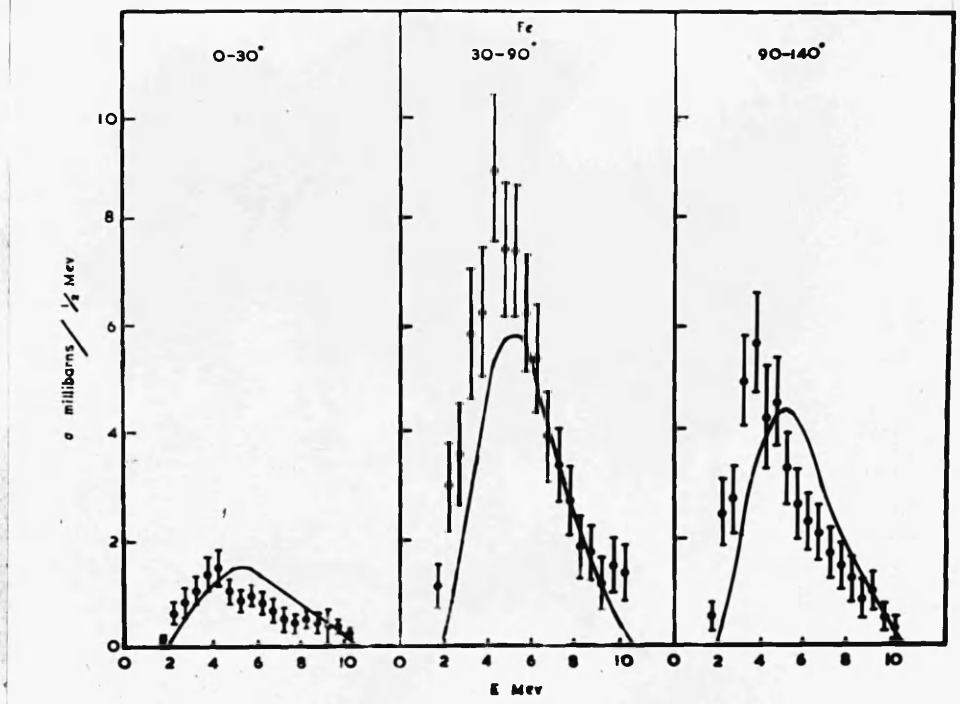

Figure 4.6: The energy spectra of the protons emitted over different ranges of angle by the interaction of 13.2 MeV neutrons with iron.

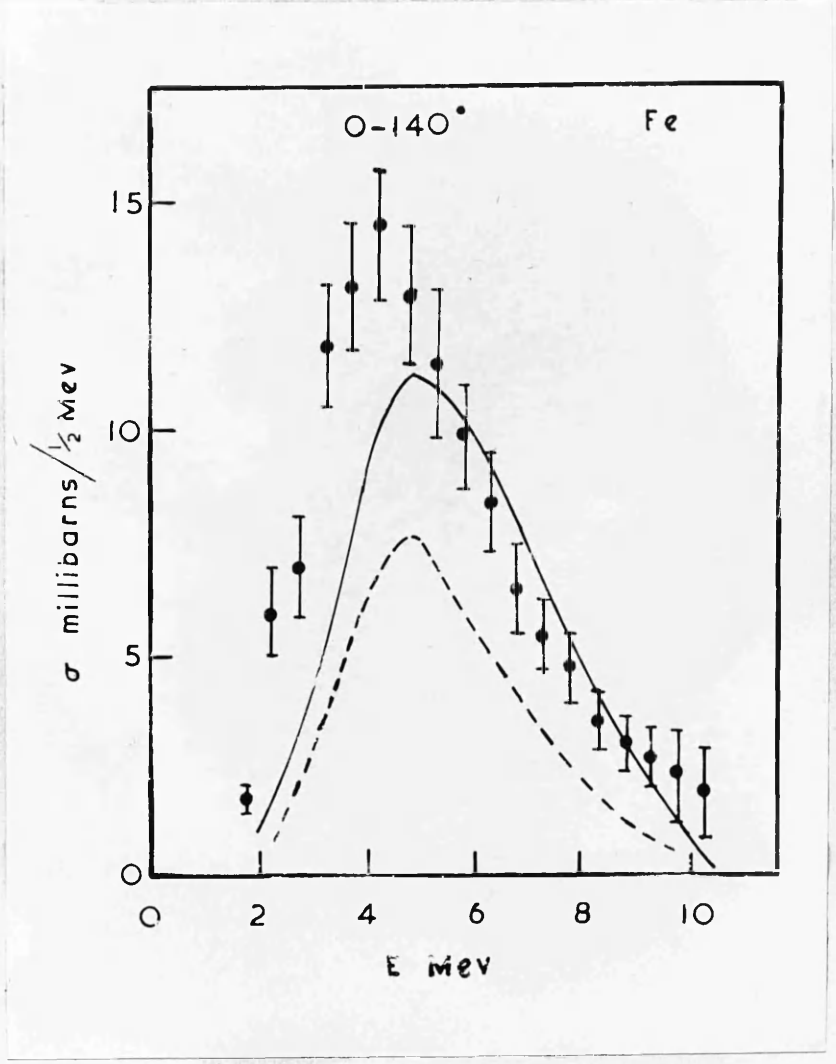

Figure 4.7: The energy spectrum of the protons emitted from iron.

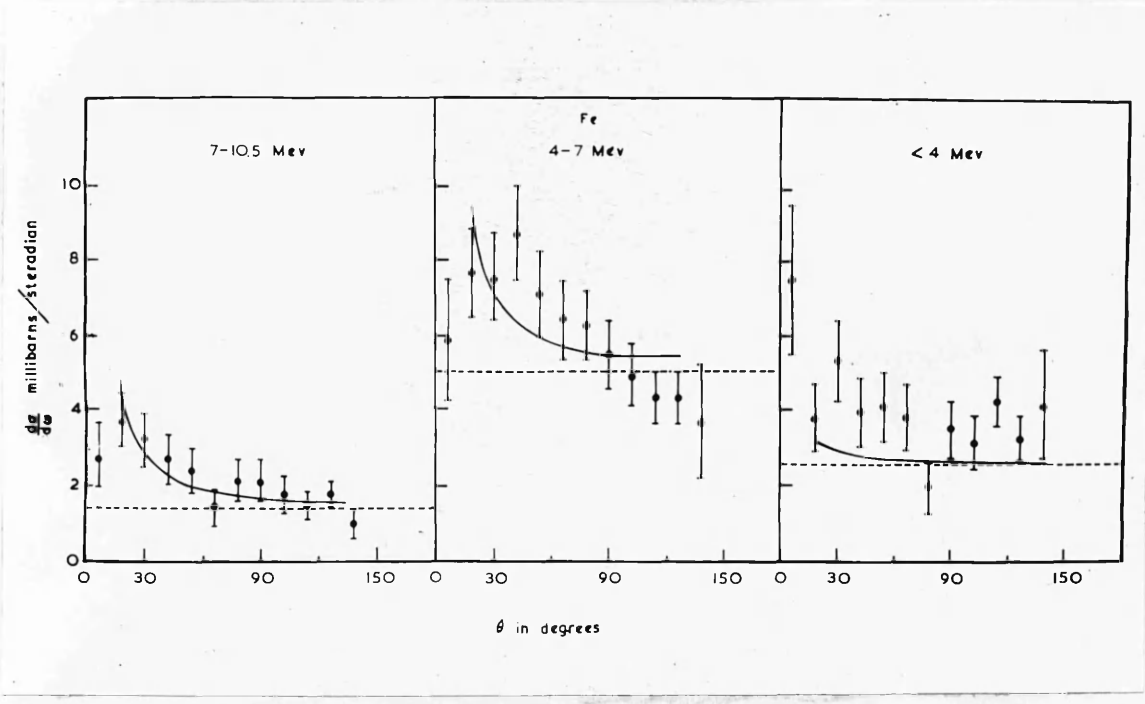

Figure 4.8: The angular distributions of the protons emitted from iron.

In the present experiment the sum of the contribution from all three reactions is observed. The processes (n,pp) and (n,d) are also energetically possible, but, due to the effects of the large negative Q-values, -12.3 MeV and -8 MeV respectively, and the Coulomb barrier are expected to make a negligible contribution to the observed data.

If it is assumed that the emission of a neutron normally accompanies that of a proton when the energy of the latter is less than 13.2 + q (where q represents the Q-value for the processes (b) and (c)), an estimate of the cross section for the process (a) can be made by integrating the observed spectra for energies greater than this limit. The correction for the reaction Fe^{56} (n,pn) is small, however, since the maximum energy of protons from this reaction is only 3 MeV. The cross section for the reaction Fe^{56} (n,pγ) is therefore effectively the total cross section of 120 $\pm$ 30 millibarns found in this experiment. This value compares favourably with values of 97 $\pm$ 12 (Paul and Clarke 1953) and 124 $\pm$ 12mb (Forbes 1952) obtained by measurements of the activity of the residual nucleus Mn^{56}.

Section 4.5 Discussion of Results.

The energy spectrum over the entire range of angles of the protons from iron has a maximum at an energy of about 4 MeV. This value is consistent with that expected from consideration of the height of the Coulomb barrier in the residual nucleus, Mn^{56}, which is about 5 MeV.

The spectrum shown for the range of angles 0 - 30° has some indication of structure at about 6.0 and 8.3 Mev.*

---

* Footnote on next page.

It is of interest to compare this spectrum of protons with the spectrum of protons emitted at an angle of $34^{\circ} \pm 20^{\circ}$ by the interaction of neutrons of 14.1 MeV with iron (Allan, private communication). The effective thickness of the iron foil was smaller in the latter experiment than in the present experiment so that better energy resolution was attained. The two spectra, normalised at 5 MeV, are shown in figure 4.9. It can be seen that the shape of the spectrum and the position of the peaks as suggested by the present results are consistent with the results obtained by Allan when account is taken of the higher neutron energy.

More convincing evidence of structure is obtained in the present investigation from the spectra of protons from aluminium and rhodium. This can be seen in figures 4.10 and 4.11. The effective thickness of foil in these exposures was again less than in the exposure to iron.

The angular distributions at all energies of the protons from iron show preferential emission of protons in the forward hemisphere although

---

* It should be pointed out that the correction applied for the use of a semi-thick target foil tends to remove any fluctuations in the shape of the spectra. The uncorrected spectrum of protons from iron emitted at an angle of dip between 20° and 30° exhibited peaks at energies of 5.5, 8.0, and 9.5 MeV. A correction of the observed energy spectrum for transversal of half the thickness of the foil at a mean angle of dip of 25° would shift these peaks to an energy of 6.0, 8.25, and 9.75 MeV, corresponding to the excitation of levels or groups of levels in Mn^{56} at about 4.3, 2.0 and 0.6 MeV respectively. These assignments are extremely tentative.

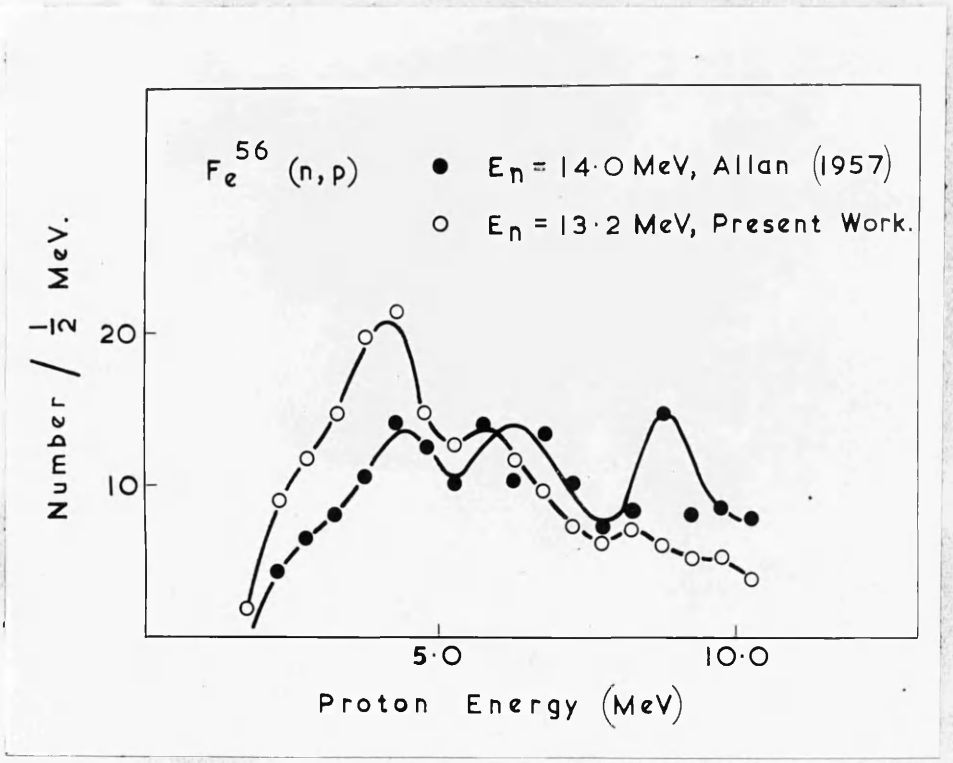

Figure 4.9: Comparison of the energy spectrum of protons emitted from iron in the forward direction; the spectra have been normalised at 5.75 MeV.

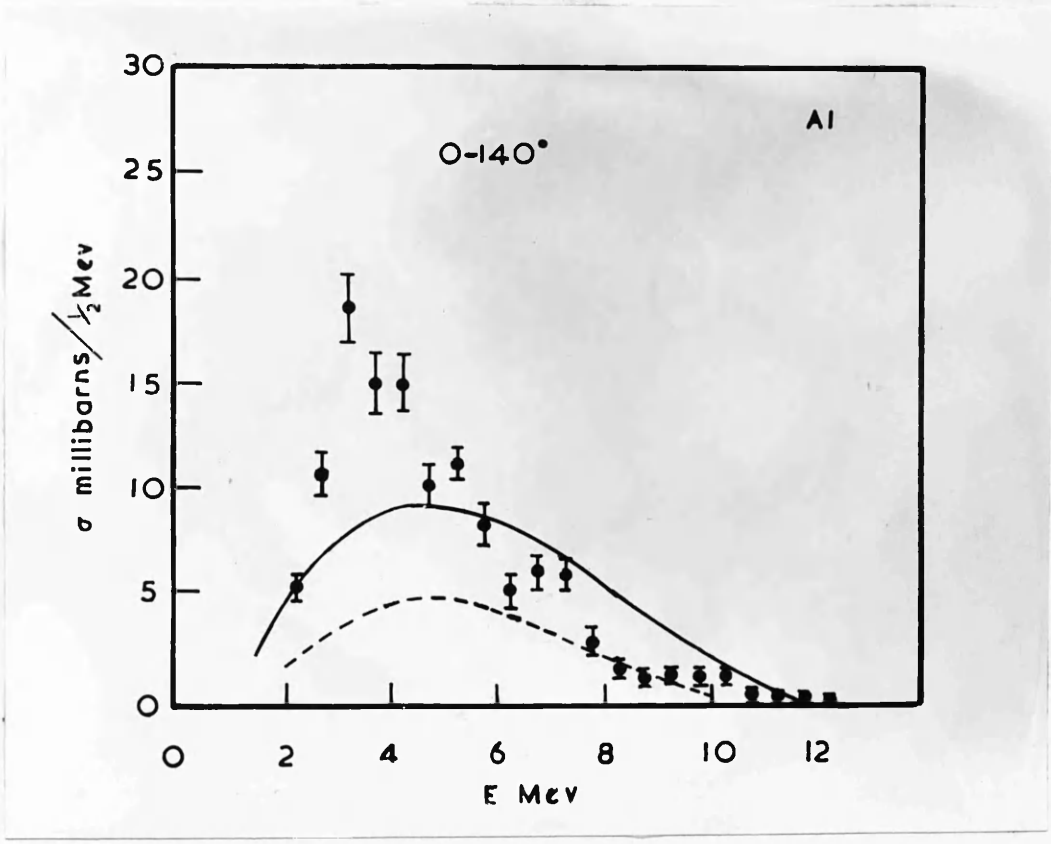

Figure 4.10: The energy spectrum of the protons emitted from aluminium.

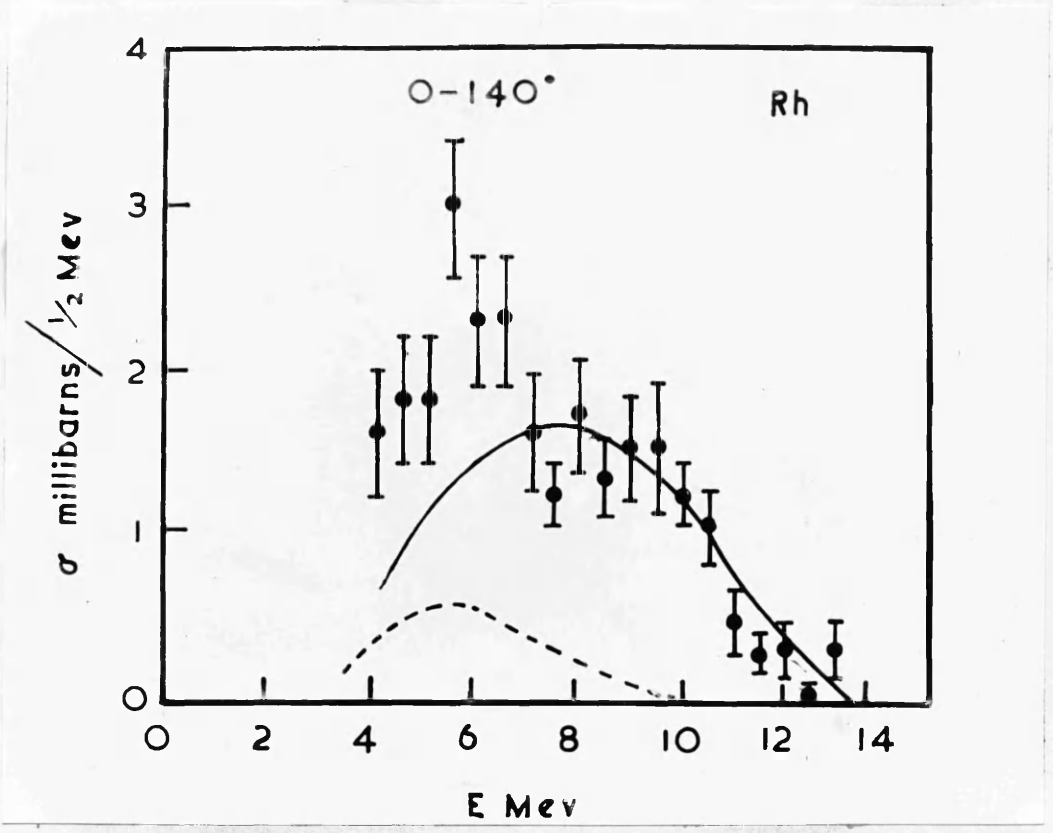

Figure 4.11: The energy spectrum of the protons emitted from rhodium.

the distribution of protons for energies less than 4 MeV is not inconsistent with symmetry about 90° . The angular distributions of protons from aluminium and rhodium also show assymmetry at all energies as can be seen in figures 4.12 and 4.13. A similar trend in the angular distribution of the high energy protons emitted when Zn^{64} is bombarded by neutrons of 14 MeV has been reported recently (Rosen, private communication).

A preferential emission of this nature would be expected if some protons were emitted following the direct collision of the incident neutron with a proton inside the nucleus. The angular distribution in the laboratory system for a free nucleon nucleon collision vanishes in the backward hemisphere. However, when account is taken of the mementum of the struck nucleon, the differential cross section for a single nucleon nucleon collision inside the nucleus would be extended to backward angles while preserving the overall forward anisotropy. It would be expected that the direct emission of protons should be enhanced relative to the emission from the decay of a compound nucleus for protons of high energy and nuclei of high atomic number. It can be seen that, experimentally, the lack of symmetry about the position of 90° is most evident for protons of high energy and that it is greatest for rhodium.

The experimental results can be compared with the predictions of a simple model which takes into account both the direct emission and that from the decay of the compound nucleus (Brown and Muirhead 1957). This model assumes that nucleon-nucleon interactions can occur throughout the nuclear volume in a similar manner to the model of nucleon nuclear inter-

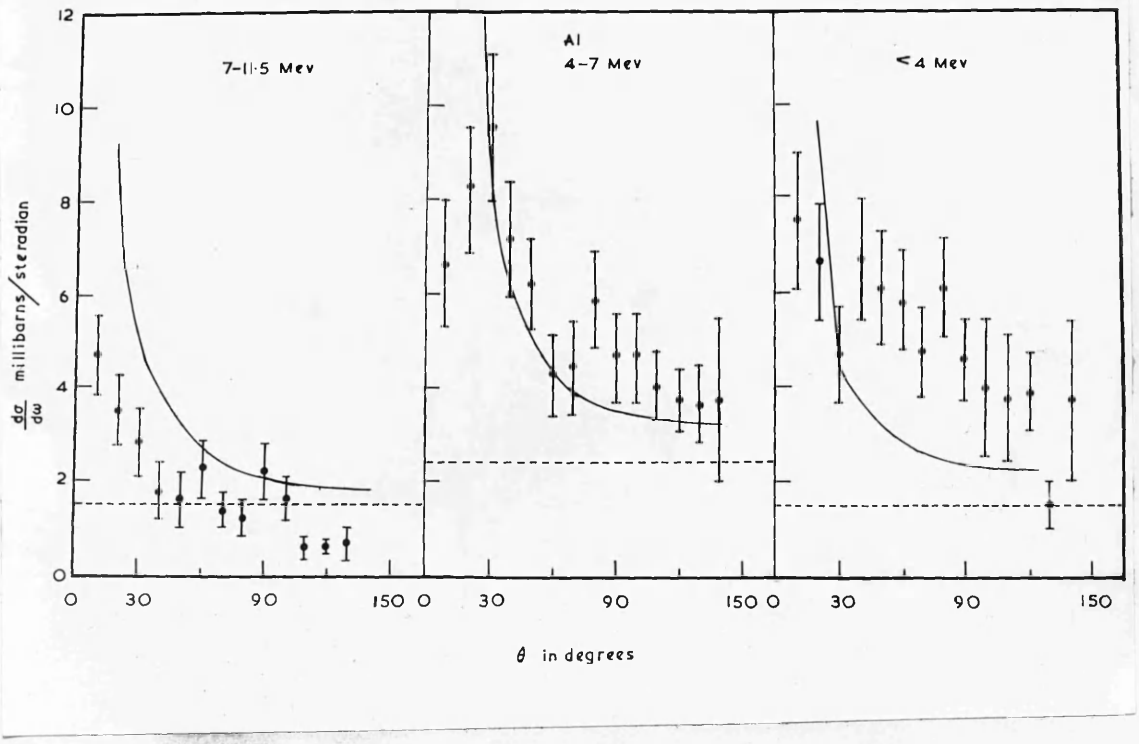

Figure 4.12: The angular distributions of the protons emitted from aluminium.

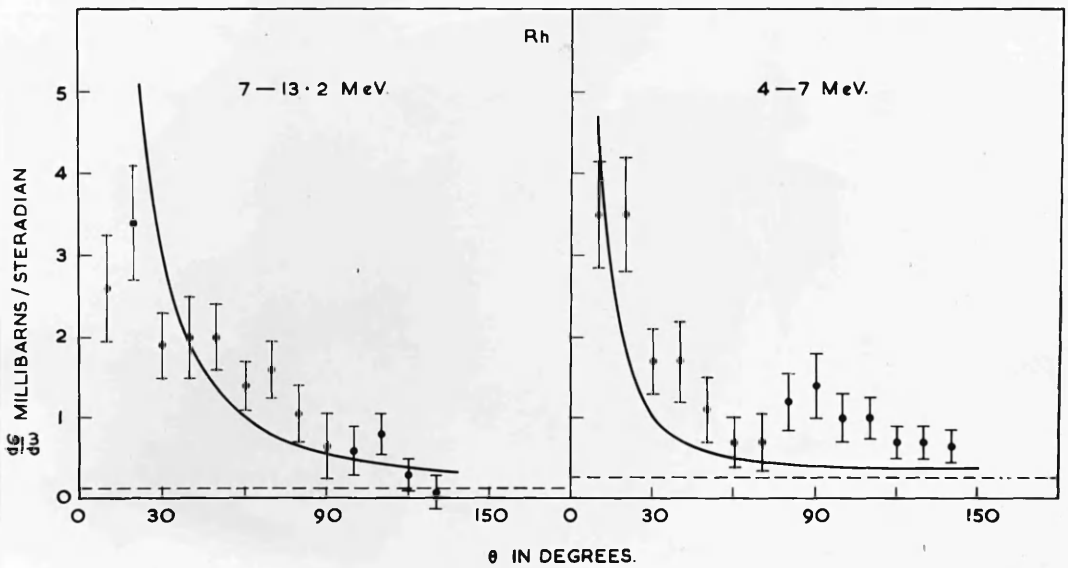

Figure 4.13: The angular distribution of the protons emitted from rhodium.

action introduced in chapter 3. At intermediate energies, however, only the first collision can lead to the direct emission of a nucleon, so that the details of the prediction of the model can be calculated analytically.

The magnitudes of the cross sections for the emission of protons in the reactions, (n,pγ) and (n,pn) have been calculated using this model. The calculated cross sections, σ_p(dir) for the emission of protons by direct collisions in Fe^{56} and Fe^{54} are 25 and 50 mb respectively. The calculated cross sections σ_p(comp) for the emission of protons by the decay of an excited nucleus are 50 and 500 mb for Fe^{56} and Fe^{54} respectively. The total cross section of 95 mb for the emission of protons from Fe^{56} is therefore in good agreement with the experimentally derived cross section of 120 mb.

In order to make a comparison with the experimental distributions, the calculated differential cross sections were added according to the isotopic mixture of Fe^{56} and Fe^{54} in natural iron. The calculated energy and angular distributions are shown in figures 4.6, 7 and 8. The calculated energy and angular distributions for aluminium and rhodium are shown also in figures 4.9, 10, 11 and 12. The broken line represents the cross section for emission of protons from the decay of a compound nucleus, while the full curve is the sum of this cross section and that for the emission of protons by direct collision.

The apparent difference in the calculated and experimental energy spectra for iron at low energies can be possibly accounted for by considering the contribution of protons from the (n,np) reaction in Fe^{54}

(Allan, private communication). The difference between the Q-values of -9.2 MeV and -13.8 MeV for the processes (n,np) and (n,2n) in Fe^{54} respectively, results in the favoured emission of protons over a region of the energy spectrum from 0 - 4 MeV. Allan finds a cross section of 220 millibarns for this reaction. More direct evidence for the importance of the (n,np) reaction is obtained in the present investigation from the excess of protons of low energy emitted from aluminium. The difference between the Q-values of -8.3 MeV and -13.0 MeV for the processes(n,np) and (n,2n) in Al^{27} respectively, results in the favoured emission of protons over a region of the energy spectrum from 0 - 4.7 MeV. In the case of Fe^{56} and Rh^{103} the effect is reduced considerably since there is no favoured emission of protons over the region of the observed energy spectrum.

Section 4.6 Conclusions

The present results for the total cross section for the (n,p) reaction in iron are in satisfactory agreement with those of other workers. Moreover, evidence for the process of direct interaction has been obtained from the angular distributions of the protons emitted in the (n,p) reaction in iron, and in the results obtained subsequently for aluminium and rhodium.

It can be seen also that the application of the model of Brown and Muirhead (loc. cit.) to these reactions leads to fair quantitative agreement with the experimental results. However, in this model conservation laws other than those for energy and momentum are neglected and the problem of transmission of the nuclear surface is oversimplified. Thus it is not surprising that detailed comparisons do not show more than semi-quantitativ

agreement.

At energies where coulombic effects are important the possibility of the enhanced production of protons at the nuclear surface should be considered (Austern et al.1953). Conservation of angular momentum, which is taken into account in this theory, could then impose more stringent conditions on the angular distributions of the outgoing protons than is assumed in the model of volume production. It is of interest, therefore, that in some cases, the observed angular distributions exhibit maxima at an angle considerably greater than 0°, whereas the calculated angular distributions always peak in the forward direction at very small angles ($\sim 5^{\circ}$). However, the statistics of the present experiment do not permit a detailed interpretation of the distributions in terms of the difference in angular momentum of the incoming neutron and outgoing proton as suggested by Austern et al. (loc. cit.)

It can be seen that considerable refinements are required in future experiments performed in this energy range. Improvement in the energy resolution is required before the suggestion of structure obtained in this investigation can be convincing. Indeed, none of the experiments so far reported for examining the (n,p), (n,n) or (p,n) processes could have detected satisfactorily the existence of discrete states superimposed on a continuum as suggested by the experiments of Gugelot (1954) on the inelastic scattering of protons.

Furthermore, improvement in the angular resolution is necessary to obtain confirmation of the appearance of maxima in the observed angular

distributions. Apart from the need for experimental improvements, however, there is an obvious need to extend the theory of nuclear reactions at intermediate energies to contain direct interaction effects.

CHAPTER 5

Nucleon Nuclear Scattering at Low and Intermediate Energies on a Simplified Free Particle Model of the Nucleus.

Section 5.1 Introduction

It has been seen that a nuclear interaction at high energies can be described in terms of a series of single nucleon-nucleon collisions inside the nucleus (Goldberger 1948). Moreover, the value of the mean free path in nuclear matter derived from the analysis of the experimental results using the optical model (the 'transparent nucleus' model) can be predicted in terms of the free nucleon-nucleon cross sections suitably modified by the restrictions of the Pauli Exclusion Principle inside the nucleus (Fernbach, Serber and Taylor 1949). Thus at high energies the transparent nucleus model and the Goldberger description of the nuclear interaction are consistent in their interpretation of the experimental results.

Recent experiments at low and intermediate energies have again been interpreted by an optical model of the nucleus. At low energies it is found that the value of the imaginary potential necessary to reproduce the experimental results implies a relatively long mean free path for nucleons in nuclear matter (Feshbach, Porter and Weisskopf 1954). At intermediate energies the application of the model indicates a reduction of the mean free path (Woods and Saxon 1954).

In chapter 3 a similar energy dependence of the mean free path was deduced from the Monte Carlo calculation on the development of a nucleon cascade inside the nucleus. On this basis the variation of the mean free

path was interpreted as a result of the reduction of the number of allowed collisions at lower energies due to the operation of the Pauli Principle. The agreement suggests therefore that the interaction of a nucleon of low and intermediate energies may be described in terms of the collisions with individual particles inside the nucleus - the free particle model of the nucleus. The description preserves the identity of the incident particle inside the nucleus without the immediate formation of a compound nucleus.

The model is therefore analogous to that employed at high energies. At high energies, however, it appears to be physically realistic to consider single nucleon-nucleon collisions because of the very small wavelength of the incident nucleon. Nevertheless, even at low energies there appears to be some physical basis to such a description. Since the nuclear potential well is comparatively deep (~ 40 MeV), when even a slow nucleon enters nuclear matter it will possess a wavelength of roughly inter-nucleon dimensions and so might be considered to move as a free particle through the nucleus.

The main work presented in this chapter is a calculation based on this model of the magnitudes of the real and imaginary potential employed in nucleon nuclear scattering problems. This was necessary in the first place to verify the consistency of the model at lower energies. The chapter is concluded with a short description of the application of the model to the detailed prediction of the course of a nuclear reaction at intermediate energies.

Section 5.2 Application of the Model

2(a) Selection of Potentials

In the optical model introduced by Feshbach, Porter and Weisskopf (1954) a complex potential of the form V + iW was used to describe the interaction between the incident nucleon and the target nucleus. The values of V and W were chosen empirically to give a best fit with the experimental data. The central part of V is close to 40 MeV; the central part of W increases from W ~ 2 MeV at zero bombarding energy to W ~ 15 MeV at an energy of 32 MeV. It is the purpose of this section to show that the magnitudes of both the real and imaginary potentials may be qualitatively predicted with the aid of data on free nucleon-nucleon scattering and a Fermi gas model of the nucleus.

The choice of the Fermi gas model is primarily dictated by the need for a mathematical approach which would be both simple and consistent. However, there appears to be some justification for considering it as an approximate physical description of the normal state of a heavy nucleus. Thus an assembly of non interacting particles, which is the basis of the model, approximates reasonably to the requirements of the shell model of the nucleus in which definite physical states exist for considerable periods of nuclear time.

The Real Potential, V

It is assumed that the target nucleus may be represented as two Fermi gases of neutrons and protons. The depth of the real well V is defined to be the sum of the maximum Fermi energy of the neutron gas E_F (n) and

the binding energy of the last neutron in the nucleus. The maximum Fermi energy is given by the well known formula,

$$E_F(n) = \frac{\hbar^2}{2M}\left(\frac{3\pi^2 N}{V_o}\right)^{\frac{2}{3}}$$

where N is the number of neutrons, V_o is the nuclear volume and M is the mass of a nucleon. The radius R of the neutron gas was assumed to be given by $1.37\ A^{\frac{1}{3}} \times 10^{-13}$cm, where A is the atomic weight of the nucleus. This value of the radius appears to fit the experimental results at high energies With this assumption, a value of the maximum Fermi energy of 28 MeV is obtained for A 100 which leads to a value of V of 38 MeV. The value of V is almost insensitive to A in the range of A from 50 to 200 as can be seen from table 5.1. The binding energies were obtained from the tables of Feather (1953).

The further assumption was made that the real potential V is the same for the proton gas as for the neutron gas. Since the binding energy of the last proton is about 7 MeV throughout the periodic table (Feather, loc. cit.), the maximum Fermi energy of the protons $E_F(p)$ has a value of 31 MeV. Then the radius of the proton gas is fixed at a value of $(1.18 \pm 0.04)\ A^{\frac{1}{3}} \times 10^{-13}$cm.

The Imaginary Potential, W

An expression relating the imaginary potential W and the mean free path λ of a particle in nuclear matter has been given by Francis and Watson (1953):

$$W = \frac{\hbar}{\lambda}\left(\frac{E_1}{2m}\right)^{\frac{1}{2}} = \frac{\hbar}{\lambda\sqrt{2m}}\left(E + V\right)^{\frac{1}{2}},$$

Table 5.1: Calculated Values of the Real Potential V.

Nucleus	Maximum Fermi Energy in MeV	Binding Energy of Last Neutron in MeV.	Depth of Real Potential im MeV
Na^{23}	26.8	12.2	39.0
Fe^{56}	27.3	11.2	38.5
Ag^{109}	28.3	9.1	37.4
Pb^{208}	29.7	7.4	37.1
U^{238}	29.9	6.1	36.0

where E_1 represents the kinetic energy of the incident nucleon inside the nucleus, E the kinetic energy outside the nucleus and m the nucleon mass. Thus the imaginary potential W can be calculated from a knowledge of the mean free path λ.

On the free particle model, the mean free path λ can be expressed in terms of the cross section for free particle scattering modified by the restrictions of the Pauli Exlcusion Principle in the manner first described by Fernbach et al (1949):

$$1/\lambda = \alpha_{Np}\,\sigma_{Np}\,\rho_p + \alpha_{Nn}\,\sigma_{Nn}\,\rho_n$$

where α_{Np} = Pauli factor for a nucleon N in collision with a proton inside the nucleus

σ_{Np} = free nucleon-proton scattering cross section

ρ_p = proton density in the nucleus

and the other three terms represent the corresponding quantities related to a collision with a neutron. In the model a collision is only allowed if both nucleons possess a final energy greater than the maximum Fermi energy; the Pauli factor α is the probability that a collision will be allowed under these conditions. Hence, the problem is now resolved into one of determining the Pauli factors α.

The term α has been calculated by Goldberger (1948) for nucleons whose energies inside the nucleus are greater than twice the maximum Fermi energy, $E_1 \geq 2\,E_F$. He obtains the following simple expression for α:

$$\alpha = \left(1 - \frac{7}{5}\,\frac{E_1}{E_F}\right)$$

where the symbols have their previous definition. In the present work the calculation was extended to lower energies to enable the imaginary potential W to be determined in the region of interest. The calculation included correction factors for the difference in binding energy of the last neutron and protons which becomes of increased importance at low energies, and the non-isotropy of neutron-proton scattering in the centre of mass system for energies greater than about 20 MeV. The priniciple of the calculation is given in appendix 4.

The calculated variation of the Pauli factor α for proton-proton or neutron-neutron scattering inside the nucleus as a function of the ratio $\frac{E_F}{E_1}$ is shown in fig 5.1 for $E_F \leq E_1 \leq 2E_F$. The predicted variation of α for $E_1 \geqslant 2E_F$ using the Goldberger formula is also shown. For proton-proton collisions, $E_1 = 2E_F$ corresponds to an energy of the incident proton of 24 MeV outside the nucleus. The Pauli factor for neutron-proton or proton-neutron scattering inside the nucleus can also be obtained from figure 5.1 when the corrections given in the appendix 4 are taken into account. Thus the mean free path λ in the interior of the nucleus can be obtained at different energies using the published data on n-p and p-p scattering and assuming that the latter is equivalent to n-n scattering.

From the calculated variation of λ the imaginary potentials in the interior of the nucleus were estimated to be

$$W \sim (3.0 + 0.35E) \text{ MeV for neutrons ,}$$

$$\sim (1.3 + 0.35E) \text{ MeV for protons ,}$$

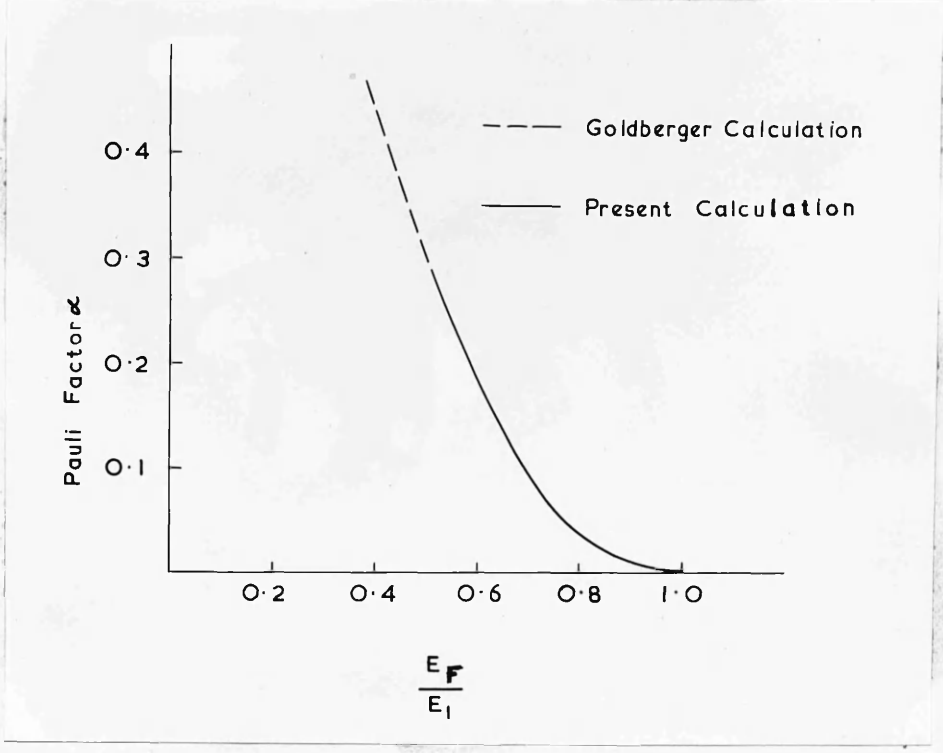

Figure 5.1: Calculated variation of the Pauli Factor for the scattering of identical nucleons inside the nucleus.

where E is expressed in MeV. The calculated expressions are appropriate for values of E lying between 0 and 24 MeV and for a nucleus in the middle of the periodic table. However, like the value of V, the expressions are fairly insensitive to the nucleus involved, over the range A = 50 - 200. The expressions are also fairly insensitive to changing the value assumed for the nuclear radius, since the resulting change in the Pauli factors α, is of the opposite sign to the changes produced in the density ρ and the real potential V.

In figure 5.2 the variation of the imaginary potentials are shown as a function of energy. The 'experimental' points are those derived by various authors in successful applications of the optical model to the analysis of scattering experiments at different energies. The experimental points at low energies have been obtained using a square well potential. The use of a rounded well, which is a physically more realistic representation of the nucleus (c.f. Woods and Saxon loc. cit.) would require a larger imaginary potential to fit the same experimental data; the smaller time spent on the average by a nucleon inside the nucleus as a result of the reduction of the internal reflection can only be compensated by an increased rate of absorption during that time. Thus the agreement might be improved at low energies.

However, the most striking feature of the results is the manner in which the empirical reduction in W at lower incident energies is reproduced In the theoretical curves the fall-off arises purely from the effect of the Pauli Principle which prevents an increasing number of collisions as

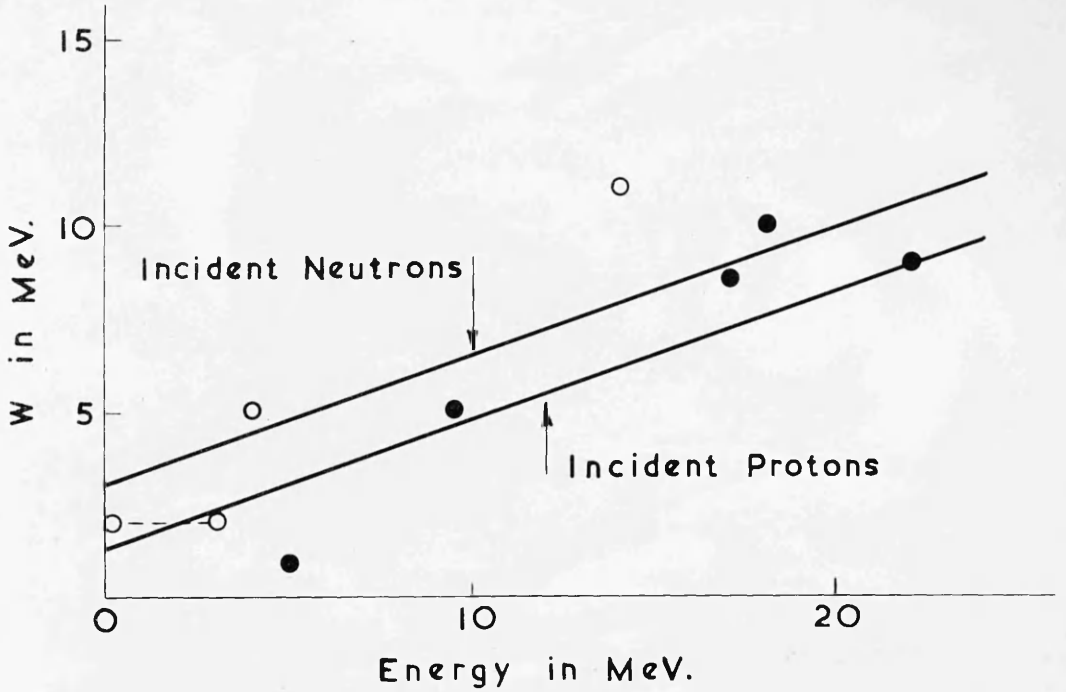

Figure 5.2: The imaginary part of the complex potential W as a function of the energy of the incident particle;

——— calculated variation;

o value derived from the analysis of neutron scattering data:
0 to 3 MeV - Feshbach, Porter and Weisskopf (1954),
4 MeV - Walt and Beyster (1955),
14 MeV - Culler, Fernbach and Sherman (1956);

● value derived from the analysis of proton scattering data:
5 and 17 MeV - Melkanoff et al. (1956),
9.5 MeV - Prowse and Hossain (1956),
18 and 22 MeV - Woods and Saxon (1954).

the incident energy is lowered. A similar conclusion has been reached also by Lane and Wandel (1955) and Clementel and Villi (1955). The successful application of the model to predict the absolute behaviour of W as a function of the energy of the incident particle serves therefore to establish the consistency of the free particle model at low energies.

2(b) Direct Interaction Effects.

The application of the free particle model at low energies shows that the mean free path can be interpreted in terms of the cross section for collision with individual nucleons inside the nucleus. The result suggests therefore that a nuclear reaction at these energies may be capable of a similar description to that employed at high energies (c.f. the Goldberger model). The products of a nuclear reaction may again be separated into two categories: those emitted by direct interaction and those from the decay of a compound nucleus. In view of the long period of decay of the compound nucleus it seems reasonable to assume that the two processes of emission can be examined separately.

At intermediate energies only the first collision should be important in contributing to the direct interaction process. Subsequent collisions are most likely to leave both particles with insufficient energy to escape from the nucleus. Thus it should be possible to calculate analytically the magnitude of the direct interaction effects at these energies without resort to the Monte Carlo type of calculation which was necessary at high energies.

The cross section for producing a nucleon (either a neutron or a

proton) inside the target nucleus N with kinetic energy between ϵ and $\epsilon + d\epsilon$ is given by

$\left(\frac{d\sigma}{d\epsilon}\right)_N$ = cross section for the collision with a nucleon inside the nucleus x the probability of the nucleon having an energy ϵ after collision.

The derivation of the Pauli factor α was based on the calculation of the latter probability. Thus the cross section for direct emission of a nucleon can be obtained from the previous procedure if suitable assumptions can be made concerning the penetration of the surface of the nucleus by the outgoing particles. A particle can only escape from the nucleus if its energy ϵ is greater than V the depth of the nucleon potential well. The cross section for direct emission of nucleons of energy $E = \epsilon - V$, can be written as

$$\frac{d\sigma}{dE} = \left(\frac{d\sigma}{d\epsilon}\right)_N \phi(E)$$

where $\phi(E)$ represents the probability of escape from the nucleus.

After allowance has been made for the direct emission of particles by the initial collision of the incident nucleon, it can be assumed that all subsequent collisions lead to the formation of a compound nucleus. Thus, in this model the cross section for formation of a compound nucleus is simply the difference between the reaction cross section (predicted by the optical model) and the cross section for the emission of particles by direct interaction. The decay of the compound nucleus can then be described by the statistical theory using the formula presented in section 1.3(c).

The procedure described here is the basis of a calculation of the cross section for direct interaction processes which has been carried out by Brown and Muirhead (1957). A calculation of the differential cross section for the direct scattering of a nucleon by a Fermi gas of nucleons has been given by Hayakawa et al. (1955). The predictions of the model with regard to the energy and angular distribution of the direct interaction in the (n,p) reaction have been considered in chapter 4.

Section 5.3: Discussion

The free particle model of a nuclear reaction is a completely classical description of the interaction. It is based on a concept of the nucleus as a well defined sphere of nucleons with a sharp nuclear surface; direct interaction is considered to take place throught the nuclear volume.

Recent interpretation of experiments on the elastic scattering of high energy electrons by nuclei (Hahn et al. 1956) has shown that a more realistic description of the nucleus is one with a tapered density distribution; in consequence the nuclear potential falls off comparatively slowly. Thus it may be that there are more states available to a scattered nucleon in the surface of the nucleus than throughout the volume. For this reason direct interaction at the nuclear surface may be enhanced, since it may be possible to relax the restrictions of the Pauli Exclusion Principle on a collision in the nuclear surface. Such an effect could be particularly important for protons since the escape of protons produced by direct collision processes within the nuclear volume is severely reduced by the coulomb

barrier at the surface of the nucleus. A calculation of the surface direct interaction has been considered by Eisberg (1954) and Austern, Butler and McManus (1952).

Chapter 6

Conclusions

It is apparent that during the time that this research has been carried out considerable progress has been made towards a better understanding of the mode of interaction of nucleons with nuclei. Thus it appears that an optical model which preserves the identity of the incident particle inside the nucleus is capable of a description of nuclear reactions over a much wider range of energies than was thought possible only a few years ago. At low energies the assumption of the immediate absorption of the incident particle has been revised to admit a nucleon mean free path which is comparable with the nuclear dimensions. Furthermore the occurrence of direct interaction has been recognised as a distinctive feature of nuclear reactions at intermediate energies. The research presented in the thesis has been influenced by and was of importance to the change in outlook which has taken place.

It is important to note that it is possible to retain many useful features of the compound nucleus model within the framework of the optical description. The formation of a long-lived compound nucleus is now regarded as the final phase of the interaction. The theory of the compound nucleus is still widely applicable as a description of a nuclear reaction at intermediate energies.

In view of the wide success of the optical model, it is natural that theoretical attention should now be given to the attempt to understand the validity of the model from a fundamental point of view (c.f. Lane, Thomas and Wigner 1955, Breuckner 1956). At low

energies the weak interaction which apparently exists inside the nucleus is in marked contrast to the strong interaction observed between isolated nucleons. It is possible that the independent particle behaviour can be explained as a property of a system of strongly interacting particles of low excitation energy.

At high energies, the scattering of particles by a nucleus can be satisfactorily described in terms of the observed two body scattering cross sections which have been reduced to allow for the Pauli Exclusion Principle. At low energies it has been shown that the Exclusion Principle can be of much greater importance in limiting the collisions of a nucleon inside the nucleus. At low energies, however, it is no longer clear that a collision inside the nucleus may be specified as occurring between individual nucleons. At the present time, therefore, the success of the optical description of strongly interacting particles by an effective average potential is still incompletely understood.

Appendix 1 The range-energy relationships for protons in Ilford G.5 x 2 and G.5 x 4 diluted emulsions.

The extremely sensitive nuclear emulsions employed in recent years have contained a very high silver halide to gelatin ratio, the silver halide occupying approximately half of the volume of emulsion. Their sensitivity was mainly dependent on this feature. However, it has been estimated that up to a 50% increase of gelatin content could be made without loss of the ability to recognize tracks. The results obtained at Ilford with actual emulsions agreed with these predictions. A series of emulsions which, whilst capable of recording the passage of particles at minimum ionisation, possess a much smaller silver halide content have been made generally available by Ilford. These are known as diluted Ilford G.5 emulsions.

Such diluted emulsions are of value for several reasons; for example in the study of nuclear reactions induced in light elements, or for investigations in which multiple scattering of particles passing through the emulsion needs to be minimised, it is advantageous to use emulsions with a higher relative content of light elements than is present in normal emulsions. It is also advantageous (c.f. Chapter 3) to have electron sensitive emulsions of different constitutions from the normal G.5 emulsions. However before these diluted emulsions can be used in nuclear physics research, a knowledge of the range-energy relationships for particles recorded by them is essential. A determination of the range-energy relationship for protons is only necessary, since that for other

singly charged particles and doubly charged alpha-particles can be reliably deduced.

The range-energy relationship for protons and alpha-particles has been experimentally determined in a number of investigations. There seems to be no difference in the stopping powers of the standard Ilford emulsions (Ilford B1 to G.5 emulsions), so that a range-energy relationship can be found which is satisfactory for all the emulsions of standard composition. However, the charge in constitution of the dilute emulsions should alter this relationship.

The experimental determination of this relationship was carried out by exposing the Ilford G.5 x 2 and G.5 x 4 dilute emulsions (that is, emulsions with twice and four times the normal value of the gelatin to silver halide ratio) under vacuum conditions to protons produced by the bombardment of Li and B with 550 KeV deuterons from the Glasgow H.T. set. The energies of the proton groups from the different reactions (table 1) were reduced by passage through an aluminium window before entering the diluted emulsions. The effective energies were determined by exposing Ilford G.5 emulsions under identical conditions. Using the experimental range-energy curves for this emulsion (Rotblat 1950, 1951), the kinetic energy of the incident proton groups was determined. The proton ranges were measured with a calibrated eyepiece scale taking into account the dip and scattering of the tracks in the emulsion, and using a shrinkage factor appropriate to the emulsion considered. However, to eliminate any uncertainty in the shrinkage factor, only approximately horizontal

Table 1: Ranges of Protons in Ilford G.5 Emulsions

Reaction	Exptl.range (μ)	Energy (MeV)	Calc.range (μ)
(i) $^{2}_{1}H + {}^{2}_{1}H \rightarrow {}^{3}_{1}H + {}^{1}_{1}H$ $^{12}_{6}C + {}^{2}_{1}H \rightarrow {}^{13}_{6}C + {}^{1}_{1}H$	67.6 ± 0.2	2.84	67.5
(ii) $^{6}_{3}Li + {}^{2}_{1}H \rightarrow {}^{7}_{3}Li^{*} + {}^{1}_{1}H$	130.9 ± 0.3	4.27	129
(iii) $^{6}_{3}Li + {}^{2}_{1}H \rightarrow {}^{7}_{3}Li + {}^{1}_{1}H$	152.6 ± 0.3	4.68	150.5
(iv) $^{10}_{5}B + {}^{2}_{1}H \rightarrow {}^{11}_{5}B^{\dagger} + {}^{1}_{1}H$	283.0 ± 0.9	6.81	284
(v) $^{10}_{5}B + {}^{2}_{1}H \rightarrow {}^{11}_{5}B + {}^{1}_{1}H$	444.0 ± 0.8	8.90	446

* excited state of 440 KeV
† excited state of 2.14 MeV

Table 2: Ranges of Protons in Ilford G.5 x 2 and G.5 x 4 Emulsions

Energy MeV	2.84	4.27	4.68	6.81	8.90
Exptl.range in G.5 x 2(μ)	75.3±0.2	144.6±0.3	169.0±0.3	316±1.4	498±0.9
Calculated range in G.5 x 2 (μ)	75.0	145	169	319	506
Exptl.range in G.5 x 4 (μ)	82.9±0.2	161±0.4	188±0.3	361±1.0	565±0.8
Calculated range In G.4 x 4 (μ)	81	158	185	354	562

tracks were considered for measurement. The proton ranges fall into different groups related to the expected energies of the protons from the deuteron induced reactions. The experimental results are given in tables 1 and 2, the quoted range in all cases being the arithmetic mean of the ranges in a group.

Calculated values of the range were also obtained, by a consideration of the dependence of the stopping power of the emulsion upon its chemical constitution in the manner described by Webb (1948). From a knowledge of the atomic stopping power of the different constituents of the emulsion to a particle, and the fractional weight of each constituent in the emulsion, the ratios $\frac{\Delta R}{\Delta R_o}$ of the differential ranges for small energy increments can be calculated, where R_o is the range in air and R is the range in emulsion of the particle. For a specific material $\frac{\Delta R_o}{\Delta R} = \left(\frac{N}{N_o}\right) S$ by definition, where S is the atomic stopping power of the material, N_o and N are the effective number of atoms per cc in air at S.T.P. and the number of stopping atoms per cc, respectively. A generalisation of the above equation leads to the ratio $\frac{\Delta R_o}{\Delta R}$ for emulsion. From this relation the differential ranges in emulsion can be calculated and hence the integral emulsion ranges R for different energies.

The atomic constitutions used in the calculation correspond closely to vacuum conditions of the emulsion. The agreement between the calculated and experimental values shown in tables 1 and 2 was always within 2%. The experimental results for protons can be represented by the following empirical formulae in the range 2.5 - 9 MeV with an error of less than 1%:

$$E = 0.227\ R^{0.602} \text{ for G.5 emulsion},$$

$$E = 0.221\ R^{0.595} \text{ for G.5 x 2 emulsion},$$

$$E = 0.220\ R^{0.583} \text{ for G.5 x 4 emulsion},$$

where E is in MeV and R in microns.

The results presented above are valid for plates exposed under vacuum conditions. If exposed under normal atmospheric conditions the ranges are longer due to the water absorbed by the gelatin of the emulsion The increase in range at a relative humidity of 60% was calculated for proton energies of 2 and 10 MeV. For G.5 emulsions the amount of water absorbed per cm^3 at various relative humidities is known (Wilkins 1951) If it is assumed that the amount of water absorbed by an emulsion is proportional to the amount of gelatin in that emulsion, and that the volume of the emulsion increases by the amount of water absorbed, then the atomic constitutions can be recalculated. The increases in range were then derived using Webb's method. The results are shown in table 3.

For protons of energy below 2.5 MeV the calculated range-energy relationships were expected to hold. Their validity for protons of energy as low as 1.4 MeV was checked by making measurements on the ranges of polonium and thorium C^1 α - particles.

For two particles a and b of the same velocity the ranges are related by the equation $R_b(v) = \left(\frac{Z_a}{Z_b}\right)^2 \frac{M_b}{M_a} R_a(v)$, where R (v) refers to the range of the particle of velocity v, and M and Z refer to the mass and charge of the particles respectively. In terms of the particles of the same energy, we then have

Table 3: Calculated Increase in Range at 60% Relative Humidity

Emulsion	G.5		G.5 x 2		G.5 x 4	
Proton energy (MeV)	2	10	2	10	2	10
% increase in range at 60% relative humidity	3.3	4.0	3.6	4.5	4.2	5.0

$$R_b(E) = \left(\frac{Z_a}{Z_b}\right)^2 \cdot \frac{M_b}{M_a} \cdot R_a\left(\frac{M_a}{M_b} E\right).$$

This expression is strictly only true when $Z_a = Z_b$. The residual ranges of protons and alpha-particles are connected by the following expression, $R_p(E) = 1.0069\ R_\alpha(3.973E) - c$, where the constant c arises from the difference in the random capture and loss of electrons for particles of different Z at low energies. The constant is given as 1.5 μ for G.5 emulsions (Wilkins loc. cit.). A value for c of 1.65 μ and 1.8 μ for the G.5 x 2 and G.5 x 4 emulsions respectively was derived by considering the percentage increase of the ranges of protons in these emulsions. From this formula the energy of an alpha-particle can be determined from its range using the range-energy relationship for a proton.

In order to check the calculated range-energy relationships for protons of energy less than 2.5 MeV, corresponding to alpha-particles of energy less than 10 MeV, measurements were made on the ranges of polonium and thorium C[1] α - particles of energies 5.3 and 8.78 MeV respectively using Ilford G.5, G.5 x 2 and G.5 x 4 emulsions. The expected ranges of α- particles of energies 5.3 and 8.78 MeV were calculated from the above expression involving R_p and R_d using the calculated proton ranges, and are compared in table 4.

In actual experiments, however, the α- particle tracks were obtained by dipping the plates in radioactive solution and drying quickly to normal atmospheric conditions, the plates being kept under the same conditions until developed. The experimental ranges were, as a result, ~~no~~ longer than those calculated for vacuum conditions due to the absorption of water

Table 4: Range of α - particles in Ilford G.5., G.5 x 2 and G.5 x 4 Emulsions.

Emulsion	α- particle source	Experimental	Calculated	
			Vacuum Conditions	60% R.H.
G.5	Polonium	22.88 ± 0.04	21.85	22.84
	Thorium C'	47.87 ± 0.08	46.5	47.7
G.5 x 2	Polonium	24.86 ± 0.06	23.6	24.7
	Thorium C'	52.8 ± 0.13	51.2	52.6
G.5 x 4	Polonium	26.63 ± 0.66	25.3	26.5
	Thorium C'	58.29 ± 0.15	56.0	58.2

vapour. Values were also calculated assuming a relative humidity of 60%, and gave good agreement with those obtained experimentally. Thus the use of the calculated range-energy relations for proton energies below 2.5 MeV is justified.

The range-energy curves are presented in figure 1. Above 2.5 MeV, the curves pass through the experimental points; below 2.5 MeV, the curves represent the calculated variation of the range.

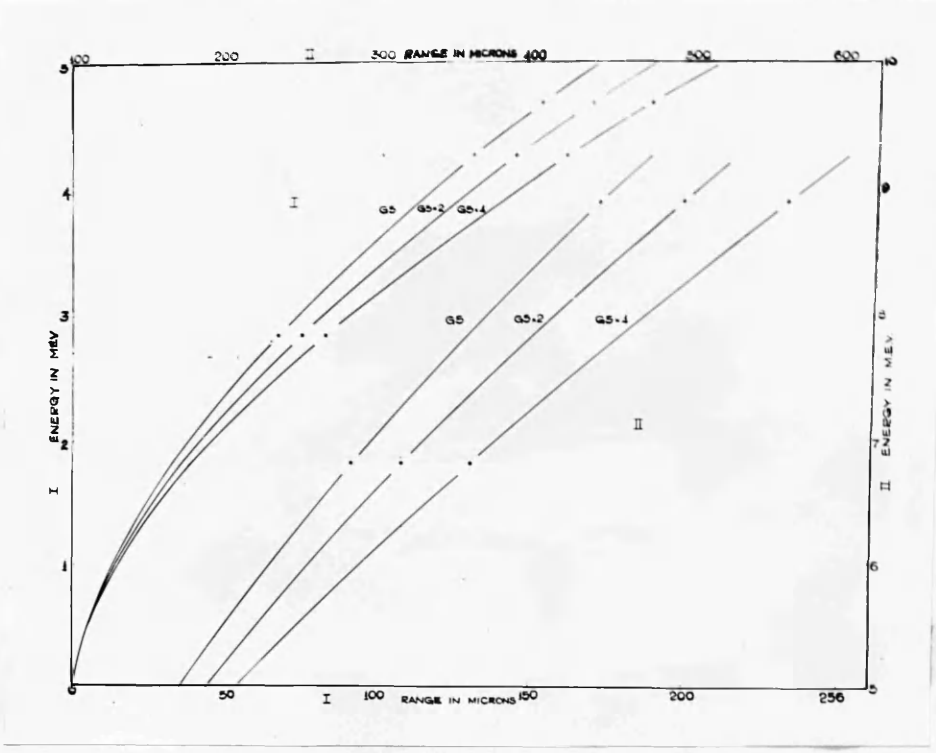

Figure 1: The range-energy curves for protons in G5, G5 x 2 and G5 x 4 emulsions.

Appendix 2: The Correction for the Energy Loss of Protons Produced in a Semi-thick Target.

Because of the variation in the thickness of foil traversed for protons with different angles of dip with respect to the surface of the emulsion the protons observed to originate in the iron foils were separated into two regions of dip angle, 10 - 20° and 20 - 30°; the protons which were observed with angles of dip less than 10° were ignored because of the large thickness of foil they might traverse. The analysis was performed first for the interval 20 - 30° since the energy loss is least in this region. An energy spectrum of protons, which will be called the "source spectrum" was chosen, say of the form $N_S(\epsilon)\, d\epsilon$.

The semi-thick target was then replaced by six thin targets each 2 mg/cm^2 thick and it was assumed that the source spectrum for the protons starting in each of these sections was the same. The number of protons $N(\epsilon)\, d\epsilon$ which would then be emergent from the thick target is given by

$$N(\epsilon)d\epsilon = \sum_{k=1}^{k=6} N_k(\epsilon + x_k)\, d\epsilon \quad ,$$

where x_k is the loss in energy of a proton, which starts in section k with an energy $(\epsilon + x_k)$, in traversing the remainder of the thick target.

The energy spectrum of the protons obtained from this choice of source spectrum was compared with that observed experimentally; a relaxation method was then applied to find the source spectrum which, after allowance for the energy loss, gave a spectrum consistent with that observed experimentally. This calculation was performed for the two intervals

20 - 30° and 10 - 20° dip. The spectra obtained in the two intervals were in good agreement. The results presented in chapter 4 are those corrected by this method.

After the above correction was applied, it was realised that the source spectra could be also obtained if the problem is considered in terms of the range rather than the energy of the particles. If the observed energy spectra is plotted in intervals of range ΔR, then the maximum thickness of foil traversed by a proton, allowing for the angle of dip, can be converted into an equivalent range in the emulsion, $n\Delta R$. In this way, the semi-thick target is replaced by n thin targets. It follows, as previously, that the observed number of protons $N(R)\,dR$ emerging from the thick target is given by

$$N(R)dR = \sum_{k=0}^{n-1} N_k\left[R + (k+\tfrac{1}{2})\Delta R\right]dR \quad ,$$

where $N_k(R)\,dR$ is the range distribution of protons which start in the kth section of the target.

This representation possesses the advantage that the distribution of particles from the first section of the target (and hence from all other sections) can be obtained directly without resort to the relaxation method.

The observed number of protons in each interval of range can be successively corrected, starting from the high energy side of the distribution, for the contribution of protons produced in sections of the target other than the first. The corrected range distribution obtained

in this way can be immediately expressed as the corrected energy spectrum.

As a check on the results obtained by the former method, a correction according to the range was carried out for the same intervals, 20 - 30° and 10 - 20° dip. It was found that the spectrum obtained by each method was in good overall agreement as can be seen from examination of table 1.

The angular distribution of the protons in the 'source' spectrum can also be obtained from the angular distribution of the protons observed experimentally. It was assumed that there is no scattering through very large angles for the protons passing through the iron foil. Thus a proton observed at an angle is the emulsion can be related to an angle of emission in the ~~emulsion~~ foil.

From the previous considerations, it follows that the number of protons $N_s(\epsilon)\, d\epsilon$ in the source spectrum with energies between ϵ and $\epsilon + d\epsilon$ can be expressed in terms of the energy spectrum observed experimentally as

$$N_s(\epsilon)\, d\epsilon = X\, N(\epsilon_1)\, d\epsilon + Y\, N(\epsilon_2)\, d\epsilon + Z\, N(\epsilon_3)\, d\epsilon + \ldots$$

where X is that fraction of the total observed number, $N(\epsilon_1)d\epsilon$, of protons of energy ϵ_1 which have an energy, after correction for energy loss, of ϵ. The other terms have a similar definition.

It follows therefore that the required angular distribution $f(\theta)\, d\theta$ of the protons of energy ϵ in the source spectrum is given by

$$f(\theta)\, d\theta = X\, f_1(\theta)\, d\theta + Y\, f_2(\theta)\, d\theta + Z\, f_3(\theta)\, d\theta + \ldots$$

where $f_1(\theta)$ is the angular distribution of the protons of energy ϵ_1 and the other terms are correspondingly defined.

Table 1: Number of Tracks in Source

Spectra Corrected for Energy Loss in Iron Foil.

Energy Interval in MeV	Angle of Dip, 20 - 30°		Angle of Dip, 10 - 20°	
	Correction by Energy	Correction by Range	Correction by Energy	Correction by Range
< 2.5	36	48	24	-
2.5 - 5.0	258	248	222	252
5.0 - 7.5	153	153	153	147
7.5 - 10.0	63	65	63	63
> 10.0	3	8	3	21
Total	513	522	465	483

Appendix 3: Calculation of the Solid Angle for Acceptance of Protons Emitted at an Angle θ to the Direction of the Incident Neutrons.

We consider a coordinate system in which the direction of the incident neutron is along the x-axis and the point at which the (n,p) reaction occurs in the target is at O, the intersection of the axes. It can be assumed that the point of interaction O lies on the surface of the emulsion. We now construct the sphere of unit radius with centre O, shown in figure 1. The section of the sphere perpendicular to the emulsion surface containing the direction of the incident neutron (the xy plane) is shown in figure 2a. With reference to figure 2a, we define:

ϕ = angle in the xy plane between the surface of the emulsion (ST) and the x-axis.

θ = angle of emission of the proton with respect to the x-axis; protons emitted at this angle to the x-axis intersect the unit sphere in the circle with diameter PQ (c.f. figure 1).

γ = maximum angle of dip of protons accepted; protons emitted at this angle of dip to the emulsion surface intersect the unit sphere in the circle with diameter UV (c.f. figure 1)

It will be assumed that $\gamma < \phi < 90-\gamma$ in the subsequent discussion, although the result derived for this case can be shown to be general.

The total solid angle available to protons emitted at an angle between θ and $\theta + d\theta$ is $2\pi \sin\theta \, d\theta$, i.e, it is proportional to the circumference of the circle in the plane perpendicular to the x-axis with diameter PQ

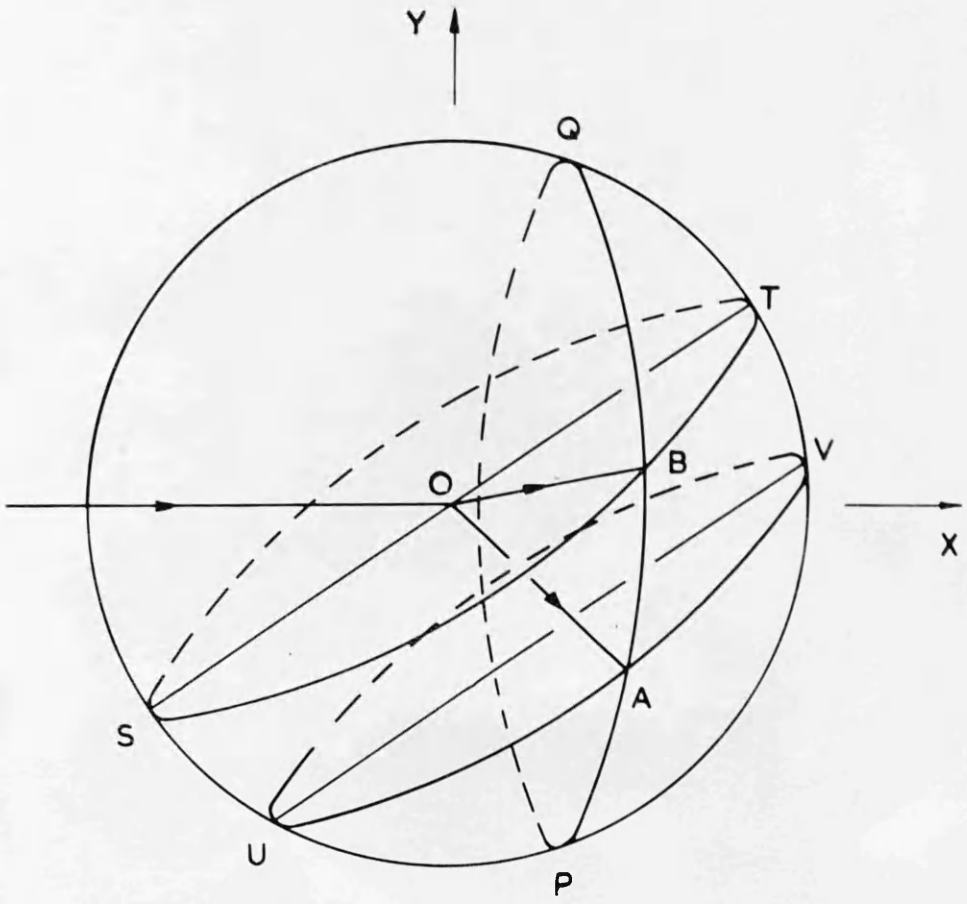

Figure 1: Unit sphere illustrating the restrictions imposed on the solid angle available for acceptance of protons.

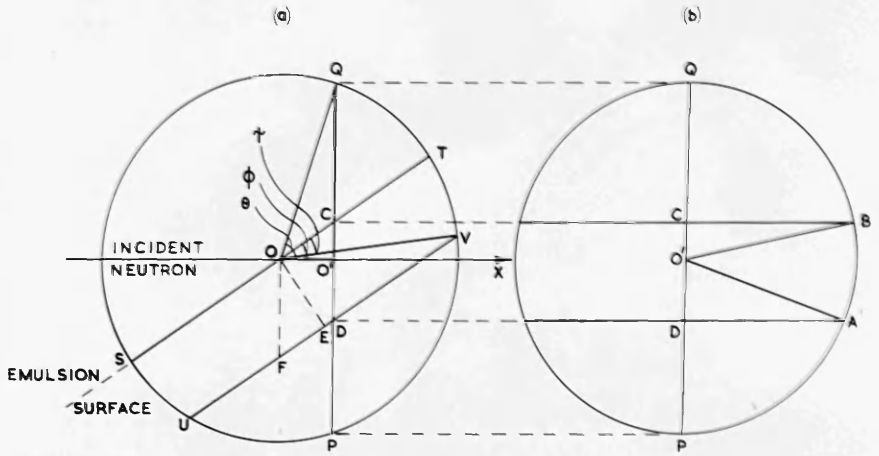

Figure 2: Geometry considered in the calculation of the solid angle;

(a) Section of unit sphere perpendicular to emulsion surface containing direction of the incident neutron;

(b) Section of unit sphere perpendicular to direction of incident neutron as shown.

(= 2 sin θ). This circle is shown in figure 2b. However, as a result of the geometrical restrictions imposed on the observation of a proton track at an angle θ, the end of the unit vector representing the direction of the emitted proton can only lie on part of the circumference of this circle, namely twice that part between A and B. This is clear from figure 1, where OB defines a track emitted at an angle θ with dip angle of 0° and OA defines a track emitted at an angle θ with dip angle of ψ Thus, the solid angle available for acceptance of a proton emitted at an angle θ is given by

$$d\Omega_\theta = 2AB\, d\theta$$

The problem is now reduced to a determination of the dependence of AB on θ, ϕ and ψ. This can be carried out with the aid of the constructions shown in figures 2a and 2b.

From figure 2b

$$AB = \underline{/AO'B} \times O'A$$
$$= \underline{/AO'B} \sin\theta$$
$$= (\hat{AO'C} - \hat{BO'C}) \sin\theta$$
$$= \left(\cos^{-1} \frac{O'C - DC}{O'A} - \cos^{-1} \frac{O'C}{O'A}\right) \sin\theta$$

From figure 2a

Construction: OE perpendicular to OC

OF parallel to CD

Since UV is parallel to ST, it follows that

$$DC = FO = \frac{OE}{\cos\phi} = \frac{\sin\psi}{\cos\phi},$$
$$O'C = OO' \tan\phi = \cos\theta \tan\phi$$

Hence $d\Omega_\theta = 2AB\, d\theta$

$$= 2 \left\{ \cos^{-1} (\cot\theta \tan\phi - \frac{\sin\gamma}{\sin\theta \cos\phi} \right.$$
$$\left. - \cos^{-1} (\cot\theta \tan\phi) \right\} \sin\theta \, d\theta \, .$$

From this formula, the solid angle available for acceptance of a proton emitted at an angle θ was calculated for the particular case considered in chapter 4, namely $\phi = 30^{\circ}$ and $\gamma = 30^{\circ}$.

Appendix 4: The Calculation of the Pauli Factors.

In order to compute the Pauli factor α it is necessary to calculate the probability for a nucleon to possess an energy in the range ϵ to $\epsilon + d\epsilon$ inside the nucleus after a collision, since the collision can only occur if $\epsilon > E_F$. In the general case of the collision of a nucleon of energy E_1 with a nucleon inside the nucleus of energy E_2 and momentum P_2 moving in a direction ϕ with respect to the incident nucleon, the cross section for scattering between the limits ϵ and $\epsilon + d\epsilon$, $\frac{d\sigma}{d\epsilon}$ is given by the expression:

$$\left(\frac{d\sigma}{d\epsilon}\right)_{\vec{P}_2} = \frac{X(P_1)\, 2m}{|\vec{P}_1 - \vec{P}_2||\vec{P}_1 + \vec{P}_2|} \cdot \frac{P_1^2}{|\vec{P}_1 - \vec{P}_2|^2} \cdot \frac{|\vec{P}_1 - \vec{P}_2|}{P_1}$$

between the limits

$$\left[|\vec{P}_1 + \vec{P}_2| + |\vec{P}_1 - \vec{P}_2|\right]^2 \geq 8m\epsilon \geq \left[|\vec{P}_1 + \vec{P}_2| - |\vec{P}_1 - \vec{P}_2|\right]^2$$

and $\left(\frac{d\sigma}{d\epsilon}\right)_{\vec{P}_2} = 0$, outside these limits.

The subscript to $\frac{d\sigma}{d\epsilon}$ refers to fixed values of P_2 and ϕ. The first term in the expression is the energy spectrum which results from a two body collision assuming that the scattering cross section is independent of energy; the second term allows for the energy variation of the free scattering cross section (assuming that the cross section varies inversely as the energy of the incident particle in the centre of momentum system); the third term takes into account the variation of the rate of flow of particles in the nucleus past the incident nucleon. The allowed energy spectrum $\frac{d\sigma}{d\epsilon}$ can be obtained from this expression by integrating over the range of ϕ and P_2 present in the Fermi gas.

Integration of $\left(\frac{d\sigma}{d\epsilon}\right)_{\vec{P}_2}$ over all possible values of ϕ yields the following expression for the cross section for the collision with a nucleon of fixed momentum P_2

$$\left(\frac{d\sigma}{d\epsilon}\right)_{P_2} = \frac{m\,X(P_1)}{2\sqrt{2}\,P_2(P_1^2+P_2^2)^{\frac{1}{2}}}\left[\log_e \frac{(P_1^2+P_2^2+2P_1P_2\cos\phi)^{\frac{1}{2}}+\sqrt{2}\,(P_1^2+P_2^2)^{\frac{1}{2}}}{(P_1^2+P_2^2+2P_1P_2\cos\phi)^{\frac{1}{2}}-\sqrt{2}\,(P_1^2+P_2^2)^{\frac{1}{2}}}\right]_{\phi}^{\pi-\phi}$$

The form of $\frac{d\sigma}{d\epsilon}$ as a function of ϵ is displayed in figure 1.

At this stage it is convenient to introduce the restrictions of the Pauli Exclusion Principle. For the collision of the incident nucleon of energy E, with a nucleon of energy E_2 the Pauli Principle is only satisfied if the energy of struck nucleon is raised to a value ϵ such that

$$E_F \leq \epsilon \leq (E_1 + E_2) - (E_F - Q)$$

where Q defines the release of energy in the nuclear process and E_F is the maximum Fermi energy. The upper limit $(E_1 + E_2) - (E_F - Q)$ ensures that the incident nucleon is also left with sufficient energy that the Pauli Principle is not violated. In the collision of an incident neutron with a proton inside the nucleus $Q = E_F\,(p) - E_F\,(n)$ and similarly for the inverse reaction. In the scattering of identical particles in the target nucleus, $Q = 0$. In figure 1 the shaded area defines the region of allowed collisions.

It follows that the only struck nucleons which can participate in such collisions must possess energies which lie between the limits:

$$\epsilon + E_F - Q - E_1 \leq E_2 \leq E_F$$

The allowed energy spectrum $\frac{d\sigma}{d\epsilon}$ averaged over the various velocities of the nucleons inside the nucleus is obtained therefore by performing the

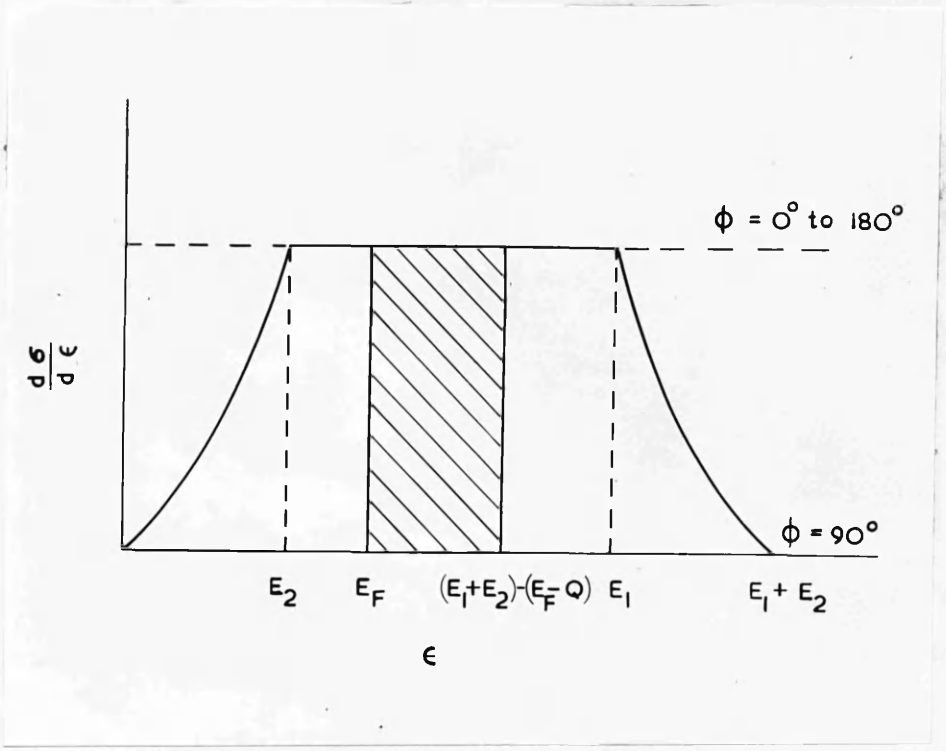

Figure 1: The distribution in energy of the particles produced by the scattering of two nucleons of energies E_1 and E_2. The shaded area represents those collisions which are allowed by the Pauli Exclusion Principle.

integration

$$\frac{d\sigma}{d\epsilon} = \frac{\int_a^b \left(\frac{d\sigma}{d\epsilon}\right)_{P_2} P_2^2 \, dP_2}{\int_0^b P_2^2 \, dP_2}$$

where $b = 2mE_F^{\frac{1}{2}}$ and $a = 2m\,(\epsilon + E_F - E_2 - Q)^{\frac{1}{2}}$. The term P^2dP takes account of the distribution of momentum in a Fermi gas of nucleons.

The Pauli Factor α for an incident nucleon energy E_1 is given by the ratio of the area of the allowed energy spectrum to the area of the energy spectrum for free nucleon scattering which is equivalent to $X(P_1)$, the cross section for free nucleon scattering. Thus:

$$\alpha = \frac{1}{X(P_1)} \int_{E_F}^{E_1 + Q} \left(\frac{d\sigma}{d\epsilon}\right) d\epsilon$$

The variation of the Pauli factor for the scattering of identical particles, $Q = 0$, which has been derived by this procedure, has been shown in figure 5.1. The Pauli factor for the scattering of non identical particles can be derived by the same procedure when the non-zero Q-value of the process is taken into account throughout the treatment. However, the relation between the different Pauli factors is not obvious from the above formula for α. The connection that exists between the different Pauli factors at the same incident energy will therefore be amplified in the following discussion.

As can be seen from figure 5.1, the Pauli factor α is a decreasing function of $\frac{E_F}{E_1}$. Since $E_F = 31$ MeV for protons and $E_F = 28$ MeV for neutrons, the following inequality holds:

$$\alpha_{nn} > \alpha_{pp}$$

However, the difference in the maximum energy of the Fermi gases also implies the following for the collision of a neutron and proton inside the nucleus. A collision is only allowed if the final neutron energy is greater that E_F (n) and the final proton energy is greater than E_F (p) Hence the following inequalities also hold

$$\alpha_{nn} > \alpha_{pn} \quad \text{and} \quad \alpha_{pp} < \alpha_{np}$$

where the first subscript refers to the incident particle in each case. Finally, in the collision of an incident neutron with a proton inside the nucleus, the struck proton can have a maximum energy greater than the maximum energy of the struck neutron in the inverse reaction. Hence the following inequality also holds:

$$\alpha_{np} > \alpha_{pn}$$

There exists therefore the following relationships between the different Pauli factors:

$$\alpha_{pp} < \alpha_{pn} < \alpha_{np} < \alpha_{nn}$$

Empirical expressions for α_{np} and α_{pn} can be derived in terms of the factors α_{pp} and α_{nn} when the preceding discussion is given a mathematical basis. The final expressions are:

$$\alpha_{np} = \alpha_{pp} + \frac{E_F(p) - E_F(n)}{E_1} \left(1 - 0.083 \frac{E_F(p)}{E_1}\right)$$

$$\alpha_{pn} = \alpha_{nn} - \frac{E_F(p) - E_F(n)}{E_1} \left(1 - 0.083 \frac{E_F(n)}{E_1}\right)$$

They illustrate more clearly than the previous formula their dependence on the difference in binding energy of the last neutron and proton (the Q-value).

The non isotropy of the neutron-proton scattering at high energies in the centre of mass system also effects the Pauli factors. The measured values (Hadley et al. 1949) for the differential cross section of neutron-proton scattering at 40 MeV can be represented by the expression

$$\frac{d\sigma}{d\omega} \sim (13 + 8 \cos^2 \theta) \text{ mb. ster}^{-1}$$

where θ = angle of scattering in the centre of mass system. This energy is of a similar magnitude to that considered in the present calculations.

Numerical calculations show that collisions with a Fermi gas of nucleons at this energy are virtually forbidden for $\theta < 50^\circ$. Since the term involving $\cos^2 \theta$ quoted above only makes a significant contribution at angles less than 50° the Pauli factors, α_{np} and α_{pn} are reduced compared with the corresponding factors calculated for isotropic scattering. The extent of the correction is about 20%.

To illustrate the effects of the different corrections, the Pauli factors α at an incident energy of 24 MeV, corresponding to an energy inside the nucleus E_1 of 62 MeV, areshown in table 1.

Table 1: Calculated Values of the Pauli Factors at an Incident Energy of 24 MeV

$$\frac{E_F(n)}{E_1} = 0.452 \qquad \frac{E_F(p)}{E_1} = 0.5$$

Pauli Factors	α_{nn}	α_{np}	α_{pn}	α_{pp}
From figure 5.1	0.355	-	-	0.29
α_{np} and α_{pn} corrected for difference in binding energy.	0.355	0.336	0.309	0.29
α_{np} and α_{pn} corrected for non-isotropy ($x \frac{1}{1.2}$)	0.355	0.28	0.257	0.29

REFERENCES

Allan, D.L., 1956, private communication.

Allan, D.L., 1957, Proc. Phys. Soc., A, 70, 195.

Austern, N., Butler, S.T., and McManus, H., 1952, Phys. Rev., 87, 188.

Barschall, H. H., 1952, Phys. Rev., 86, 431.

Barschall, H. H., Coon, J. H., and Graves, E.R., 1952, Phys. Rev., 88, 562.

Bernardini, G., Booth, E. T., and Lindenbaum, S. J., 1952, Phys. Rev., 85, 826; Ibid., 88, 1017.

Blaser, J.P., Boehm, F., Marmier, P., and Scherrer, P., 1951, Helv. Phys. Acta, 24, 441.

Blatt, J. M., and Weisskopf V. F., 1953, Theoretical Nuclear Physics, New York: J. Wiley and Son.

Bleuler, E., Stebbins, A. K., and Tendam, D. J., 1953, Phys. Rev., 90, 460.

Bohr, N., 1936, Nature, 137, 344.

Bosley, W., and Muirhead, H., 1952, Phil. Mag., 43, 63.

Bradt, H. L., and Tendam, D. J., 1947, Phys. Rev., 72, 1117.

Breuckner, K. A., 1956, Phys. Rev., 103, 172.

Britten, R., 1952, Phys. Rev., 88, 283.

Brown, G., and Muirhead, H., 1957, Phil. Mag., 2, 473.

Cassels, J. M., and Lawson, J. D., 1954, Proc. Phys. Soc., A, 67, 125.

Chamberlain, O., and Segrè, E., 1952, Phys. Rev., 87, 81.

Chen, F. F., Leavitt, C.P., and Shapiro, A. M. 1955, Phys. Rev., 99, 857

Christian, R. S., 1952, Rep. Progr. Phys., 15, 68.

Cladis, J. B., Hess, W. N., and Moyer, B. J., 1952, Phys. Rev., 87, 425.

Clementel, E., and Villi, C., 1955, Nouvo Cimento, 11, 176.

Cohen, B. L., Newman, E., Charpie, R.A., and Handley, T. H., 1954, Phys. Rev., 94, 620.

Conner, J. P., Bonner, T. W., and Smith, J. R., 1952, Phys. Rev., 88, 468.

Culler, G., Fernbach, S., and Sherman, N., 1956, Phys. Rev., 101, 1047.

Dilworth, C. C., Occhialini, G. P. S., and Payne, R. M., 1948, Nature, 162, 102.

Eisberg, R. M. 1954, Phys. Rev., 94, 739.

Feather, N., 1953, Advance Phys., 2, 141.

Fernbach, S., Serber, R., and Taylor, T. B., 1949, Phys. Rev., 75, 1352.

Feshbach, H., Peaslee, D.C., and Weisskopf, V. F., 1947, Phys. Rev.,71,145

Feshbach, H., Porter, C., and Weisskopf, V. F., 1953, Phys. Rev., 90, 166; 1954, Ibid., 96, 448.

Forbes S. G., 1952, Phys. Rev., 88, 1309.

Fowler, P. H., and Perkins, D. H., 1951, Fundamental Mechanisms of Photographic Sensitivity: Butterworths Scientific Publications.

Francis, N. C., and Watson, K. M., 1953, Amer. Phys., 21, 659.

Fry, W. F., 1952, Phys. Rev., 85, 676.

Frye, G. M., 1954, Phys. Rev., 93, 1086.

Gatha, K. M., and Riddell, R. J., 1952, Phys. Rev., 86, 1035.

Ghoshal, S. N., 1950, Phys. Rev., 80, 939.

Goldberger, M. L., 1948, Phys. Rev., 74, 1269.

Graves, E. R., and Rosen, L., 1953, Phys. Rev., 89, 343.

Gugelot, P. C., 1951, Phys. Rev., 81, 51; 1954, Ibid., 93, 425.

Hadley, J., Kelley, E., Segrè, E., Wiegand, C., and York, H., 1949, Phys. Rev., 75, 351.

Hahn, B., Ravenhall, D. G., and Hofstadter, R., 1956, Phys. Rev., 101,1131.

Hayakawa, S., Kawai, M., and Kikuchi, K., 1955, Prog. Theor. Phys., 13, 41

Hildebrand, R. H., and Leith, C. E., 1950, Phys. Rev., 80, 842.

Hintz, N. M., 1952, Phys. Rev., 86, 1042.

Igo, G. J., and Eisberg, R. M., 1954, Phys. Rev., 93, 1039.

Lane, A. M., Thomas, R. G., and Wigner, E. P., 1955, Phys. Rev., 98, 693.

Lane, A. M., and Wandel, C. F., 1955, Phys. Rev., 98, 1524.

Le Couteur, K. J., 1950, Proc. Phys. Soc., A, 63, 259; 1952, Ibid, 65,718.

Le Levier, R. E., and Saxon, D. S., 1952, Phys. Rev., 87, 40.

Lock, W. O., March, P. V., and McKeague, R., 1955, Proc. Roy. Soc., A, 231, 368.

Mandl, F., and Skyrme, T. H. R., 1952, Proc. Phys. Soc., A, 65, 107.

Melkanoff, M. A., Moskowski, S. A., Nodvik, J., and Saxon, D. S., 1956, Phys. Rev., 101, 507.

Menon, M. G. K., Muirhead, H., and Rochat, O., 1950, Phil. Mag., 41, 583.

McManus, H., and Sharp, W. T., 1952, Phys. Rev., 87, 188.

Nedzel, V. A., 1954, Phys. Rev., 94, 174.

Paul, E. B., and Clarke, R. L., 1953, Canad. J. Phys., 31, 267.

Peaslee, D. C., 1952, Phys. Rev., 86, 269.

Perry, A. M., 1952, Phys. Rev., 85, 497.

Pickavance, T. G., and Cassels, J. M., 1952, Nature, 169, 520.

Prowse, D. J., and Hossain, A., 1956, Phil. Mag., 1, 19.

Richardson, R. E., Ball, W. P., Leith, C. E., and Moyer, B. J., 1952, Phys. Rev., 86, 29.

Rochester, G. D., and Rosser, W. G. V., 1951, Rep. Progr. Phys., 14, 227.

Rosen, L., 1953, Nucleonics, 11, No. 7, 32.

Rosen, L., 1956, private communication.

Rotblat, J., 1950, Nature, 165, 387; 1951, Ibid., 167, 550.

Serber, R., 1947, Phys. Rev., 72, 1114.

Taylor, T. B., 1953, Phys. Rev., 92, 831.

Tiomno, J., and Wheeler, J. A., 1949, Rev. Mod. Phys., 21, 153.

Ulam, S., and Neumann, J. von, 1947, Bull. Amer. Math. Soc., 53, 1120.

Walt, M., and Beyster, J. R., 1955, Phys. Rev., 98, 677.

Webb, J. H., 1948, Phys. Rev., 74, 511.

Weisskopf, V. F., 1937, Phys. Rev., 52, 295.

Weisskopf, V. F., 1950, Helv. Phys. Acta, 20, 187.

Weisskopf, V. F., and Ewing, D. H., 1940, Phys. Rev., 57, 472.

Wilkins, J. J., 1951, A.E.R.E. Report, G/R 664.

Wolfenstein, L., 1951, Phys. Rev., 82, 690.

Woods, R. D., and Saxon, D. S., 1954, Phys. Rev., 95, 577.

~~Ford,~~ Feshbach, H., and Weisskopf, V. F., 1949, Phys. Rev., 76, 1550.